Ministry of Higher Education
and Scientific Research
Karbala University
College of Science

Synthesis and Identification of Heterogeneous Catalysts from Rice Husk as Schiff Base and It's Application on the Hydrolysis of Cellulose to Glucose.

A Thesis

Submitted To The College of Science , Karbala University In Partial Fulfillment of the Requirements for The Master Degree in Chemistry

By

Mosa Jaafar Mosa Al-Ghaliby

B. Sc. University of Karbala (2011)

Supervision by

Dr. Hayder Hamied Al-Hmedawi .

Assist. Prof. Dr. Kasim Mohammed Hello Al-Mahmudawi

2014

بسم الله الرحمن الرحيم

« ((قُلْ كُلٌّ يَعْمَلُ عَلَىٰ شَاكِلَتِهِ فَرَبُّكُمْ أَعْلَمُ بِمَنْ هُوَ أَهْدَىٰ سَبِيلًا))

صدق الله العلي العظيم

سورة الاسراء اية 84

Dedication

To the souls of martyrs of my dear country

Iraq

وزارة التعليم العالي والبحث العلمي

جامعة كربلاء

كلية العلوم

تحضير وتشخيص محفزات غير متجانسة من قشور الرز و قواعد شف واستخدامها في تفاعل تحلل السليلوز الى الكلوكوز

رسالة مقدمة الى كلية العلوم - جامعة كربلاء

كجزء من متطلبات نيل درجة الماجستير في الكيمياء

من قبل

موسى جعفر موسى الغالبي

بكالوريوس علوم في الكيمياء - جامعة كربلاء (2011)

بإشراف

د. حيدر حميد الحميداوي

أ.م.د. قاسم محمد حلو المحموداوي

2014

الاهداء

الى ارواح شهداء بلدي العزيز

العراق

الخلاصة

في هذه الدراسة تم تدعيم السيليكا المستخلصة من قشور الرز (السبوس) مع مركب 3-كلوروبروبيل تراي ايثوكسي سايلين لتحضير المركب RHACCl بعدها تم تطعيم هذا المركب مع مركبين من قواعد شف المحضرة من تفاعل السلسلديهايد مع الفنل هدرازين (PHMP) مرة ، ومرة اخرى مع قاعدة شف المحضرة من تفاعل السلسلديهايد و 4,2 داي نتروفنل هدرازين (DNPHMP) لتحضير محفزات جديدة غير متجانسة سميت RHPHMP و RHDNPH. تم التأكد من تحميل هذه المركبات العضوية على السيليكا بواسطة عدة تقنيات منها مطيافية الاشعة تحت الحمراء FTIR وتحليل العناصر CHN وتشتت الاشعة السينية EDX والمجهر الالكتروني الماسح SEM والتحليل الحراري الوزني TGA والتحليل الحراري التفاضلي DTA وتحليل امتزاز النتروجين والتي اثبتت صحة الصيغة التركيبة المتوقعة للناتج حيث ان عدم ظهور حزمة امتصاص الاصرة NH_2 وظهور حزم امتصاص لاصرتي C=N وكذلك C=C عند المنطقة المتوقعة يؤكد تكوين الناتج المتوقع لانها غير موجودة في طيف الاشعة تحت الحمراء للسيليكا ، كذلك في نتائج تحليل العناصر و EDX اظهر زيادة في نسبة الكاربون عما هي موجودة في RHACCl وظهور نسبة للنتروجين التي لم تكن موجودة في RHACCl ، فيما اظهرت التحاليل الحرارية TGA/DTA وجود مراحل تكسير للجزء العضوي ضمن تركيب المحفزات ، اضافة الى التحاليل الاخرى التي اعطت ادلة كافية على تكوين المركب المتوقع.

اما الفعالية التحفيزية للمركبات RHPHMP و RHDNPH كمحفزات غير متجانسة وكذلك المركبات PHMP و DNPHMP كمحفزات متجانسة وايضا RHA (كمرجع) في تفاعل تحلل السليلوز . وجد بان الفعالية التحفيزية لهذه المركبات تجاه تفاعل تحلل السليلوز الى الكلوكوز تتبع التسلسل الاتي :

PHMP > RHPHMP> RHDNPH > DNPHM > RHA.

فصلت المحفزات بسهولة بعد التفاعل وتم اعادة استخدامها لعدة مرات بدون فقدان فعاليتها التحفيزية .

SUPERVISORS CERTIFICATION

We certify that this thesis was prepared by ***Mosa Jaafar Mosa Al-Ghaliby*** *under our supervision at the Chemistry Department, College of Science, Karbala University, as a partial requirement for the degree of Master of Science in chemistry.*

Signature:

Name: ***Dr. Hayder Hamied Al-Hmedawi***

Address: University of Karbala

Date:

Signature:

Name: ***Asst.Prof. Dr. Kasim Mohammed Hello***

Address: University of Al-Muthanna

Date: / /

HEAD OF DEPARTMENT CERTIFICATION

In view of the available recommendation by supervisors, I foreward this thesis for debate by the examining committee.

Signature:

Name: ***Dr. Baker Abid Al-Zahra Joda***

Address: University of Karbala / College of Science

Date:

Report of Linguistic Evaluator

I certify that the linguistic evaluation of this thesis was carried out by me and it is linguistically sound.

Signature:

Name: ***Assist. Prof. Dr. Sabah Wajid Ali***

Address: University of Karbala / College of Education

Date: 26 / 11 / 2013

Report of Scientific Evaluator

I certify that the scientific evaluation of this thesis was carried out by me and it is accepted scientifically.

Signature:

Name: ***Prof. Dr. Hussien A. Salih***

Address: University of Babylon / College of Science

Date: / /

Examination Committee Certification

*We, the examining committee certify that we read this thesis "***Synthesis and Identification of Heterogeneous Catalysts from Rice Husk as Schiff Base and It's Application on the Hydrolysis of Cellulose***" and have examined the student (**Mosa Jaafar Mosa**) in its contents and that our opinion , its adequate as a thesis for the degree of master of science in chemistry with excellent .*

Signature:

Name : ***prof. Dr. Faleh Hasan Mousa***
Address : University of Baghdad
Date : / 2 / 2014
(Chairman)

Signature:

Name: ***Asst. prof .Dr. Ashour H. Dawood***
Address : University Of Al-Mustansirya
Date: / 2 / 2014
(Member)

Signature:

Name: ***Dr. Luma Majeed Ahmed***
Address: University of Karbala
Date: / 2 / 2014
(Member)

Signature:

Name: ***Dr. Hayder Hamied Al-Hmedawi***
Address: University of Karbala
Date: / 2 / 2014
(Member/supervisor)

Signature:

Name: ***Asst.Prof. Dr. Kasim Mohammed Hello***
Address: University of Al. Muthanna
Date: / 2 / 2014
(Member/supervisor)

Approve by Council of the College of Science

Signature:
Name: ***Prof. Dr. Ahmed Mehmood Abdul-Lettif***
Address: University of Karbala - Dean of the College of Science
Date: / 2 / 2014

Acknowledgment

First of all thank God Almighty for His ample grace and permanent reconcile, the owner of biggest credit that guide me and gave me the ability to complete this work.

I also extend my sincere thanks to my father, my mother and all my brothers for their continued support me throughout my research. Thanks goes to them with all my heart.

I also want to express my sincere thanks and great gratitude to the supervisors ***Dr. Hayder Hameed Al.Hmedawi****, and* ***Assist. Prof .Dr. Kasim Mohammad Hello*** *for their support to me and bearing the burden of the practical part with their helping throughout this large period, so I reiterate my thanks to them and invoke God to help them for all that is good during their scientific way.*

My thanks and gratitude are due to for the prime and all the staff of the Department of Chemistry for helping me during the period of work as well as my thanks and gratitude are present to all the Deanship staff in the College of Science.

I also want to express my sincere thanks to University of Al-Muthanna /college of science / department of chemistry.

Finally, to my loved friends I extend of my thanks and gratitude for their moral support and standing by my side in the hardest stages of research.

..... Thank you all …….

Mosa Jaafar Al.Ghaliby

Abstract

In this study the silica which extracted from rice husk ash (RHA) was immobilized with 3-chloroprpyltriethoxysilane (CPTES) to produce RHACCl. A Schiff bases which were prepared from the reaction of salisyaldehyde with phenylhydrazine (PHMP), also with 2,4-dinitrophenylhydrazine (DNPHMP),were functionalized with RHACCl to give new heterogeneous catalysts labeled as RHPHMP and RHDNPH. Many techniques have been used to prove the successfully functionalized silica with PHMP and DNPHMP such as FT-IR ,CHN, X-ray Diffraction, Scanning Electron Microscopy (SEM) / Energy Dispersive X-Ray (EDX), and Thermal Gravimetric Analysis (TGA) / Differential Thermal Analysis (DTA). The FT-IR of the prepared catalysts shows the disappearance of –NH2 absorption band and appearance of C=N and C=C absorption bands at the expected position The elemental analysis and EDX results show an increase in the carbon percentage and presence of nitrogen which is not found in RHACCl. Thermal analysis TGA/DTA shows different stages of mass loss attributed to the removal of the organic moiety in the catalysts structure. The catalytic activity of RHPHMP, RHDNPH and RHA-Blank (as control) as well as homogenous PHMP and homogenous DNPHMP were used as catalysts in the hydrolysis of cellulose . The catalytic activity of the catalysts toward the respective glucose was found to follow the sequence below.

PHMP > RHPHMP> RHDNPH > DNPHM > RHA.

The catalysts were easily regenerated and could be reused several times without loss of catalytic activity.

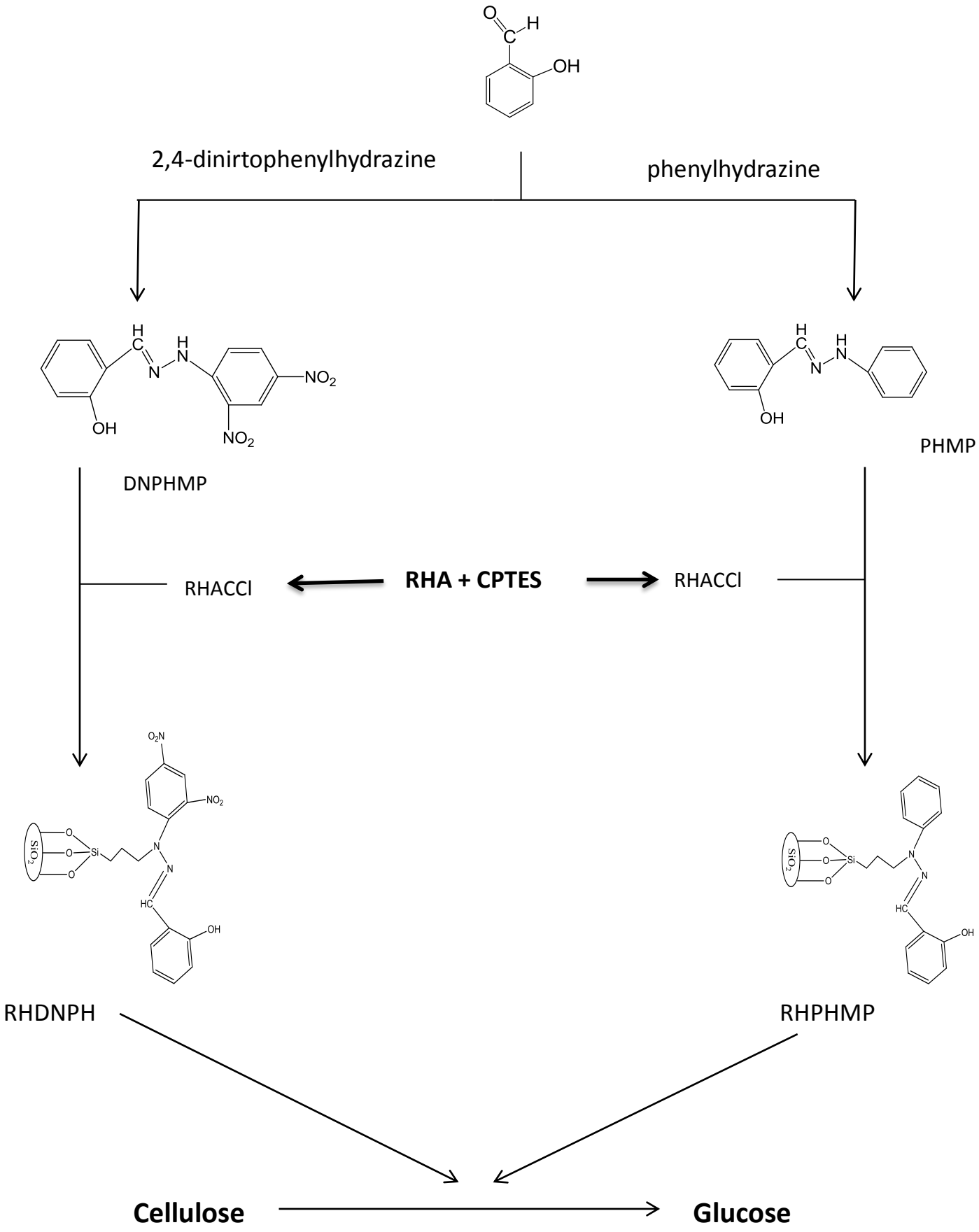
2,4-dinirtophenylhydrazine
phenylhydrazine
DNPHMP
PHMP
RHACCl
RHA + CPTES
RHACCl
RHDNPH
RHPHMP
Cellulose
Glucose

TABLE OF CONTENTS

LIST OF TABLES

LIST OF FIGURES

LIST OF SCHEMES

LIST OF SYMBOLS AND ABBREVIATIONS

APTMS	3-aminoprpyltrimethoxysilane.
Au/SiO_2	Gold particle supported on silica surface.
BET	Brunauer-Emmett-Teller
BJH	Barrett–Joyner–Halenda
ca.	Calculated
CPTES	3-chloroprpyltriethoxysilane.
CPTMS	3-chloroprpyltrimethoxysilane.
d^6-DMSO	Fully Deuterated dimethoxysulfoxide.
DCM	Dichloromethane
DMF	Dimethylformamide
DMSO	Dimethoxysulfoxide.
DNPHMP	2-((2-(2,4-dinitrophenyl)hydrazono) methyl)phenol (DNPHMP).
DNS	Dinitrosalicylic acid.
DSC	Differential Scanning Calorimetry.
DTA	Differential Thermal Analysis.
DTO	Dithioxamide.
EDX	Energy Dispersive X-ray.
Et_3N	Triethyl amine.
Fig	Figure.
H2	Hysteresis loop type 2.
IL	Ionic liquid.

KeV	Kilo electron Volt.
mp	Melting point.
MPTMS	3-marcptoprpyltrimethoxysilane.
P/P_o	Relative pressure.
PHMP	2-((2-phenylhydrazono)methyl)phenol PHMP.
p-PDA	*para*-phenylenediamine.
Ppm	Past per million.
Pt/Al_2O_3	Platinum supported on alumina
PTMS	Phenyltrimethoxysilane.
RH	Rice Husk.
RHA	Rice Husk Ash.
RHABuIm	RHA immobilized with Butylimidazole.
RHACCl	RHA immobilized with 3-chloroprpyltriethoxysilane.
RHDNPH	RHACCl immobilized with DNPHMP.
RHPHMP	RHACCl immobilized with PHMP.
Ru/Ac-SO_3H	Ruthenium nanoparticles activated with sulphonate group.
$Ru/NbOPO_4$	Niobium phosphate supported Ruthenium.
SEM	Scanning Electron Microscopy.
TA	Thermal Analysis.
TG	Thermal Gravimetric.
TGA	Thermal Gravimetric Analysis.
TLC	Thin Layer Chromotography.

XRD	X-Ray Diffraction.
μg	microgram.

CHAPTER ONE

Introduction

1.1 Catalysis

Catalysis is a term coined by Berzelius in 1835 to describe the property of substances that expedite chemical reactions without being consumed in them. A broad definition of catalysis also allows for materials that slow the rate of a reaction. Whereas catalysts can greatly affect the rate of a reaction, the equilibrium composition of reactants and products is still determined solely by thermodynamics. [1, 2].

Two types of catalyst can be distinguished, natural and unnatural. Enzymes are Nature's catalysts. They are large proteins, the structure of which results in a very shape and reactant specific active site [3]. The second type of catalysts is divided into two types homogeneous and heterogeneous. In homogeneous catalysis both the catalyst and the reactants are in the same phase. The heterogeneous catalysts involves the catalyst and reactants in different phases and, most frequently, the reactants and products are in the gas or liquid phase with a solid catalyst. Heterogeneous catalysts are preferred in industry because of the ease separation of the products from the catalyst [4].

1.2 Heterogeneous catalysts

Heterogeneous catalysts are distinguished from homogeneous catalysts by the different phases present during reaction. Homogeneous catalysts are present in the same phase as reactants and products, usually liquid, while heterogeneous catalysts are present in a different phase, usually solid [5] e.g. when the reactants chemisorb on a solid surface, the weakening of the internal bonds makes the formation of new bonds with

other molecules easier. The product must have a lower affinity with the catalyst in order to be released into the liquid phase (desorption) [6].

The main advantage of using a heterogeneous catalyst is the relative ease of catalyst separation from the product stream that aids in the creation of continuous chemical processes. Additionally, heterogeneous catalysts are typically more tolerant of extreme operating conditions than their homogeneous analogues, heterogeneous catalysis has never held a more pivotal role. Not only do a great many industrial processes rely on heterogeneous catalysts today, but as the global concerns of energy production and conversion, alternative energy sources, and climate change garner attention, the importance of heterogeneous catalysis is again paramount [1]. Although many reactions can be promoted with either homogeneous or heterogeneous catalysis, the latter generally allows for less waste, fewer toxic reagents, and easier retrieval and recycling of the catalyst [7].

1.3 Rice Husk Ash (RHA)

Rice milling generates a byproduct known as husk Fig1.1. This surrounds the paddy grain. It is reported that approximately 0.23 ton of rice husk (rice hull) is formed from every ton of rice produced. The use of any material including wastes (RH) depends on its structure, properties and mainly on chemical composition [8].

Fig1.1: Rice husk is a byproduct of rice [9].

During milling of paddy about 78% of weight is received as rice, broken rice and bran. The rest 22% of the weight of paddy is received as husk. This husk is used as fuel in the rice mills for steam generation process. It contains about 75% organic volatile matter and the balance 25% of the weight of this husk is converted into ash during the firing process, which is known as rice husk ash (RHA). This RHA in turn contains around 85–90% amorphous silica [10,11].

Amorphous silica is well known and commonly used as a support material due to its high surface area, which will provide sufficient surface area for any metal to disperse. There are very limited publications on the use of RHA as a matrix for preparing metal supported heterogeneous catalyst. In all reported cases, the incipient-wet method and ion exchange methods were used to physically incorporate the metal into the RH silica matrix [12].

1.3.1. Components of Rice Husk

Chemical compositions of rice husk are different from sample to sample. This variation is due to differences in climatic and geographical conditions, type of paddy etc. The chemical analysis of rice husk is shown in Table 1.1. The silica SiO_2 is found to be 22.12%, the organic material and water content is 74% and (Al_2O_3+Fe_2O_3+CaO+ MgO) constitute about 4% [13].

Table 1.1: Chemical analysis of raw RH [13].

Constituent	Content (wt %)
Organic material and moisture	73.87
Al_2O_3	1.23
Fe_2O_3	1.28
CaO	1.24
MgO	0.21
SiO_2	22.12
MnO_2	0.074

Sharma et al. [14] analyzed all the reported data on organic constituents of rice husk after excluding silica and gave an average composition as given in the Table 1.2. The organic part is composed of cellulose, lignin and hemicellulose; the latter is a mixture of D-xylose, L-arabinose, methylglucoronic acid and D-galactos. The fibrous nature and the small grains in RH did not seem to be disturbed by burning as shown in SEM of RHA Fig1.2.

Table1.2: Organic constituents of RH excluding silica[14].

Constituent	**Amount present in RH (wt %)**
α-cellulose	43.30
Lignin	22.00
D-xylose	17.52
L-arabinose	6.53
Methylglucuronic acid	3.27
D-galactose	2.35

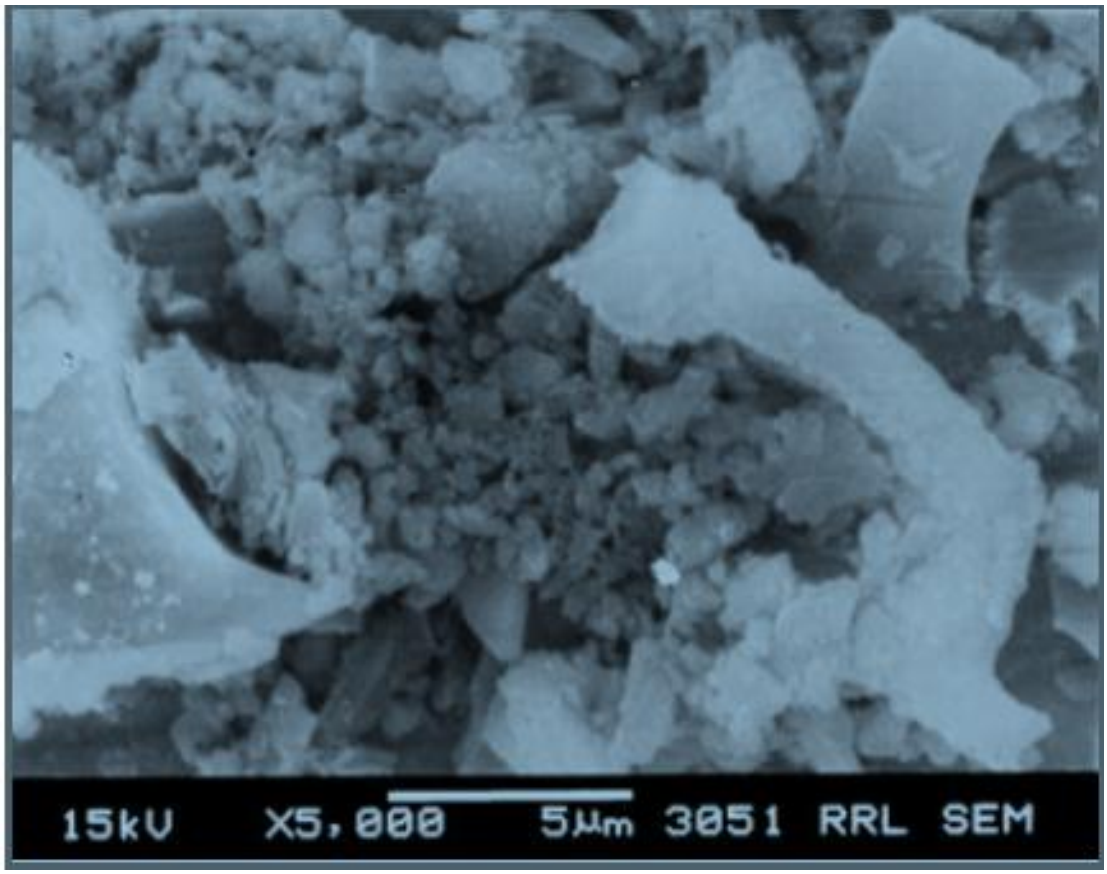

Fig.1.2: SEM of white ash of RH [11].

1.3.2 Structure of RHA

The silica is the main component in RHA. Silica has been investigated by many workers to determine its properties. The structure terminates at the surface in either a siloxane group (Si–O–Si) with the oxygen on the surface, or one of several forms of silanol groups (Si–OH). The silanols can be divided into isolated groups (or free silanols), where the surface silicon atom has three bonds in the bulk structure and the fourth bond is attached to a single –OH group, and vicinal silanols (or bridged silanols), where two single silanol groups, attached to different silicon atoms, are close enough to the hydrogen bond. The third type of silanols, geminal silanols, consists of two hydroxyl groups that are attached to one silicon atom and that are too close to form hydrogen bond between each other Fig 1.3 [15].

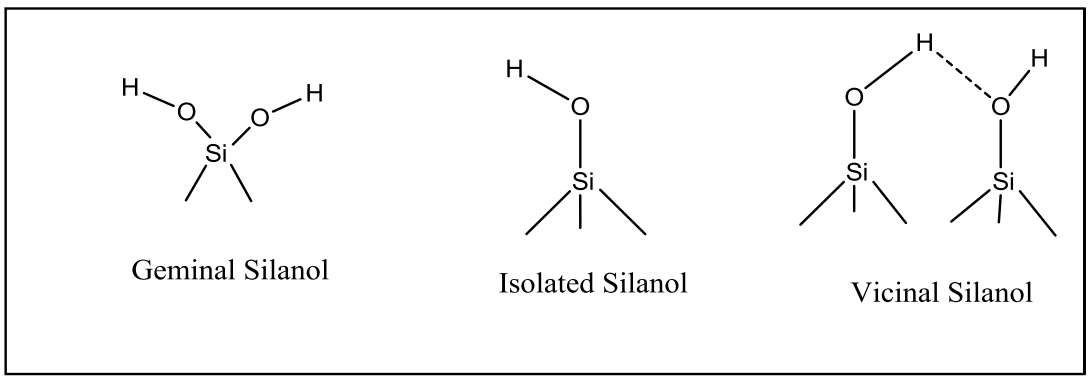

Fig. 1.3: Different types of silanol group in surface of silica [15].

The surface of silica can show strong hydrogen-bonding effects. Because of this, silica with hydroxyl surface is extremely hygroscopic. Dry silica will absorb water directly from moist air, with mass increases of up to 20% [16]. The enhanced acidity of silica surface gives it a high

degree of chemical reactivity, so it can react with many coupling agents to immobilize organo-functionalized silanes Scheme 1.1 [17].

There are two strategies for the immobilized polysiloxane ligand systems into silica. The first strategy is to prepare the silane with the complexing group and then to immobilized the complexing ligand by hydrolytic condensation reaction with tetra ethoxy silane. The second strategy is post treatment of the polysiloxane with the complexing ligand. The first strategy frequently results in a high amount of complexing ligand than the post-treatment of the polysiloxane, provided that the ligand is stable in the hydrolytic-condensation step. Therefore, the immobilized polysiloxane ligand systems can be prepared by two different methods, which are briefly surveyed by other researchers [16].

Silane coupling agents have the general formula $RSiX_3$, Scheme 1.1 where X is a hydrolysable group and R represents an organo functional group [18]. The organo functional groups are chosen for reactivity with the polymer, while the hydrolysable groups X (Cl or OR) are just intermediates in the formation of silanol groups for bonding to mineral surface. Ordinarily, trialkoxysilane is used because it is easier to handle than the trichlorosilane and the corrosive HCl formed as a byproduct of hydrolysis is undesirable [16].

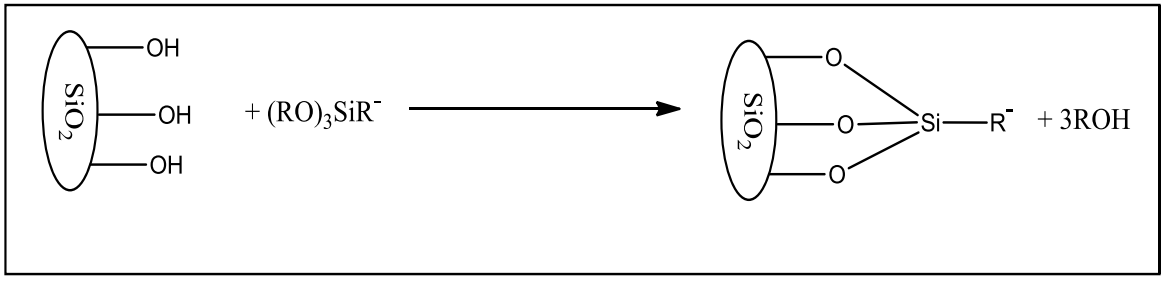

Scheme 1.1: Immobilization of silica with ethoxy or methoxy silane.
R = Me or Et, R/= Organo functionalized ligand.

1.3.3 Functionalization of silica with organic compounds

There are several studies that have benefited from the nature of the structure of amorphous silica to carry organic and inorganic compounds to synthesis heterogeneous catalyst. The main method of immobilization of the organic and inorganic moieties was via the reaction of a particular molecule with the silanol groups on the silica surface.

Yang and Chao [19] have been reported that a three method to functionalization of silica: namely grafting, coating, and co-condensation (Scheme 1.2). The products have been used to produce inorganic-organic hybrid networks and it may used in preparing of different catalysts.

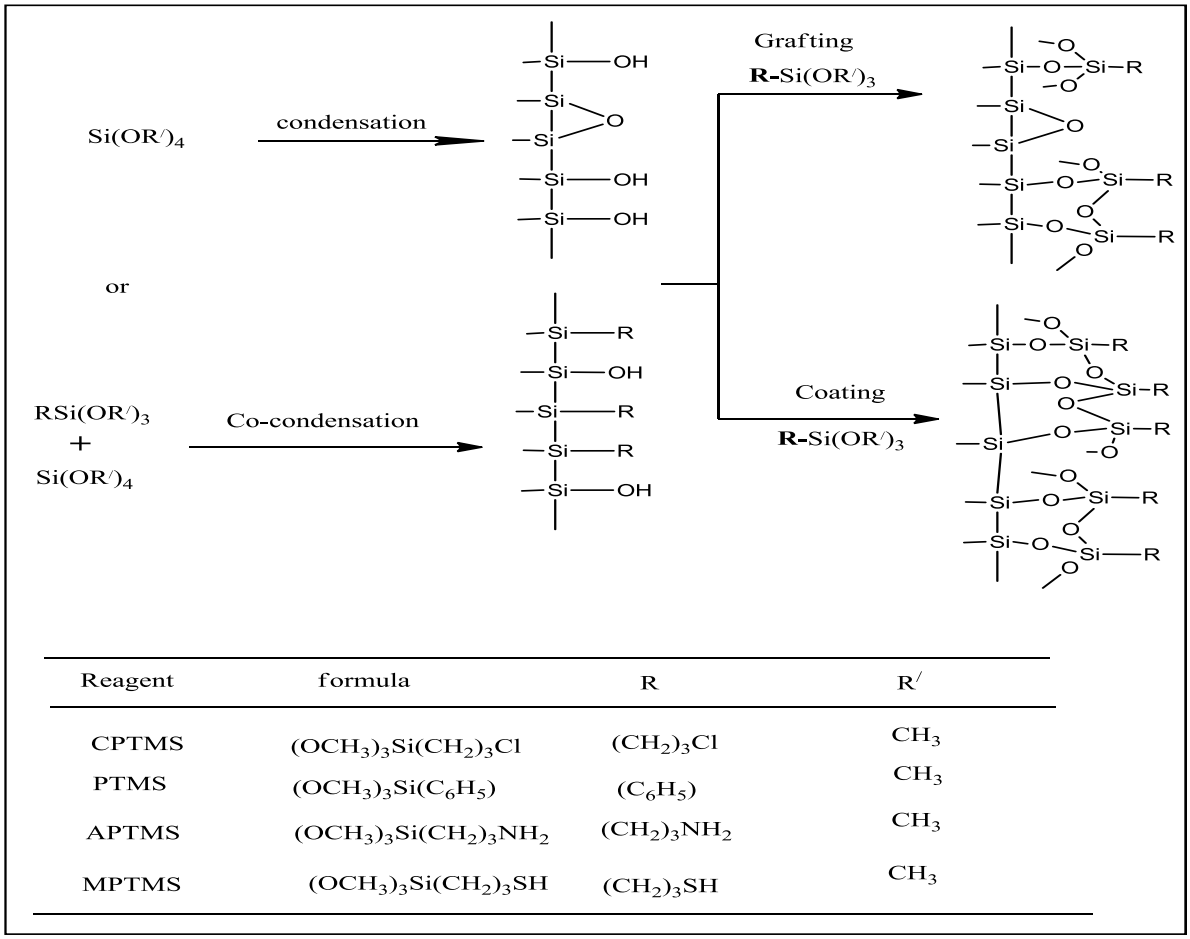

Reagent	formula	R	R/
CPTMS	$(OCH_3)_3Si(CH_2)_3Cl$	$(CH_2)_3Cl$	CH_3
PTMS	$(OCH_3)_3Si(C_6H_5)$	(C_6H_5)	CH_3
APTMS	$(OCH_3)_3Si(CH_2)_3NH_2$	$(CH_2)_3NH_2$	CH_3
MPTMS	$(OCH_3)_3Si(CH_2)_3SH$	$(CH_2)_3SH$	CH_3

Scheme 1.2: Different types of silylating agents which have been used to functionalization of silica.

Bae et al. [20] were reported that the silica can also be functionalized with 3-(chloropropyl)trimethoxysilane (CPTES) by refluxing in toluene for 24 h. This was followed by soxhlet extraction with different organic solvents. Paul et al. [21] showed that 3-(chloropropyl)trimethoxysilane (CPTMS) can also be used to functionalize silica to produce the same product. However, the reaction needs to be refluxed for 96 h at 160 ^{o}C. The same reaction was carried out by Soundiressane et al. [22] by refluxing CPTMS with silica for 24 h, followed by soxhlet extraction with dichloromethane (DCM) for 12 h.

Hello [23] was the first mention that the silica could immobilize with CPTES via sol-gel technique (Scheme 1.3). His method is simple and does not require toxic reagents and within a reasonable time of 2 h without having to resort to high refluxing temperatures. This method involves a one-pot synthesis of silica–CPTES complex from sodium silicate obtained from RHA. The technique results in high yield of the surface modified silica from a cheap waste product of the rice milling industry. Many studies have follow this method to produce RHACCl [24, 25].

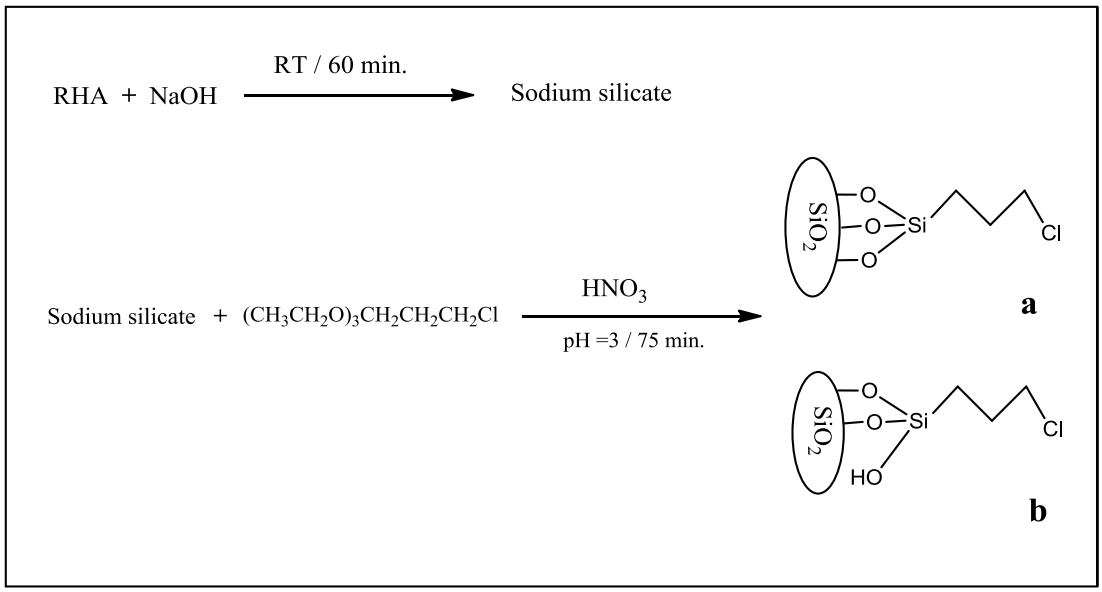

Scheme 1.3: Functionalized of silica with CPTES to produce RHACCl.

Chew et al. [26] were used the RHACCl to synthesized a heterogeneous catalyst by reaction of RHACCl with imidazole Scheme 1.4. The synthesis of silica–imidazole composite was carried out by adding imidazole to a suspension of RHACCl in dry toluene and triethylamine. The reaction mixture was refluxed at 110 ^{o}C in an oil bath for 48 h.

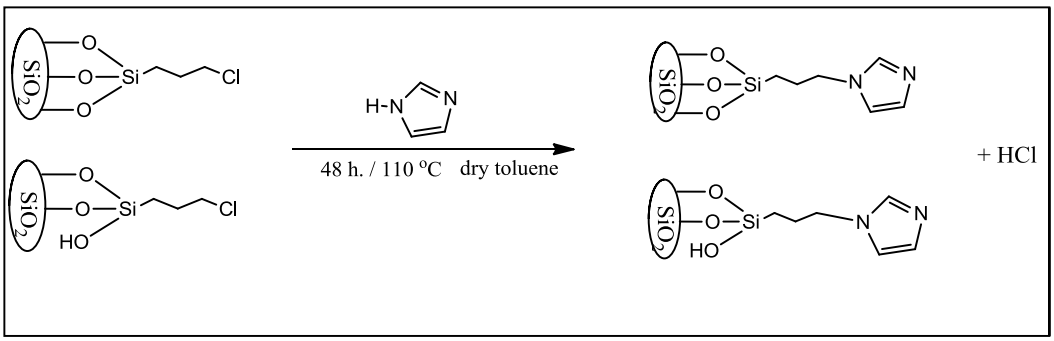

Scheme 1.4: The reaction of RHACCl with imidazole.

Adam et. al. [27] were used RHACCl to prepared a heterogeneous catalyst by its reaction with butyl imidazole Scheme 1.5. The catalyst was showed high activity in the cyclization of glycerol to cyclic acetals.

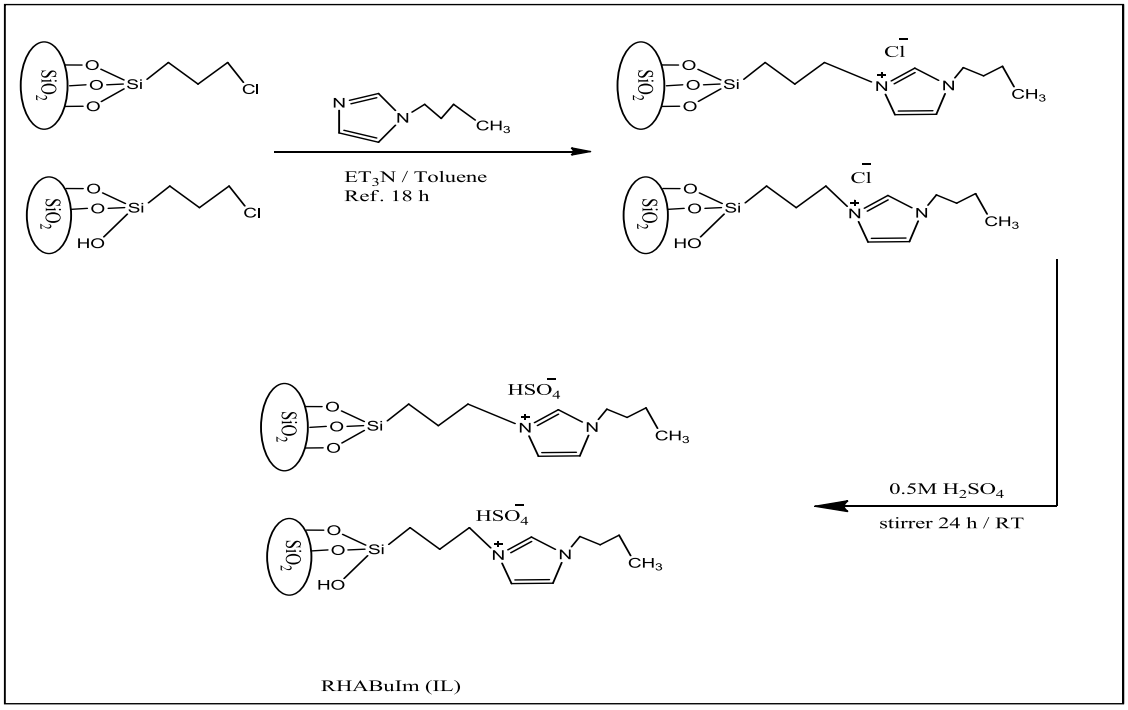

Scheme 1.5: Synthesis of ionic heterogeneous catalyst from RHACCl and BIM.

The sulfanilic acid was grafted onto the RHACCl to prepared heterogeneous acidic catalyst Scheme 1.6. The catalyst was used in the alkylation of phenol, The catalyst can be reused several times without significant loss of catalytic activity [28].

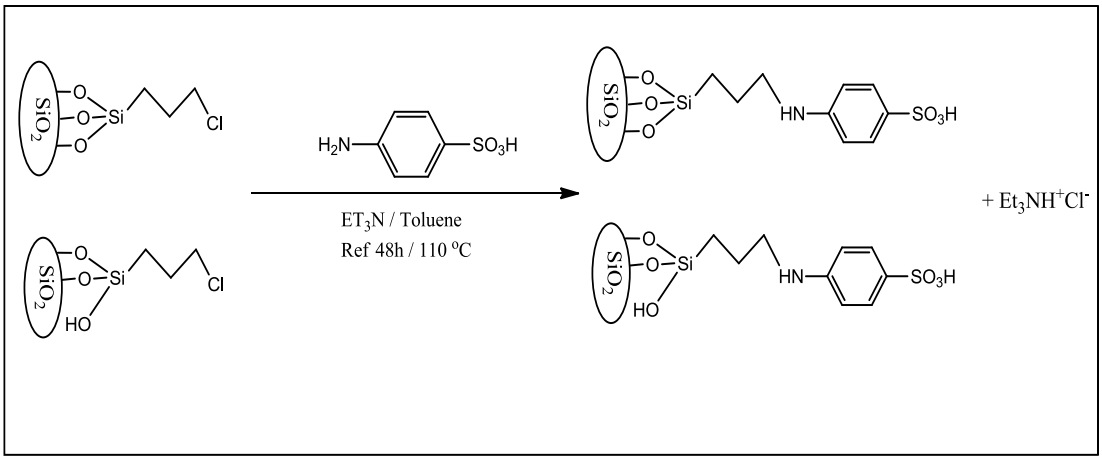

Scheme 1.6: The immobilization of RHACCl with sulfanilic acid.

Al-Hmedawi [29] was used RHACCl for the preparation of an heterogeneous catalyst. The dithiooaxamide (DTO) and P-phenylendiamine (P-PDA) were treated with RHACCl in dry toluene and Et_3N (Scheme 1.7). The catalyst was tested in the esterification of ethyl alcohol with acetic acid.

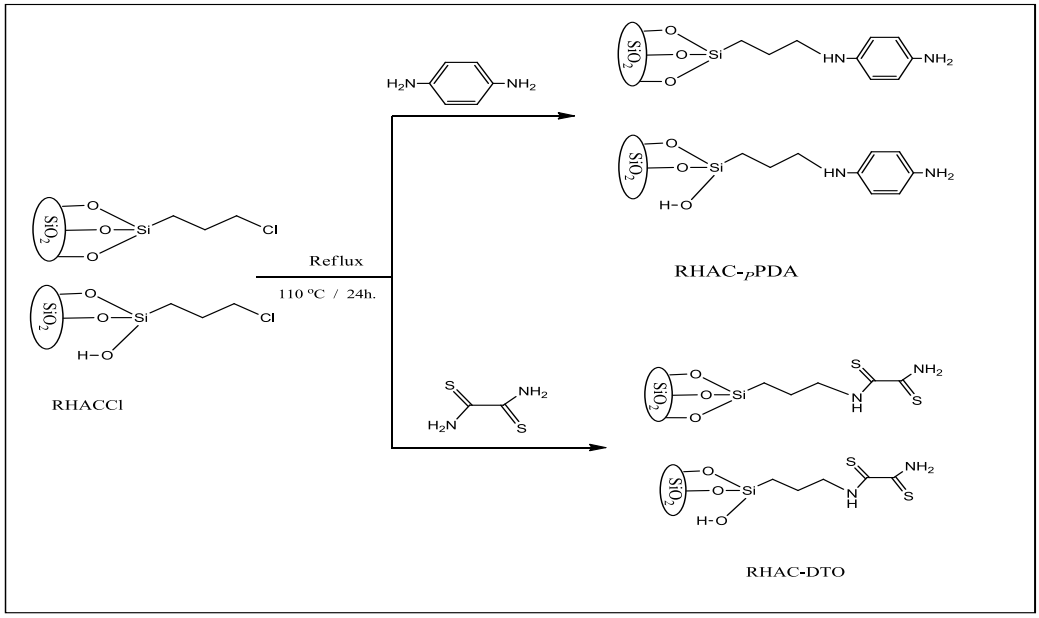

Scheme 1.7: The reaction of DTO and P-PDA onto RHACCl to form RHAC-DTO and RHAC-P-PDA.

1.4 Schiff base

Schiff bases are bimolecular condensation products of primary amines with aldehydes or ketone. It was represented valuable intermediates in organic synthesis due to the various applications [30]. The general reaction for the synthesis of shiff base was represented as in Scheme 1.8.

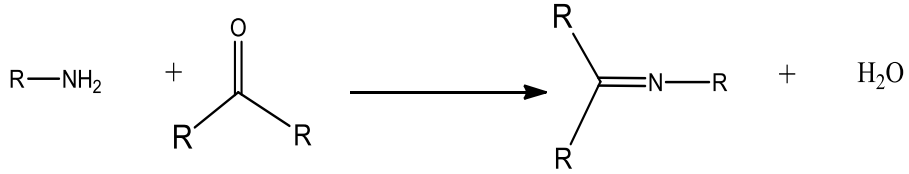

Scheme 1.8: General reaction of Schiff base preparation.

Where R an alkyl or aryl group. Schiff bases that contain aryl substituent are substantially more stable and more readily synthesized while those which contain alkyl substituent are relatively un stable and readily polymerizable [31]. Scheme 1.9 describes the general mechanism of the Schiff base reaction:

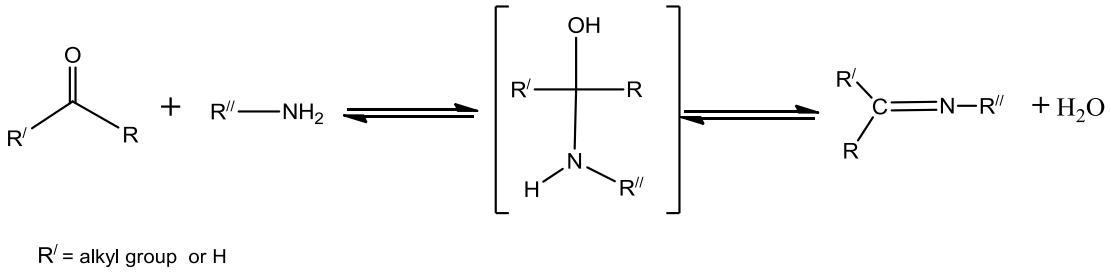

R/ = alkyl group or H

Scheme 1.9: General mechanism of Schiff base.

1.5 Hydrazones

Hydrazones are a class of organic compounds with the structure $R_2C{=}NNH_2$. They are related to ketones and aldehydes by the replacement of the oxygen atom of carbonyl group, with the $=NNH_2$ functional group. They are formed by the reaction of hydrazine derivatives with ketones or aldehydes [32].

Hydrazones have been studied as a group of the most useful spectrophotometric reagents. Combining appropriate starting materials (carbonyl compounds and hydrazine), the sensitivity as an analytical reagent and/or solubility of the hydrazones could be improved and the donating environment could be changed. The shortcoming of hydrazones was their lack of selectivity for metal ions. Much effort has been devoted to developing masking agents for use with hydrazones [33, 34].

1.6 Cellulose

Cellulose and hemicellulose are produced by plants during the photosynthesis process using sunlight energy, water and carbon dioxide [35]. Cellulosic materials have played an important role in everyday of life as constituent of wood, paper, cloth, rayon film, plastic rope and fillers. The biological decomposition of cellulose is the most important process in nature. It constitutes the major necessary steps in maintaining the balance between the synthetic and degradative phenomenon in carbon cycle [36, 37]. Cellulose is a polymer of glucose units with a molecular formula $(C_6H_{10}O_5)n$ Scheme 1.10.

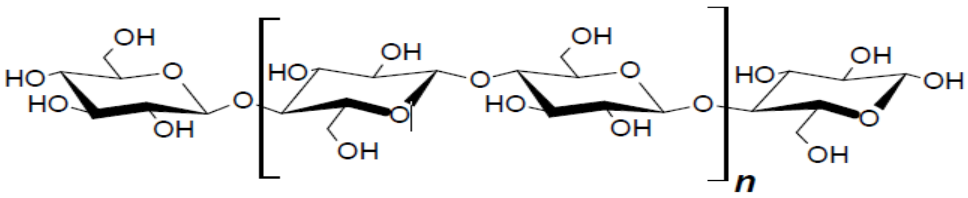

Scheme 1.10: The cellulose structure.

1.6.1 Structure of cellulose

Cellulose has a linkage of glucose with 1,4-β-glycosidic bonds (Scheme 1.11). Cellulose forms crystalline, insoluble micro fibrils in plant cell walls which are recalcitrant to enzymatic hydrolysis [35].

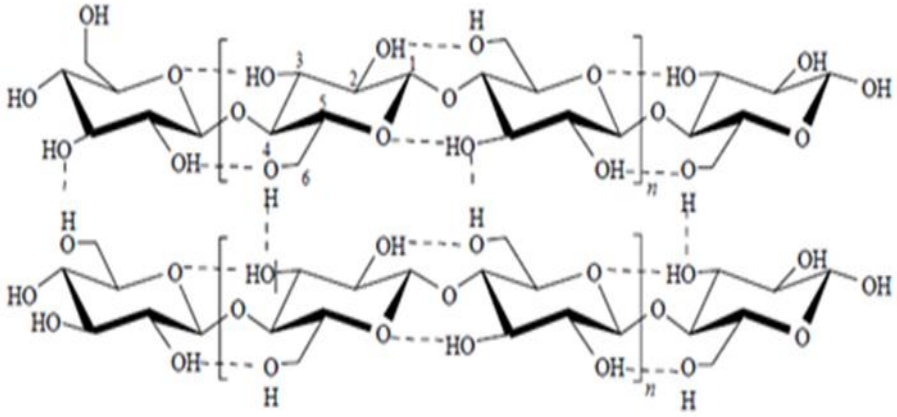

Scheme 1.11: The linkage of 1,4-β-glycosidic bonds and hydrogen bonding in cellulose.

The existence of the hierarchic networks of intra- and inter-molecular hydrogen bonds results in cellulose having stronger chemical recalcitrance in water and common organic solvents such as ethanol and acetone. Concentrated acid solutions, concentrated aqueous solutions of zinc chloride, ammoniacal copper hydroxide, and ionic liquids are exceptions, however. Cellulose exists in several crystal polymorphs, differing in unit cell dimensions and possibly in chain polarity [38, 39]. The natural cellulose (I) has two different structures, Iα and Iβ. Cellulose produced by bacteria and algae is rich in Iα while cellulose from higher plants consists mainly of Iβ. Besides cellulose I, cellulose II is another important crystalline form of cellulose. The process of the transformation of cellulose I to cellulose II is generally considered to be irreversible suggesting that cellulose II is more stable than cellulose I [40].

1.6.2 Hydrolysis of cellulose

Hydrolysis of cellulose is a hydrolytic cleavage of the β-1,4-glycosidic bonds between the glucose units in cellulose fibers is of

fundamental interest and plays an essential role in cellulose processing. As this degradation step paves the way for other catalytic transformations. Furthermore, whereas cellulose is inert to water under mild conditions it can hydrolyze at elevated temperatures for cellulose conversion have been carried out including hydrolysis with solid acid catalysts and hydrogenation or hydrogenolysis with supported metal catalysts. Therefore, it is imperative to first highlight the area of cellulose hydrolysis [41].

Hydrolysis of cellulose to fermentable sugars is virtually an essential step in any practical cellulosic biofuel production via a biological route. Furthermore, more chemical processes are seen to convert mono saccharides into fuels and value-added chemicals. Two methods including acid hydrolysis and enzymatic hydrolysis are currently known for biomass hydrolysis. To make cellulosic materials more susceptible to hydrolysis, a pretreatment process is needed to reduce the crystallinity and increase the porosity. Traditional pretreatment technologies using oxidants, organic solvents, lime, or mineral acids, remain imperfect in terms of process greenness and environmental friendliness. Therefore, the development of advanced pretreatment technologies is one of the main issues in bio-refinery. The inherent of dissolution of cellulose in ionic liquids provided a new pretreatment technology and an inert homogeneous platform for the hydrolysis of cellulose [42].

Dilute sulfuric acid based process for the hydrolysis of cellulose to glucose was first industrialized during first world war because of scarcity of fuels. In this process, glucose is formed via cellulose-acid complex with swollen cellulose. However, now handful of industries run this process due to difficulty in inhibiting further reactions of glucose,

corrosion hazards, handling of dangerous acids and generation of large amount of neutralization waste[43].

Another way to convert cellulose is based on applying high temperature, thermochemical treatment. The process is divided into two categories: gasification and pyrolysis. In the former process, cellulose is decomposed in the presence of small amount of oxygen to give syngas ($CO+H_2$) mixture. Conversely, in the latter process cellulose decomposition is accomplished in the absence of oxygen to yield a blend of products such as oils, tar and char. The major disadvantage of these processes is lack of selective formation of any compound [35].

The generation of fuels from cellulosic biomass is a promising way in renewable energy research [44]. The major challenges are linked to reducing the costs associated with production, harvest, transportation, and up-front processing in order to make cellulosic ethanol competitive with grain-based fuel ethanol and gasoline. The major processing challenges are linked to the biology and chemistry of the processing steps. Advances in biotechnology and engineering will likely make significant impacts toward achieving the goals of improving efficiency and yields in processing plant material to ethanol [45]. Table 1.3 shows the hydrolysis of cellulose over some different catalysts.

Table 1-3: The hydrolysis of cellulose over different catalysts.

Catalyst	Method	Time h.	Temp. ^{o}C	Solvent	Glucose yield %	Ref
Ru/AC-SO_3H	Acidic hydrolysis	24	165	Water	71.3	[43]
Pt/Al_2O_3	Supported metal	24	150	Water	31	[35]
Glucose oxidase	Enzyme hydrolysis	24	37	Water	32	[46]
H_2SO_4	Acidic hydrolysis	12	40	H_2SO_4	80	[47]
1-ethyl-3-methylimidazolium chloride	Ionic liquid hydrolysis	1.5	25	Water	36	[48]
H_2SO_4	Acidic hydrolysis	1	135	Water	67	[49]
1- butyl-3-methylimidazolium chloride	Ionic liquid hydrolysis	9	100	Water	43	[50]
Au/SiO_2	Supported metal	3	145	Water	67	[51]
Tungstated alumina: AlW	Solid acid	24	190	Water	47	[52]
Tungstated zirconia: ZrW	Solid acid	24	190	Water	42	[52]

C_{16} H_2PW	Heterogeneous Poly acids	8	170	Water	76	[53]
$H_3PW_{12}O_{40}$	Heteropoly acid	8	170	Water	80	[54]
H_3PO_4	Acidic hydrolysis	6	120	Water	65	[55]
$Ru/NbOPO_4$	Supported metal	24	170	Water	64	[56]
sulphated ZrO_2	Solid acid	7	190	Water	49	[57]
SO_3H on biochar	Solid acid	2	120	water	85	[58]
H_3PO、	Activated acid	4	200	Water	78	[59]
Carbon-based solid acid	Heterogeneous acid	12	150	Water	40	[60]

1.7 The equipments used in this study

1.7.1 Nitrogen adsorption analysis

Adsorption occurs whenever a solid surface is exposed to a gas or liquid. Adsorption is of great technological importance thus, some adsorbents are used on a large scale as desiccants, catalysts or catalyst supports; others are used for the separation of gases, the purification of liquids, pollution control or for respiratory protection. In addition, adsorption phenomena play a vital role in many solid state reactions and biological mechanisms. Another reason for the widespread use of adsorption techniques is the importance now attached to the characterization of the surface properties [61].

Adsorption phenomenon first studied and explained by Langmuir (1930), since He put many assumptions to express this phenomenon, These assumptions were able to explain monolayer adsorption but did not explain multilayer adsorption until discovering the BET (1938) theory which can explain the higher layer adsorption[62]. BET based on the method of using Nitrogen and Mercury to assign adsorption isotherm and to calculation the properties of porosity and surface area of material.

Porosity refers to the pore space in a material. Internal surface of the material comprises the pores and cracks that are deeper than they are wide. An open pore is a cavity or channel that communicates with the surface of the particle. Closed pores are inside the material. These open and closed pores are called intra-particular porosity of the material [63].
Pores are classified according to size into three categories; micro pores (pore diameter smaller than 2 nm), meso pores (pore diameter 2 - 50 nm) and macro pores (pore diameter larger than 50 nm). With nitrogen gas adsorption, depending on the equipment used, pore diameter range of 3 - 300 nm, i.e. meso pores and macro pores, are determined. Low-pressure

mercury porosimetry determines micro pores (pore diameter 14 - 200 µm), and high-pressure porosimetrymesopores and macropores (pore diameter 3 nm - 14 µm), depending on the equipment [64].

Brunauer, Emmett and Teller (BET), most common method used to describe specific surface area,[65] the BET equation:

$$\frac{1}{W\left(\left(\frac{Po}{P}\right)-1\right)} = \frac{1}{Wm\,C} + \frac{C-1}{Wm\,C}\left(\frac{P}{Po}\right) \ldots\ldots\ldots\ldots\ldots\ 1$$

W= weight of gas adsorbed.

P/P_o =relative pressure.

Wm = weight of adsorb.ate as monolayer

C = BET constant.

1.7.2 X-ray diffraction (XRD)

Diffraction effects are observed when electromagnetic radiation impinges on periodic structures with geometrical variations on the length scale of the wavelength of the radiation. The interatomic distances in crystals and molecules amount to 0.15–0.4 nm which correspond in the electromagnetic spectrum with the wavelength of X-rays having photon energies between 3 and 8 keV. Accordingly, phenomena like constructive and destructive interference should become observable when crystalline and molecular structures are exposed to X-rays [66].

X-ray interference are derived the interactions between X-rays and matter have to be considered. There are three different types of interaction in the relevant energy range. In the first, electrons may be liberated from their bound atomic states in the process of photoionization. Since energy and momentum are transferred from the incoming radiation to the excited electron, photoionization falls into the group of inelastic

scattering processes. In addition, there exists a second kind of inelastic scattering that the incoming x-ray beams may undergo, which is termed Compton scattering. Also in this process energy is transferred to an electron, which proce EDX analysis, however, without releasing the electron from the atom. Finally, x-rays may be scattered elastically by electrons, which is named Thomson scattering. In this latter process the electron oscillates like a Hertz dipole at the frequency of the incoming beam and becomes a source of dipole radiation [67].

The wavelength λ of x-rays is conserved for Thomson scattering in contrast to the two inelastic scattering processes mentioned above. It is the Thomson component in the scattering of x-rays that is made use of in structural investigations by x-ray diffraction [68].

XRD technique can deduce the nature of inspected sample; whether amorphous or crystalline structure as well as structural information can therefore be deduced from the knowledge of scattering intensity and angle For example, approximated as the repeating distance in the porous materials, the sum of a pore diameter and a pore wall thickness can be estimated base on the d spacing calculated from the Bragg equation [29].

$$n\lambda = 2d\sin\theta \quad \ldots\ldots\ldots\ldots\ldots 2$$

Where n is an integer, λ is the wavelength, d is the separation between planes and θ is the diffraction angle.

1.7.3 Thermal analysis

The term thermal analysis (TA) is frequently used to describe analytical experimental techniques which investigate the behavior of a sample as a function of temperature. The advantages of TA over other analytical methods can be summarized as follows: (i) the sample can be studied over a wide temperature range using various temperature

programs; (ii) almost any physical form of sample (solid, liquid or gel) can be accommodated using a variety of sample vessels or attachments; (iii) a small amount of sample (0.1 μg-10 mg) is required; (iv) the atmosphere in the vicinity of the sample can be standardized; (v) the time required to complete an experiment ranges from several minutes to several hours; and (vi) TA instruments are reasonably priced. In polymer science, preliminary investigation of the sample transition temperatures and decomposition characteristics is routinely performed using TA before spectroscopic analysis is begun [69].

Thermogravimetric analysis (TGA) is an analytical technique used to determine a material's thermal stability and its fraction of volatile components by monitoring the weight change that occurs as a specimen is heated. The measurement is normally carried out in air or in an inert atmosphere, such as Helium or Argon, and the weight is recorded as a function of increasing temperature. Sometimes, the measurement is performed in a lean oxygen atmosphere (1 to 5% O_2 in N_2 or He) to slow down oxidation. In addition to weight changes, some instruments also record the temperature difference between the specimen and one or more reference pans (differential thermal analysis, or DTA) or the heat flow into the specimen pan compared to that of the reference pan (differential scanning calorimetry, or DSC). The latter can be used to monitor the energy released or absorbed via chemical reactions during the heating process [70].

In DTA technique is measure the difference in temperature between a sample and a reference material (reference sample is made by placing a similar quantity of inert material (such as Al_2O_3)) when they are subjected to a controlled temperature program, both sample and reference material must be heated under carefully controlled conditions. If the sample undergoes a physical change or a chemical reaction, its

temperature will change while the temperature of the reference material remains the same. That is because physical changes in a material such as phase changes and chemical reactions usually involve changes in enthalpy, the heat content of the material. There is a constant temperature difference ΔT between sample and reference since they have different heat capacities. But when the sample undergoes an thermic change ΔT becomes different[71].

1.7.4 Scanning electron microscopy – energy dispersive X-ray (SEM-EDX)

The operation of the SEM consists of applying a voltage between a conductive sample and filament, resulting in electron emission from the filament to the sample. This occurs in a vacuum environment ranging from 10-4 to 10-10Torr. The electrons are guided to the sample by a series of electromagnetic lenses in the electron column [72].

The resolution and depth of field of the image are determined by the beam current and the final spot size, which are adjusted with one or more condenser lenses and the final, probe-forming objective lenses. The lenses are also used to shape the beam to minimize the effects of spherical aberration, chromatic aberration, diffraction, and astigmatism. The electrons interact with the sample within a few nanometers to several microns of the surface, depending on beam parameters and sample type. Electrons are emitted from the sample primarily as either backscattered electrons or secondary electrons. Secondary electrons are the most common chemical shift used for investigations of surface morphology. They are produced as a result of interactions between the beam electrons and weakly bound electrons in the conduction band of the sample. Some energy from the beam electrons is transferred to the conduction band electrons in the sample, providing enough energy for their escape from the sample surface as secondary electrons. Secondary electrons are low

energy electrons (<50eV), so only those formed within the first few nanometers of the sample surface have enough energy to escape and be detected. High energy beam electrons which are scattered back out of the sample (backscattered electrons) can also form secondary electrons when they leave the surface. Since these electrons travel farther into the sample than the secondary electrons, they can emerge from the sample at a much larger distance away from the impact of the incident beam which makes their spatial distribution larger. Once these electrons escape from the sample surface, they are typically detected by an Everhart-Thornley scintillator photo multiplier detector. The SEM image formed is the result of the intensity of the secondary electron emission from the sample at each x,y data point during the rastering of the electron beam across the surface [73, 74, 75].

EDX analysis depended on the **Moseley's Law** (the energy of the characteristic radiation within a given series of lines varies monotonically with atomic number). Moseley's Law can be represented in the following equation:

$$\mathbf{E = C_1 (Z- C_2)^2} \quad \text{..... 3}$$

where:

E = energy of the emission line for a given X-ray series (e.g. Kα)

Z = atomic number of the emitter

C_1 and C_2 are constants

Moseley's Law is the basis for elemental analysis with EDX analysis. If the energy of a given K, L or M line is measured, then the atomic number of the element producing that line can be determined. The K, L and M series X-rays increase in energy with increasing atomic number [76].

1.8 Objectives of the present investigation

Cellulose is an important raw material. Due to the unfavorable conditions of the using homogeneous methods in the hydrolysis of cellulose, therefore this study is to improve on these conditions. The main objectives of this work are:

1. Modified of the silica extracted from RHA with two different Schiff bases.
2. Characterized of the catalysts by using various spectroscopic and microscopic techniques such as Powder X–ray, FT-IR, Scanning electron microscopy SEM / EDX, Thermal analysis and N_2-adsorption-desorption.
3. Studied the hydrolysis of cellulose to mono saccharide over prepared heterogeneous catalysts.
4. Optimized of the catalytic activity of the catalysts.

CHAPTER TWO

Experimental part

2.1 Instruments

Most of the analyses in this thesis were done outside of Iraq. The equipment's used in this thesis were listed in Table 2.1.

Table 2.1: The equipment's used in this thesis. All companies and places of the analysis were shown.

Technique	Type of apparatus	Place of measurement
Elemental analysis	EuroEA Elemental Analyzer**,** Turkey	University of Esfahan, Iran.
FT-IR	Shimadzu-8400s, Japan	Karbala University-Iraq
Nitrogen adsorption analyses	nova2000, quantachrome, USA	University of Tehran Iran.
^{1}H and ^{13}C NMR	Bruker (400MHz), United Kingdom	University of kashan-Iran
SEM-EDX analysis	Philips XL30 Netherlands	University of Tehran Iran.
Thermal analyses TGA/DTA	STA1500, Germany	University of Tehran Iran.

X-ray diffraction (XRD).	stoe, stidy-mp Germany	University of Kashan Iran

2.2 Materials

All chemicals are of AR grade, were used directly without further purification. The (RH) was collected from a rice mill in Najaf, Iraq. The chemicals used in this thesis were listed in Table 2.2.

Table 2.2: The suppler and purity of all used chemicals.

Item	Suppler	Purity %
2,4-dinitro phenyl hydrazine	BDH, England	99
3-chloropropyltriethoxysilane	Sigma, Germany	98
Acetone	Sigma, Germany	99
Benzene	Merck, Germany	98
Butanol	Fluka, Germany	98
Cellulose	BDH, England	98
Chloroform	Sigma, Germany	98
Cyclohexanol	Riedel-de haen, England	99
Cyclopentanon	Riedel-de haen,	99
Dimethylformamide	Riedel-de haen	99
Dimethylsulfoxide	GCC, England	98
Dioxin	Hi-media, India	98

Ethanol	GCC, England	100
Ethyl acetate	Hi-media, India	98
Lithiumchloride	BDH, England	
Methanol	GCC, England	98
Nitric acid	Systerm Spain	65
Phenyl hydrazine	BDH, England	98
Salicylaldehyde	Hi-media, India	98
Sodium hydroxide	Systerm, Spain	99
Toluene	GCC, England	98
Triethylamine	Merck, Germany	98

2.3 The preparation

2.3.1 Preparation RHA

The preparation of RHA was done according to the method reported [77]. In general the rice husk 30 g was first washed with distilled water to remove adhering materials and dried at about 25 ^{o}C. It was leached with 750 mL of 1.0 M nitric acid at room temperature for about 24 h. The digested husk was then washed with distilled water and dried in a drying oven at 110 °C for 24 h. The amorphous white silica (RHA) was obtained by burning this rice husk at 800 °C in a muffle furnace for 6 h [78] .The white ash was labeled RHA.

2.3.2 Functionalization of RHA with CPTES

The functionalization of RHA with CPTES was done according to the method reported [23]. In general, about 3.0 g of the silica (obtained from RHA) was stirred in 200 mL of 1.0 M NaOH in a plastic container at temperature 60 ^{o}C for about 30 min. The sodium silicate formed was filtered to remove undissolved particles. A 6.0 mL of CPTES was added to this sodium silicate solution. The solution was then titrated slowly (1.0 mLmin^{-1}) with 3.0 M nitric acid with constant stirring. The change in pH was monitored by using a pH meter. A white gel started to form when the pH decreased to less than 11.0. The titration was continued until the pH of the solution reached 3.0. The gel obtained was aged for 2 days in a covered plastic container.

After 2 days of aging the gel was separated by centrifuge at 4000 rpm for 8 min The separation process was repeated 6 times with copious amount of distilled water. The final washing was done with acetone. The sample was then dried at room temperature. Finally, it was ground to produce a fine powder. This sample was labeled as RHACCl [79].

2.3.3 Preparation of 2-((2-phenylhydrazono)methyl)phenol PHMP

A 0.02 mol (2.4 mL) of salicylaldehyde was stirred with 10 mL of ethanol for about 20 min. and then a 0.02 mol (2 mL) of ethanolic solution of phenyl hydrazine was added gradually to solution .The mixture was refluxed at 60 ^{o}C for 3 h. The reaction was monitoring by TLC using ethyl acetate as an eluent which shows one spot of the

product. The yellow product was dried in an oven at 50 ^{o}C for 5 h. The product is labeled as PHMP. The yield was 78.0%, mp: 145.8 ^{o}C [80].

2.3.4 Preparation of 2-((2-(2,4-dinitrophenyl)hydrazono) methyl)phenol (DNPHMP)

A 0.01mol (1.98 g) of 2,4-dinitrophenylhydrazine was dissolved in 15mL of absolute ethanol and was added gradually to ethanolic solution of salicylaldehyde 0.01mol (1.06 mL). The mixture was refluxed at 60 ^{o}C for 4 h. The reaction was monitoring by TLC using a mixture of chloroform : benzene (2:1) as an eluent. A red precipitate was separated out and washed with acetone. The product was dried in an oven 50 ^{o}C for 5 h . The product is labeled as DNPHMP. The yield was 80.0 %, mp: 259.3 ^{o}C [81].

2.3.5 Synthesis of RHPHMP

RHPHMP was prepared by adding Schiff base PHMP 0.01mol (2.0 g) to the RHACCl (1.0 g) in a mixture of dry toluene (30 mL) and triethylamine (Et_3N) 0.01mol (2.0 mL), [Et_3N was used to remove the produced HCl as $HEt_3N^+Cl^-$] . The reaction mixture was refluxed at 110 °C in an oil bath for 44 h. The solid was filtered, and washed with 75 mL with three deferent solvents benzene, ethylacetate and ethanol. The solid was dried at 110 °C for 24 h. Finally, it was grind to produce a fine powder which was labeled as RHPHMP. About 0.9 g from RHPHMP was collected.

2.3.6 Synthesis of RHDNPH

RHDNPH was prepared by adding Schiff base (DNPHMP) 0.01mol (2.0 g) to a mixture of RHACCl (1.0 g) in dry toluene (30 mL) and Et_3N 0.01mol (2.0 mL), [Et_3N was used to remove the produced HCl as $HEt_3N^+Cl^-$].The reaction mixture was refluxed at 110 °C in an oil bath for 44 h. The solid was filtered, washed with (50 mL) methanol and (50 mL) DMSO and then dried at 100 °C for 24 h. Finally, it was grind to produce a fine powder which was labeled as RHDNPH. About 0.75 g from RHDNPH was collected.

2.4 Catalytic reactions

2.4.1 Cellulose hydrolysis

The cellulose hydrolysis was carried out in a liquid-phase reaction in a 250 mL round bottom flask equipped with magnetic stirrer and water condenser. 20 mL of DMF, 0.2 g of LiCl and cellulose (0.18 g) were separately transferred to the round bottom flask containing of the catalyst (pre-dried at 110 °C for 24 h and cooled in a desiccator to minimize moisture content). The reaction temperature fixed at 140 °C. The reaction mixture was refluxed for 14 h.

A 0.5 mL portion of the clear hydrolyte solution from the reaction mixture was transferred into a vial and 2.0 mL of NaOH (2M) and 2.0 mL of DNS reagent were added and the mixture was incubated in a water bath maintained at 90 °C for 5 min. The reagent blank sample was prepared with 2.50 mL of deionized water and 0.50 mL of DNS reagent and heated similar to the samples. Then the absorbance was measured at

540 nm, against the reagent blank (the color of solution was yellow at start and would be red with increasing of cellulose hydrolysis) , and glucose concentrations in solutions were calculated by employing a standard curve prepared using glucose.

2.4.2 The optimization of the catalyst mass

The catalytic activity with different mass of catalyst (50, 100, 150, and 200 mg) was studied by using the same procedure as in section 2.4.1. The reaction was carried out at 140 °C for 14 h for RHPHMP and for 11 h. for RHDNPH as hydrolysis time.

2.4.3 The optimization of reaction temperature

The catalytic activity at different temperatures (120, 130 and 140 °C) were studied by following same procedure as in section 2.4.1. The reaction was carried out using 200 mg of the catalyst RHPHMP for 14 h. and using 150 mg of the catalyst RHDNPH for 11 h.

2.4.4 The solvent effect

The catalytic activity with different solvents (cyclopentanon, n-butanol and cyclohexanol) was studied by using the same procedure as in section 2.4.1. The reaction was carried out at 140 °C, 200 mg for 14 h as hydrolysis time of the catalyst RHPHMP, and was carried out at 140 °C, 150 mg for 11 h as hydrolysis time of the catalyst RHDNPH.

2.4.5 The reusability of the catalysts

Reusability experiment was conducted by running the hydrolysis successively with the same catalyst under the same hydrolysis condition.

The hydrolysis was first run with the fresh catalyst to complete conversion and then the catalyst was filtered and washed with hot mixture of DMF and LiCl and dried at 110 °C. After regeneration, the catalysts were reused under the optimized reaction conditions.

2.4.6 Hydrolysis procedure using homogenous catalysts

The hydrolysis of cellulose using homogenous catalyst was studied with PHMP and DNPHMP. Typically, a 150 mL capacity three necked round–bottom flask, equipped with a magnetic stirrer and water condenser was used. 15 mL of DMF was added to into the round bottom flask containing 0.18 g of cellulose, 0.5 g of lithium chloride and 0.001mol [0.25 g] from PHMP or 0.001mol [0.31 g] from DNPHMP. The mixture was refluxed at 140 ^{o}C and the glucose was monitoring according to the general procedure in section 2.4.1.

2.4.7 Hydrolysis procedure using RHA catalysts

The hydrolysis of cellulose by using RHA catalyst was studied by following the procedure as in section 2.4.1. The hydrolysis was carried out at 140 °C for 14 h as hydrolysis time using 200 mg of RHA.

2.4.8 Hydrolysis procedure without catalysts

The hydrolysis of cellulose without using any catalyst was studied by following the procedure as in section 2.4.1. The hydrolysis was carried out at 140 °C for 14 h as hydrolysis time using 20 mL of DMF and 0.2 g of LiCl. No catalyst was added at this step.

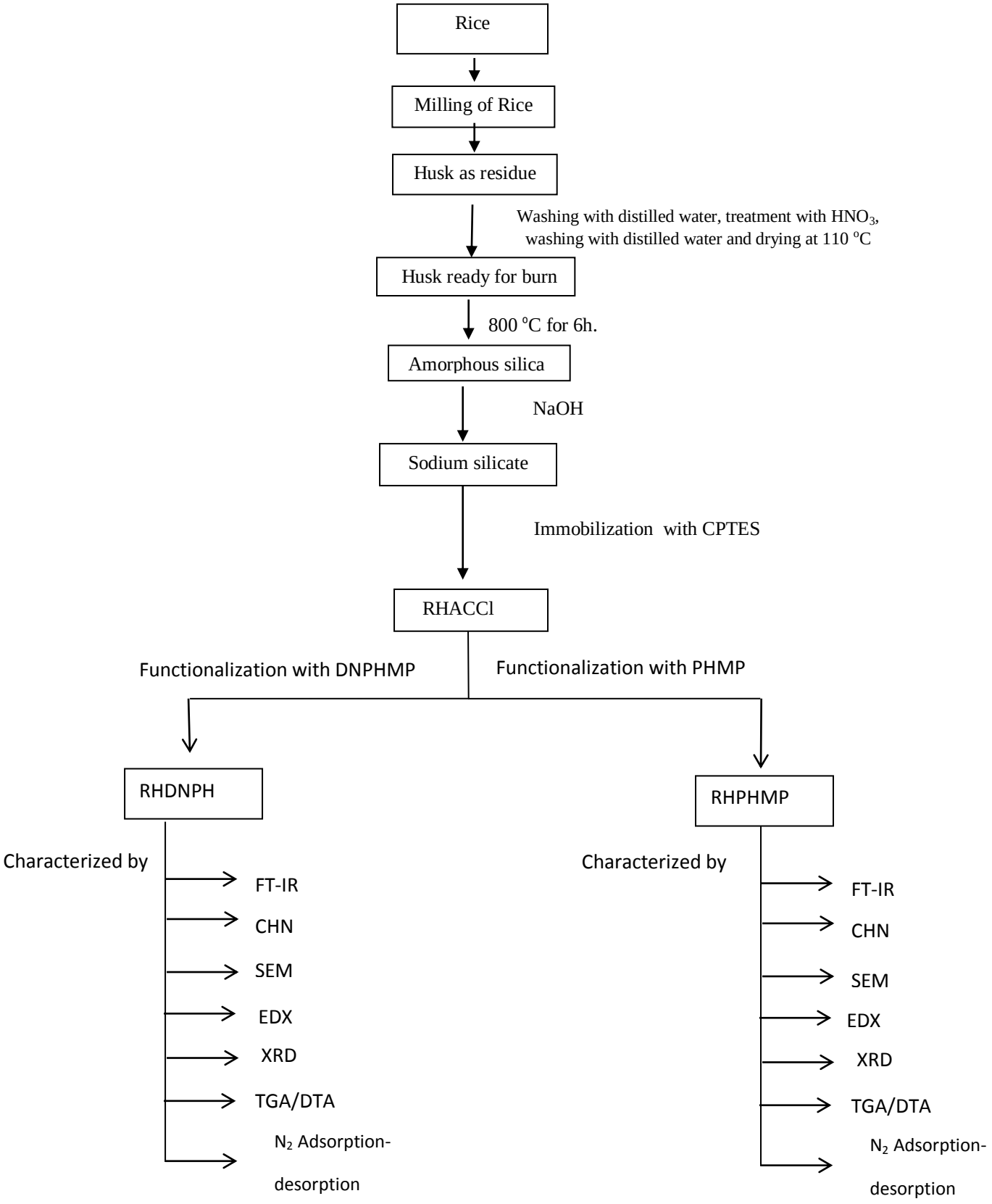

Scheme 2.1: Research progress during the catalysts preparation

CHAPTER THREE

The Characterization of RHPHMP

In this respect, 3-chloropropyltriethoxysailine (CPTES) was immobilized onto silica extracted from RHA within a short time (45 min). These hybrid organic–inorganic material with an organic end group, –CH_2–Cl as part of the solid network has important and unique properties and many application possibilities. The organic end group –CH_2–Cl was replaced with PHMP to form new catalyst labeled as RHPHMP. The following subtitles are described the characterization of the new catalyst RHPHMP.

3.1 Characterization of PHMP

This compound was prepared by the condensation reaction of amine group with the carbonyl group Scheme 3.1 shows the synthesis of PHMP.

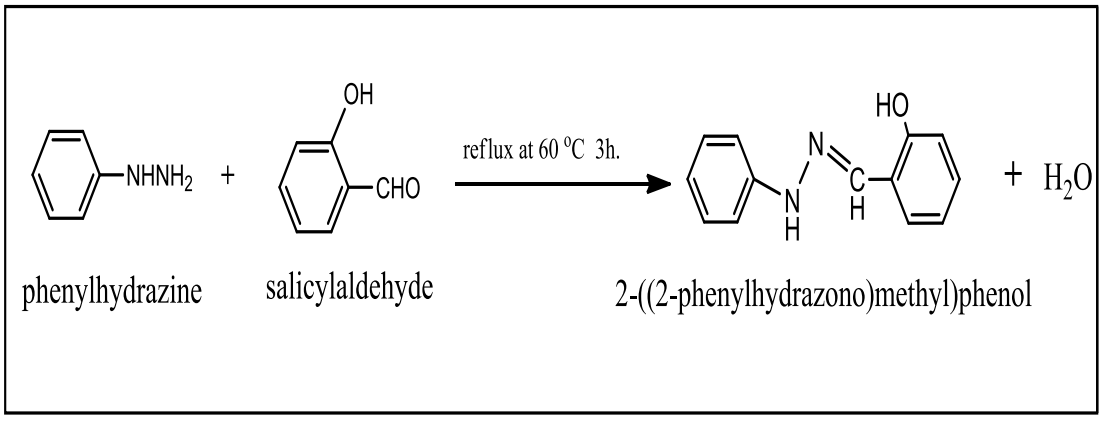

Scheme 3.1: The synthesis of PHMP.

3.1.1 Fourier transformed infrared spectroscopic analysis (FT-IR)

The FT-IR spectrum of PHMP is shown in Fig 3.1. The absorption band at 3450 cm^{-1} attributed to the stretching vibration of –OH group[82]. The band around 3290 cm^{-1} attributed to the stretching vibration of N-H[83]. The stretching vibration of C-H (aromatic) was observed around 3047 cm^{-1}[84]. The band at 1599 cm^{-1} attributed to stretching vibration of imine C=N bond[85].The band at 1535 cm^{-1} attributed to stretching vibration of aromatic C=C bond[86]. The presence of N-H and C=N bands clearly indicated to the successfully formation of PHMP.

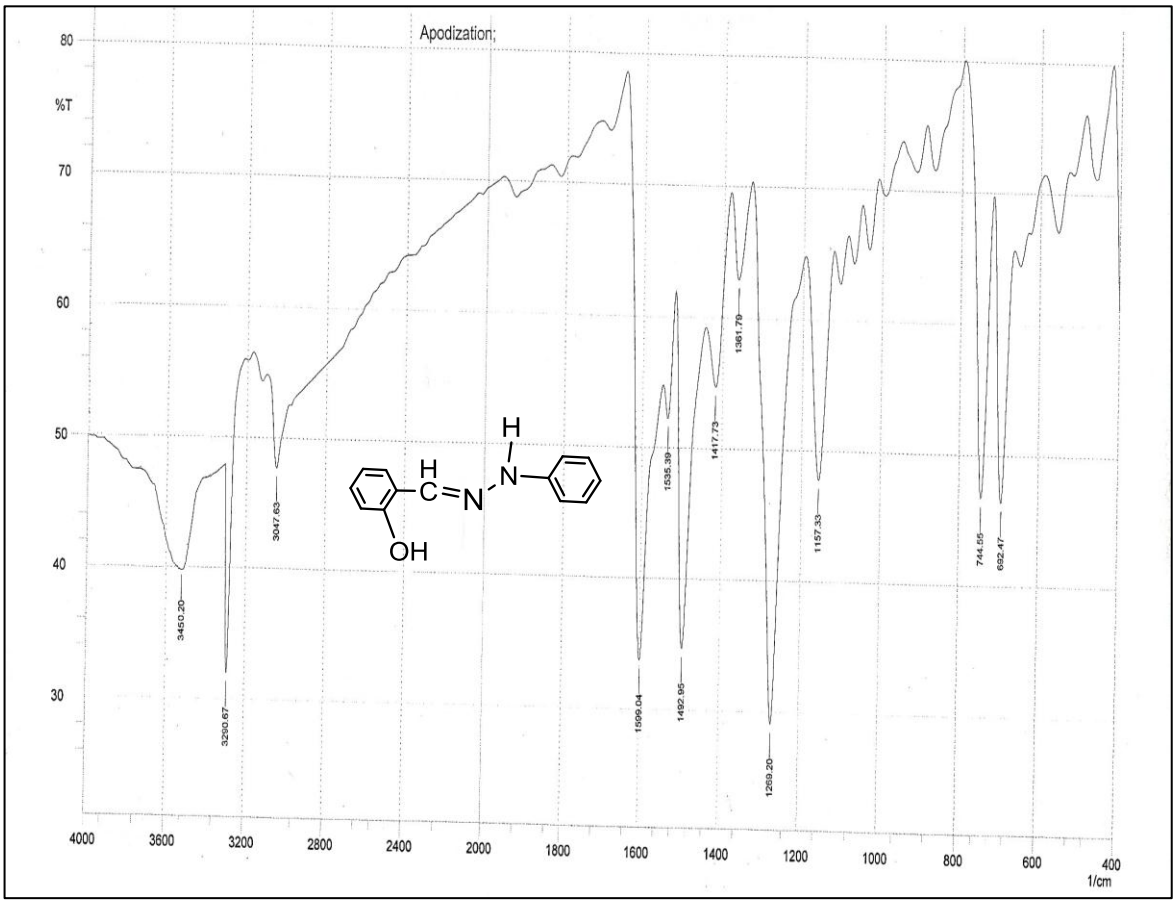

Fig 3.1: FT-IR spectrum for compound PHMP.

3.1.2 Proton nuclear magnetic resonance ^{1}HNMR of PHMP

The ^{1}HNMR spectrum of the PHMP is shown in Fig.3.2. The spectrum showed different chemical shifts at different positions. The chemical shift at 2.4 ppm attributed to the C-H proton of the solvent (DMSO) [85,86]. The chemical shift at 3.3 ppm with an integration value =1 is due to the hydrazonic N-H proton [88]. The chemical shifts between 6.6-7.5 ppm are assigned to the aromatic rings protons [89]. The chemical shift at 8.12 ppm is due to the benzylic protone C-H [90]. The doublet signal at 10.3-10.5 ppm is attributed to the hydroxyl proton (O-H) [91]. The ^{1}HNMR spectrum of the PHMP is clearly shown that the suggested structure is in agreement well with observed result.

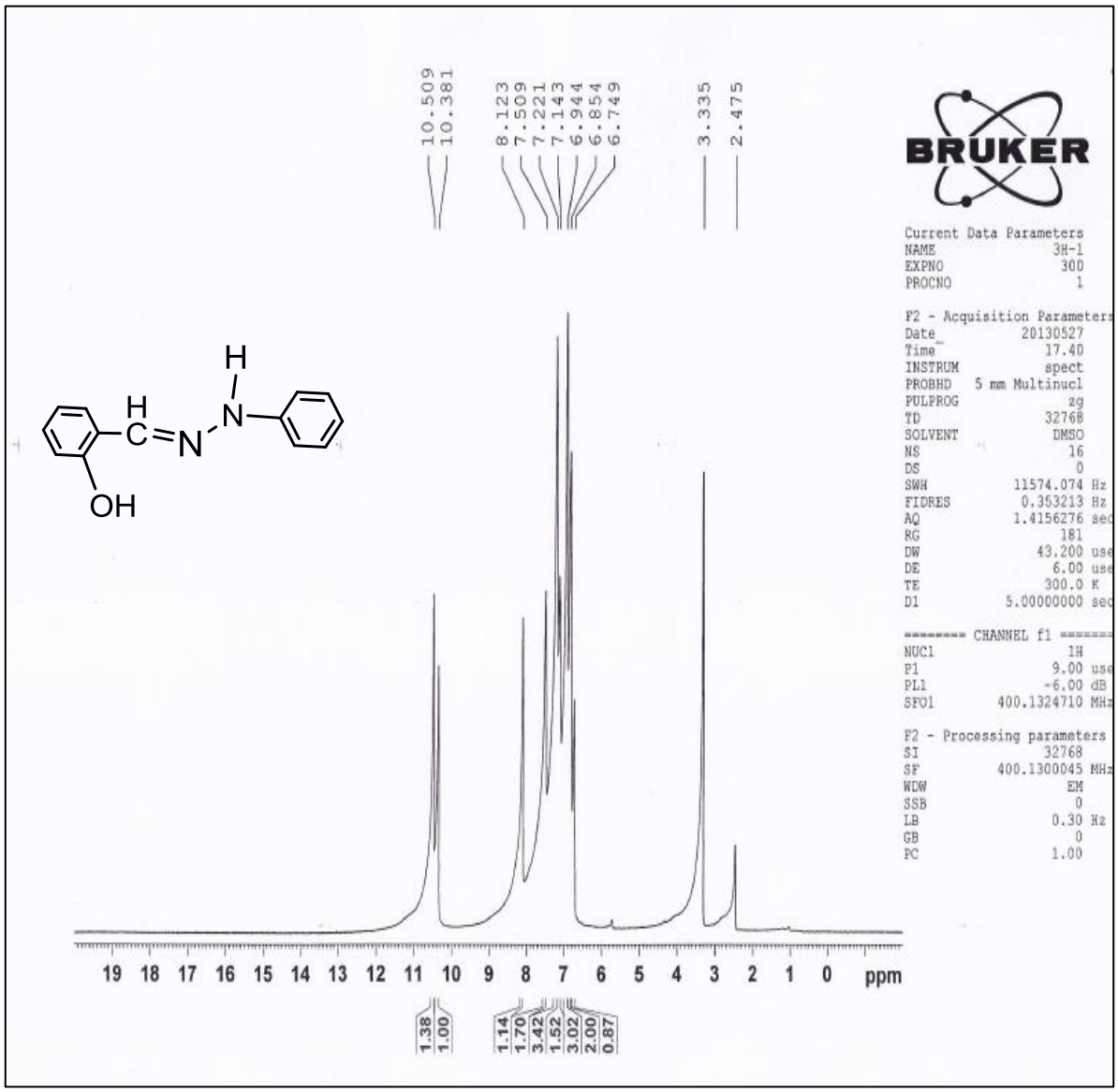

Fig 3.2: The ^{1}HNMR spectrum of PHMP in d^{6}-DMSO.

3.1.3 The ^{13}C Nuclear magnetic resonance of PHMP

Fig. 3.3 shows the ^{13}CNMR spectrum for PHMP (dissolved in DMSO – d^{6}). The analysis of this spectrum shows a chemical shift at δ =113.35 ppm attributed to the C9 (2×C9) aromatic carbon which is chemically equivalent. The chemical shifts at δ =11.52, 120.60, 120.99, 122.06, 139.0 ppm was assigned to the aromatic carbon C2, C4, C11, C5, C3 respectively. The chemical shift at δ =128.99 ppm attributed to the

C10 (2×C10) aromatic carbon which is chemically equivalent. The chemical shift at δ =130.85 ppm attributed to the C6 aromatic carbon which is directly bonded with imine group[92]. The chemical shift at δ =146.35 ppm attributed to the C8 aromatic carbon which is directly bonded with the secondary amine (N-H)[93]. This chemical shift is combined with the C7 carbon atom [94]. The C1 aromatic carbon which is directly bonded with the hydroxyl group –OH is observed at chemical shift δ =157.31 ppm [30]. The ^{13}CNMR spectrum of the PHMP is clearly shown that the experimental result is in agreement well with suggested structure**.**

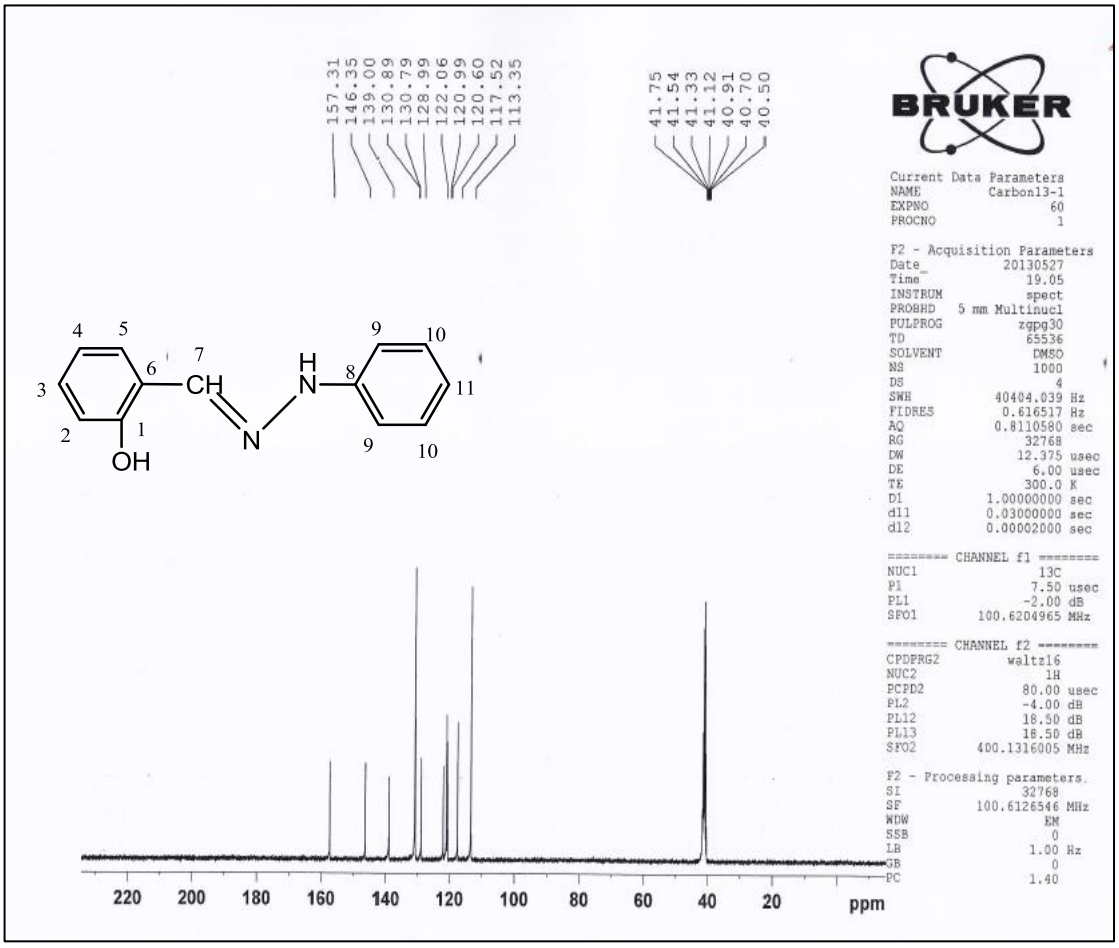

Fig 3.3: The ^{13}CNMR spectrum for compound PHMP.

3.2 The characterization of RHPHMP

The immobilization of PHMP onto RHACCl was carried out in a heterogeneous reaction. In the heterogeneous reaction one or more than one of the reactant could be in different state. In this reaction the dry toluene was used as solvent and the reaction mixture was reflux for 44 h, yielding the products as shown in Scheme 3.1.

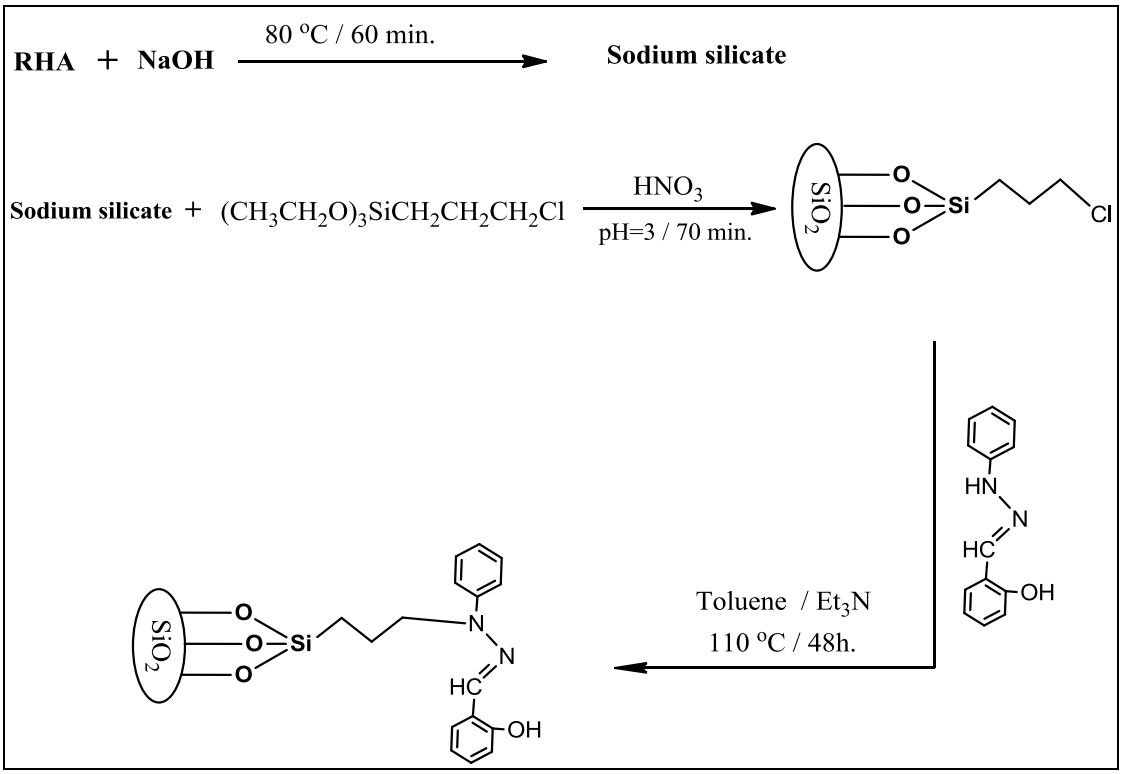

Scheme 3.2: The reaction sequence and the possible structures for RHPHMP. The reaction time and temperature were shown.

3.2.1 The FT-IR analysis of RHPHMP

The FT-IR spectrum of RHPHMP is shown in Fig. 3.4. The strong and broad band in the range 3319 cm^{-1} region corresponds to the hydroxyl

groups–OH in Si-O–H and free –OH phenolic group [82,95]. The stretching vibration of C–H aromatic ring was observed at 3047cm^{-1} [84]. The stretching vibration of C–H aliphatic was observed at 2939 cm^{-1} [96]. The band appear at 1625 cm^{-1} was due to the stretching vibration of C=N bond [85]. The band appear at 1600 cm^{-1} was due to the stretching vibration of C=C bond in aromatic rings [86]. The symmetrical and asymmetrical bending vibration of aliphatic CH_2 bonds was appeared at 1489 cm^{-1} [27]. The band appear at 1267.27 cm^{-1} was due to the stretching vibration of C-N bond. The doublet and strong band at 1066 cm^{-1}, 1143 cm^{-1} attributed to Si-O-Si stretching vibration [23]. The FT-IR clearly show the appearance of newly C–H aromatic and C=N bands onto the spectrum. The appearances of these bands [C-H aromatic, and C=N] and disappearance of N-H band indicate the presence of PHMP in RHACCl, and also confirms the successful replacement of chloride by the PHMP.

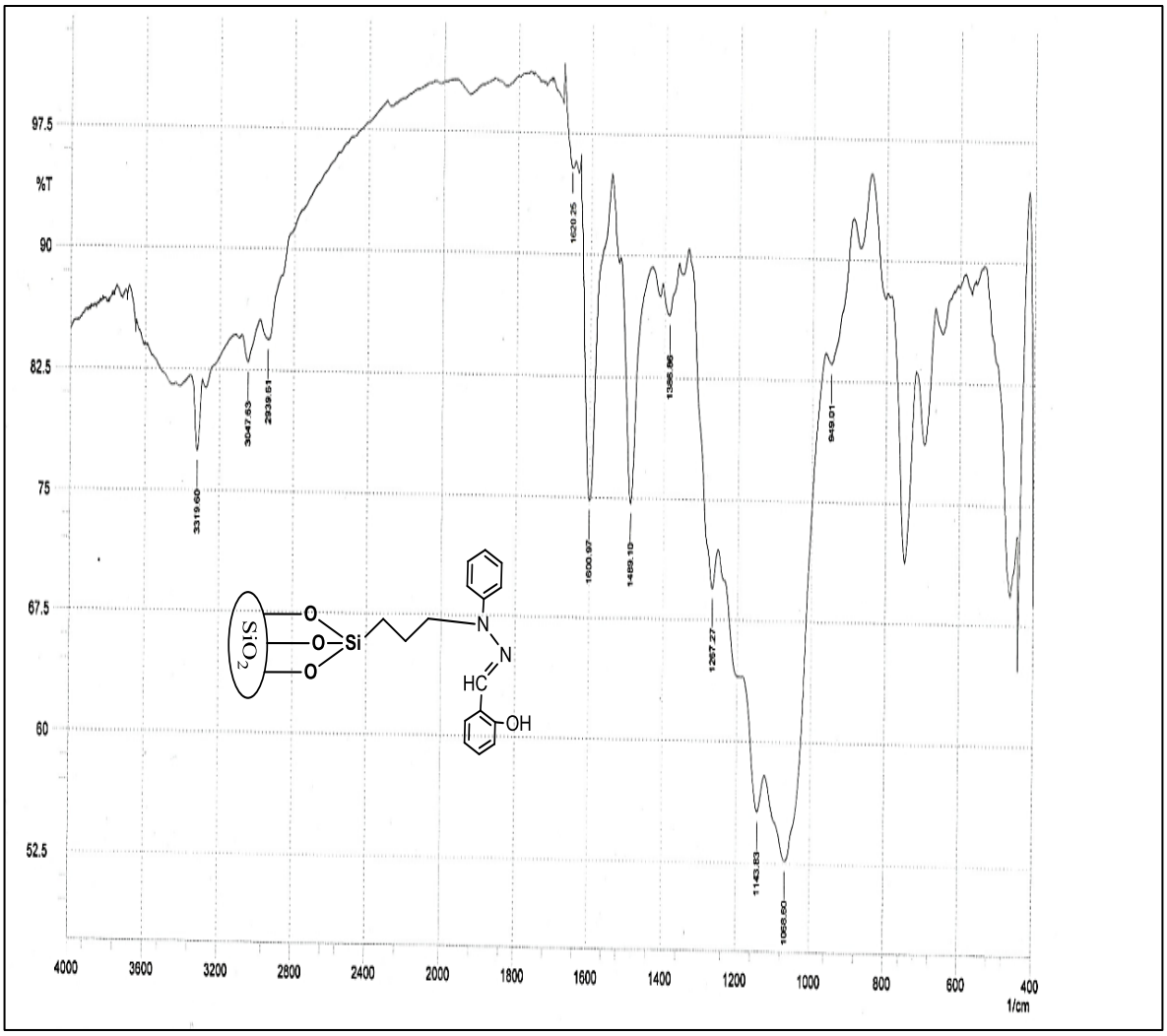

Fig 3.4: The FT-IR spectrum for RHPHMP compound.

3.2.2 Elemental analysis

Table 3.1 shows the elemental analyses of RHA, RHACCl and RHPHMP. The percentage of carbon and hydrogen in RHPHMP were higher than that of RHA and RHACCl [29]. The elemental analysis of RHPHMP shows the presence of nitrogen 2.88 %, while both RHA and

RHACCl do not show this element. These results clearly indicate that the PHMP was successfully immobilized onto RHACCl.

Table 3.1.Elemental analysis data for RHA, RHACCl and RHPHMP

Sample	Elemental analysis %		
	C	H	N
RHA	1.60	0.84	-
RHACCl	9.98	1.61	-
RHPHMP	18.74	3.37	2.88

3.2.3 The Nitrogen adsorption analysis

The Brunauer-Emmett-Teller (BET) gas adsorption method has become the most widely used standard procedure for the determination of the surface area of finely-divided and porous materials therefore; the specific surface area of the prepared compounds were calculated using the BET model. The pore diameter and pore size distribution of the materials were obtained from the adsorption isotherms, using the Barrett–Joyner–Halenda (BJH) method [29].

The nitrogen adsorption isotherm obtained for RHPHMP is shown in Fig. 3.5. Inset is the pore size distribution graph. The hysteresis loop observed in the range of $0.4 < P/Po < 0.8$ this is associated with capillary

condensation according to IUPAC classification. The isotherm shown is of type IV and exhibited an H2 hysteresis loop.

Materials that give rise to H2 hysteresis contain a more complex pore structure in which network effects (e.g., pore blocking/percolation) are important [97].

The specific surface area of RHPHMP was 137.68 m^2g^{-1}, this was decreased compared with the specific surface area of RHACCl (633 m^2g^{-1}), this reduce could be due to the reduction of the surface sites due to the immobilization of PHMP on it, causing the surface to be over crowded with the compound network on the surface and thus blocking the pores. The average pore diameter of RHPHMP was obtained 1.41 nm, which is in the microporous range, while for RHACCl it was reported to be 6.07 nm. It can be seen that RHPHMP had a narrower pore size compared to RHACCl. This was probably due to the presence of PHMP inside the silica matrix. RHPHMP showed a distinct pore size distributions between 2 and 4 nm. These fall within the mesooporous region. The results obtained by the nitrogen adsorption–desorption analysis for RHPHMP is summarized in Table 3.2.

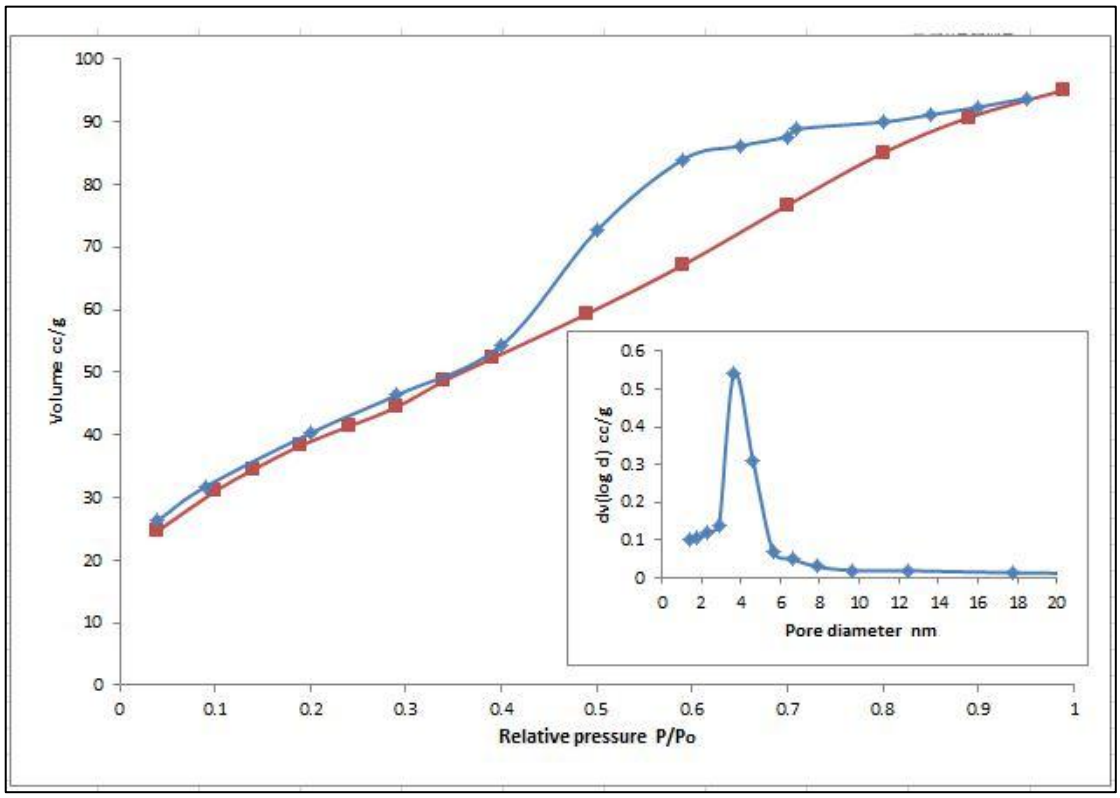

Fig 3.5: The nitrogen adsorption–desorption isotherms of RHPHMP. Inset the pore size distribution graph.

Table 3.2: The result of BET analysis for RHA [adapted from Ahmed and Adam [76]], RHACCl and RHPHMP.

Sample	Specific surface area (m^2g^{-1})	Average pore volume (cc g^{-1})	Average pore diameter(nm)
RHA	347	0.87	10.4
RHACCl	633	0.70	6.07
RHPHMP	137.68	0.16	1.41

3.2.4 X-Ray diffraction pattern (XRD)

The X-ray diffraction pattern spectrum of RHPHMP is shown in Fig.3.6. A broad band at 2θ angle of ca. 22.5° was observed which was typical for amorphous silica. A few sharp peaks in different pattern are observed this could be as a result of immobilizing PHMP onto silica which shows some crystallinity on the catalyst.

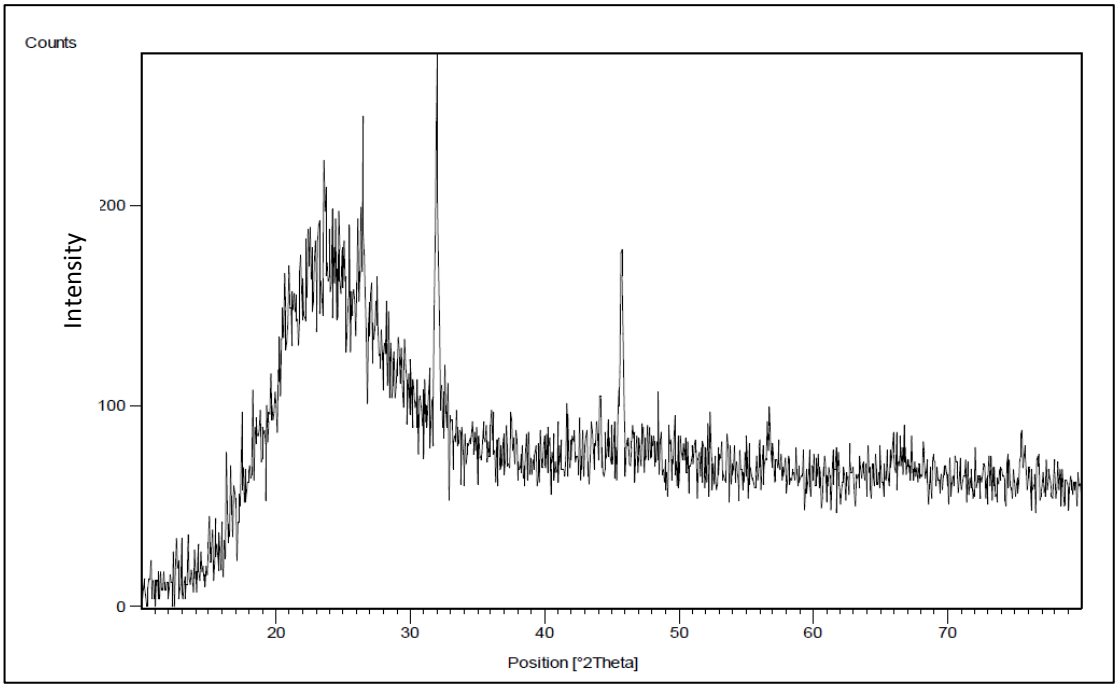

Fig 3.6: The X–ray diffraction pattern for RHPHMP.

3.2.5 Thermogravimetric analysis (TGA)/Differential thermal analysis (DTA)

Thermogravimetric analysis is commonly employed to determine the moisture content, the level of inorganic and organic components, the stability of organic groups, decomposition point, etc. Absorbed moisture content of materials gives an indication on the hydrophobicity of the materials studied. A derivative weight loss curve (DTA) can be used to

tell the point at which weight loss is most apparent. The TGA/DTA of RHA and RHACCl were published by Hello, [23]. The Fig. 3.7(a, and b) shows the TGA/DTA of both RHA and RHACCl. The TGA/DTA of RHA and RHACCl was given for the comparison with the prepared catalyst.

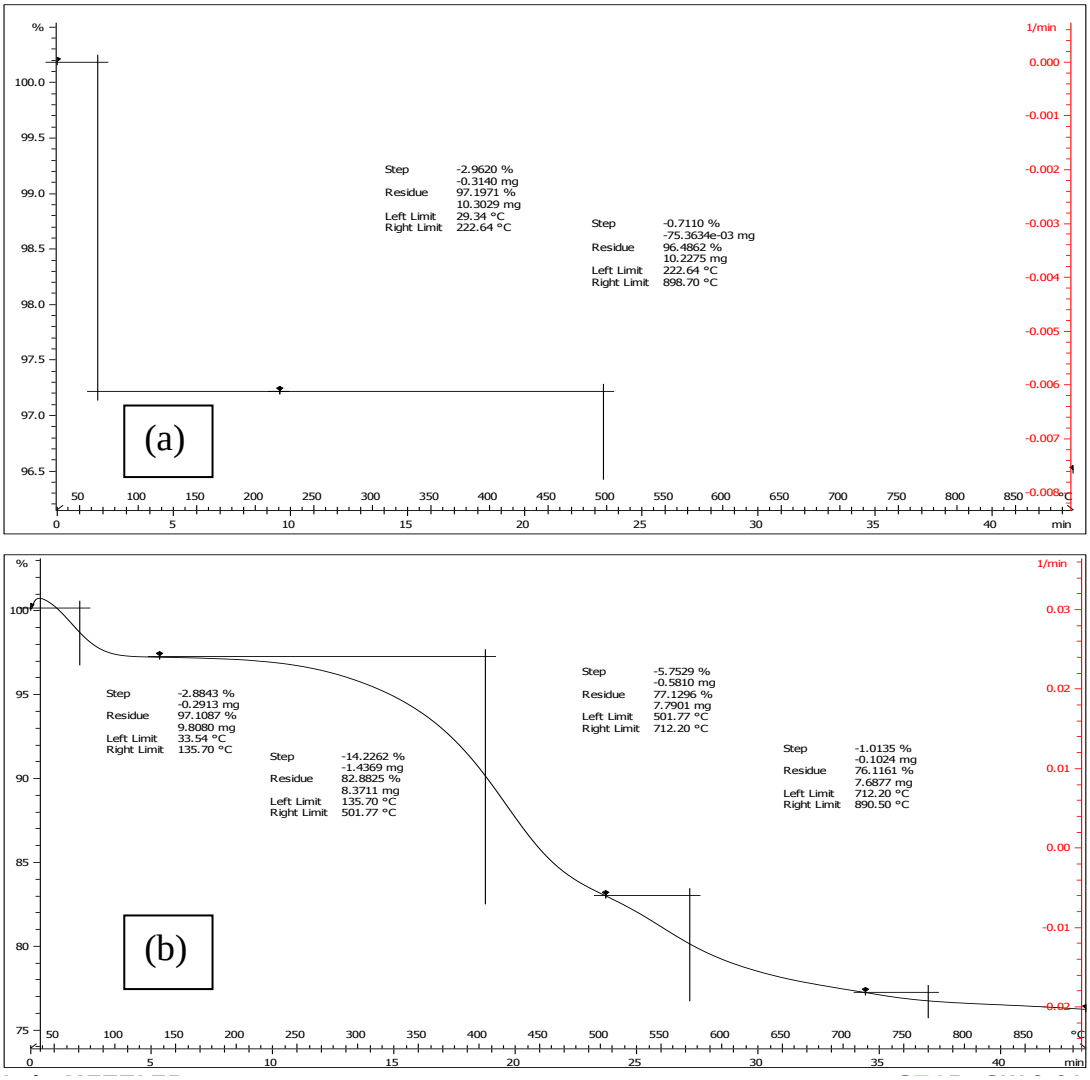

Fig. 3.7: Thermogravimetric analysis (TGA)/differential thermal analysis (DTA) of (a) RHA, (b) RHACCl (adapted from Hello [23])

Fig. 3.8 the TGA result for compound RHPHMP catalyst is shown in Fig 3.8. The graph shows three characteristic decomposition stages.

The first started at 30 to 208 ºC, due to the loss of adsorbed water (ca. 0.24 %), and the second mass loss (ca. 12.15 %) occurred between 215 – 380 ºC due to the decomposition of the PHMP and propyl groups anchored onto the silica. The continuous weight loss (ca. 15.55 %) between 380 – 700 ºC was due to decomposition of the remaining organic PHMP and propyl anchored on the silica surface and also due to the condensation of silanol groups at higher temperatures.

In the DTA curve Fig.3.8 it was observed four exothermic transformations the first is a peak which occurs between 40 °C and 208 °C, with a maximum at 100 °C and the second occurs between 215 °C and 380 °C, with a maximum at 290 °C, while the third occurs between 380 °C and 700 °C with a maximum at 480 °C. The first exothermic change due to the loss of adsorbed water, while the second, and third attribute to the arrangement of the structure of the polymer [98]. The TGA/DTA provided further evidence for the successful immobilisation of PHMP onto rice husk silica.

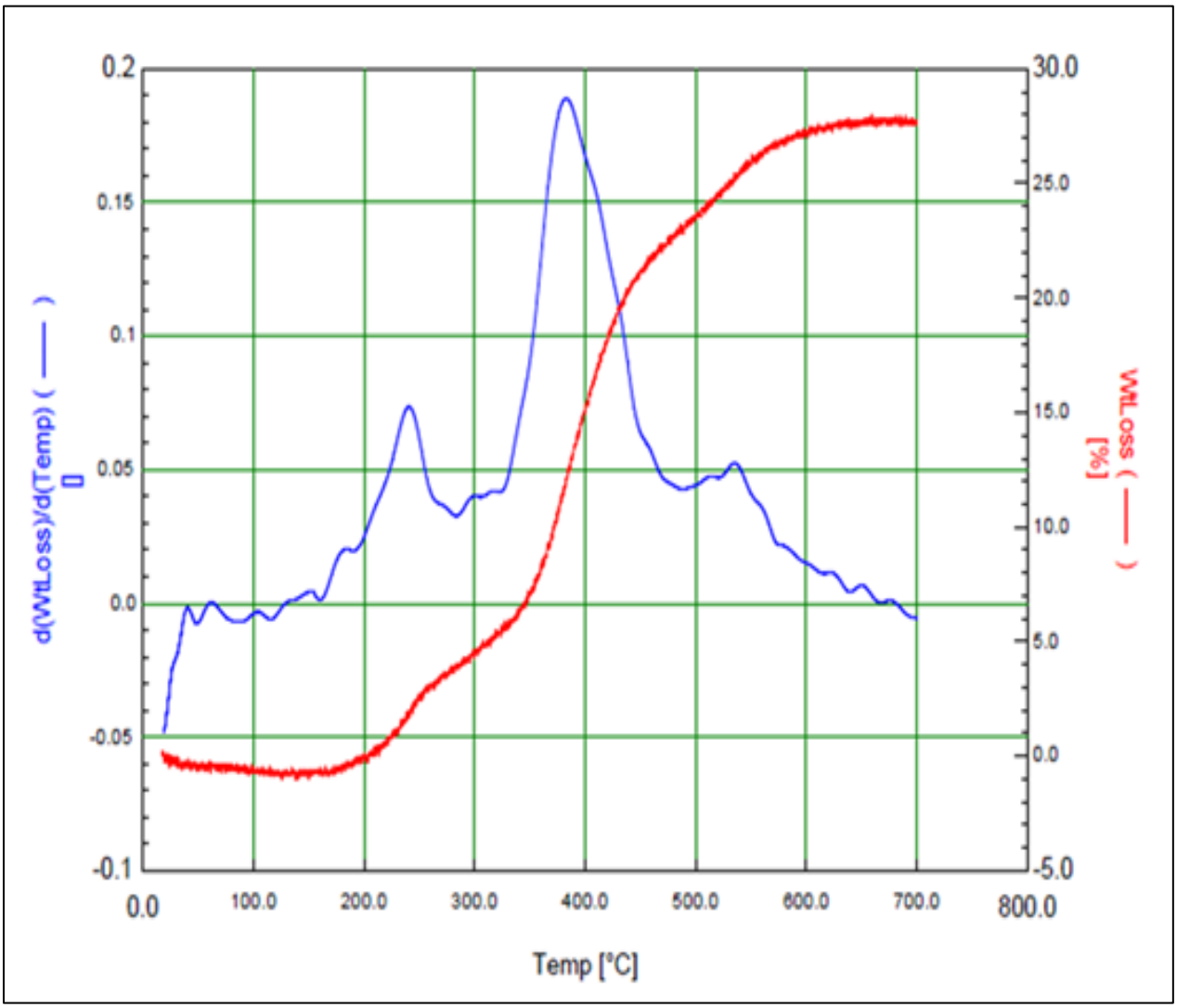

Fig. 3.8 : The TGA for compound of RHPHMP.

3.2.6 Scanning electron microscopy SEM

The scanning electron micrographs (SEM) for the RHPHMP are shown in Fig. 3.9. The SEM shows that the sample is granular. The granular particles of different sizes are arranged randomly on the surface.

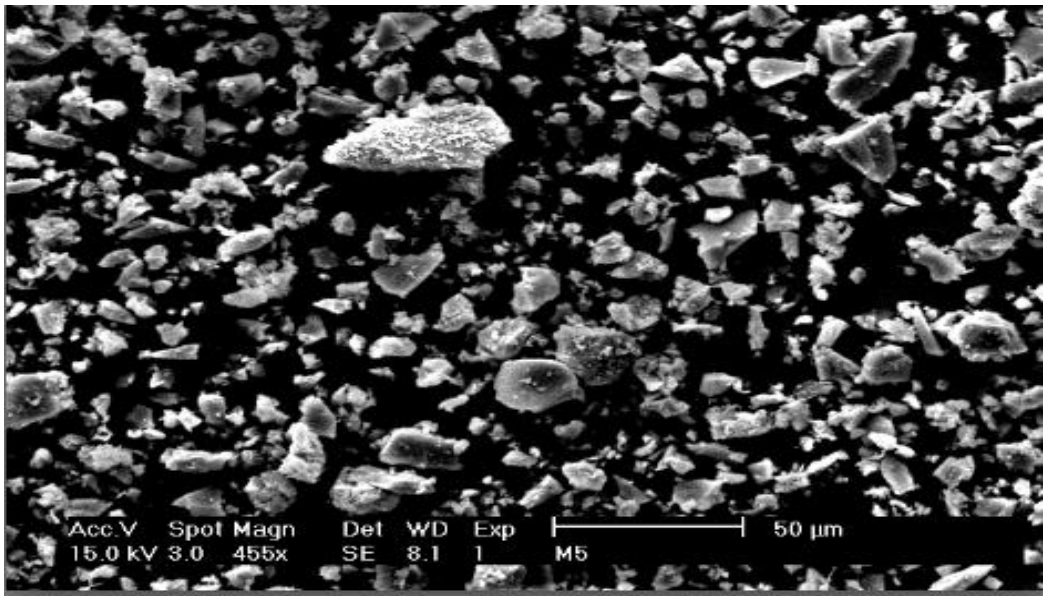

Fig 3.9: The SEM micrograph of RHPHMP.

3.2.7 Energy dispersive X-ray (EDX)

Fig. 3.10 show the EDX results of RHPHMP. The EDX result show the presence of C, Si, O, and N. These entire elements were found into RHACCl. The only nitrogen is not found in the formula of RHACCl. The presence of the nitrogen give very good indication for the successfully immobilization of PHMP onto RHACCl.

Table 3.3 shows the percentage of the elements components of RHPHMP. It was observed the presence of Cl in the analysis, this indicates that not all chlorine onto RHACCl was replaced by the PHMP. The reason behind this phenomenon was due to the fact that it follows a heterogeneous bath during the synthesis of RHPHMP. On the heterogeneous method one or more than one of the reaction components could not be soluble on the reaction solvent which may lead to the not all the functional group could replaced.

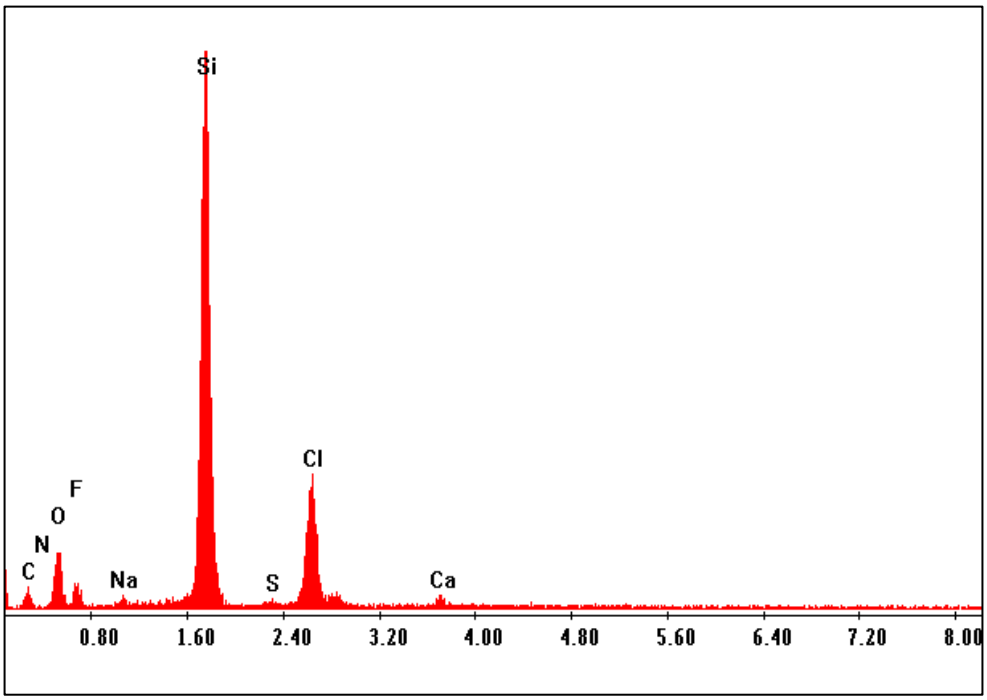

Fig 3.10: The EDX result of RHPHMP.

Table 3.3: The percentage of elements obtained from EDX analysis.

Elem.	Elements %
C	26.5
N	1.6
O	28.9
Si	25.7
Cl	6.7

CHAPTER FOUR

The Characterization of RHDNPH

The DNPHMP was immobilized onto silica via RHACCl to form new catalyst labeled as RHDNPH. The following subtitles are shown the characterization of DNPHMP and the new catalyst RHDNPH.

4.1 The characterization of DNPHMP

This compound was prepared by the condensation reaction of amine group with the carbonyl group. Scheme 4.1 shows the synthesis of DNPHMP.

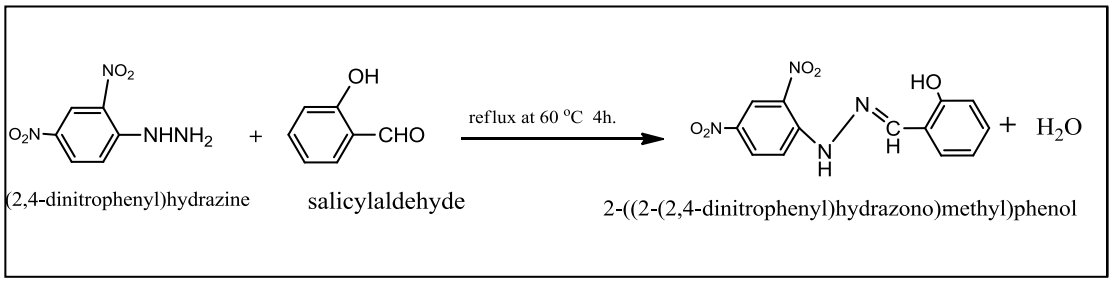

Scheme 4.1: The synthesis of DNPHMP.

4.1.1 FT-IR analysis of DNPHMP

Fig. 4.1 shows the FT-IR of DNPHMP. The bands at 3410 cm^{-1} was attributed to the stretching vibration of –OH group [82]. The stretching vibration of N-H group was shown at 3271 cm^{-1} [83]. The sharp peak at 3105 cm^{-1} was attributed to the stretching vibration of C-H aromatic bond [84]. The band at 1616 cm^{-1} was attributed to the stretching vibration of imine C=N bond [99]. The band at 1587 cm^{-1} was

attributed to the stretching vibration of aromatic C=C bond [86]. The presence of N-H and C=N bands clearly indicated to the successfully formation of DNPHMP.

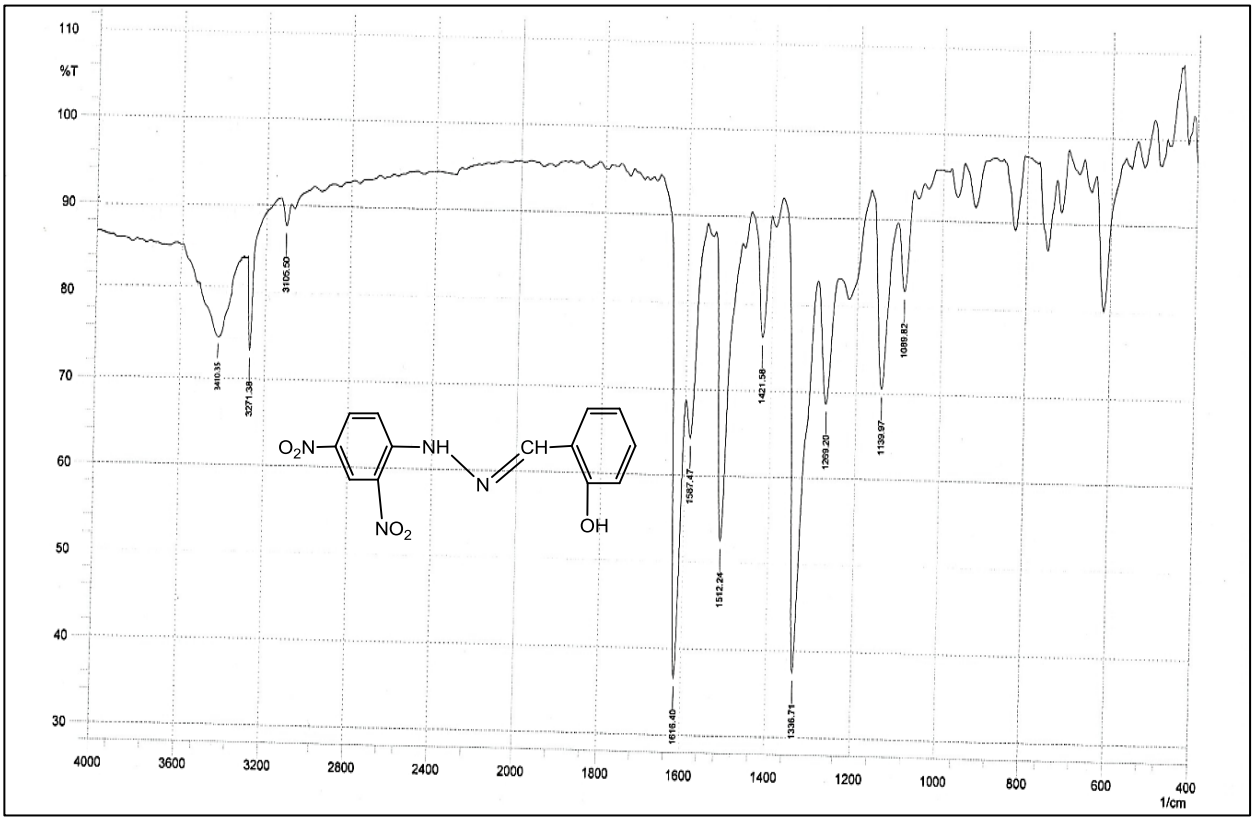

Fig 4.1: FT-IR spectrum of DNPHMP.

4.1.2 Proton nuclear magnetic resonance ^{1}HNMR of DNPHMP

The ^{1}HNMR spectrum of DNPHMP is shown in Fig.4.2. The spectrum showed different chemical shifts at different positions. The chemical shift at 2.7 ppm attributed to the C-H proton in DMSO [85]. The chemical shift at 3.3 ppm is due to the hydrazonic N-H proton [88]. The chemical shifts between 6.6-8.2 ppm are assigned to the aromatic rings protons [100]. The chemical shift at 10.1 ppm is attributed to the

hydroxyl proton (O-H) [90]. The benzylic proton (C-H) was observed at chemical shift 11.7 ppm [91]. The ^{1}HNMR spectrum of the DNPHMP is clearly shown that the suggested structure was in agreement well with observed result.

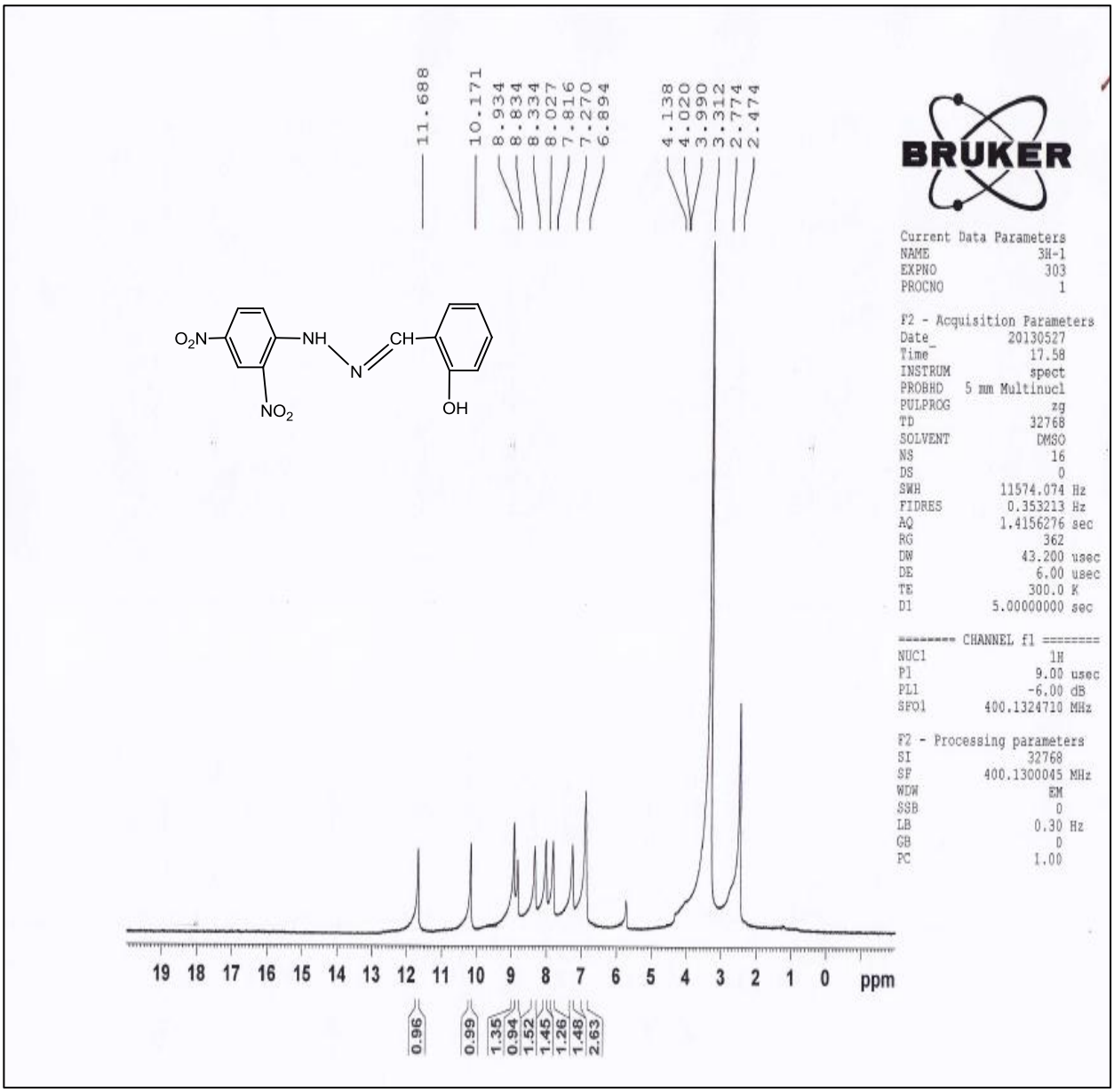

Fig 4.2 ^{1}HNMR spectrum of DNPHMP.

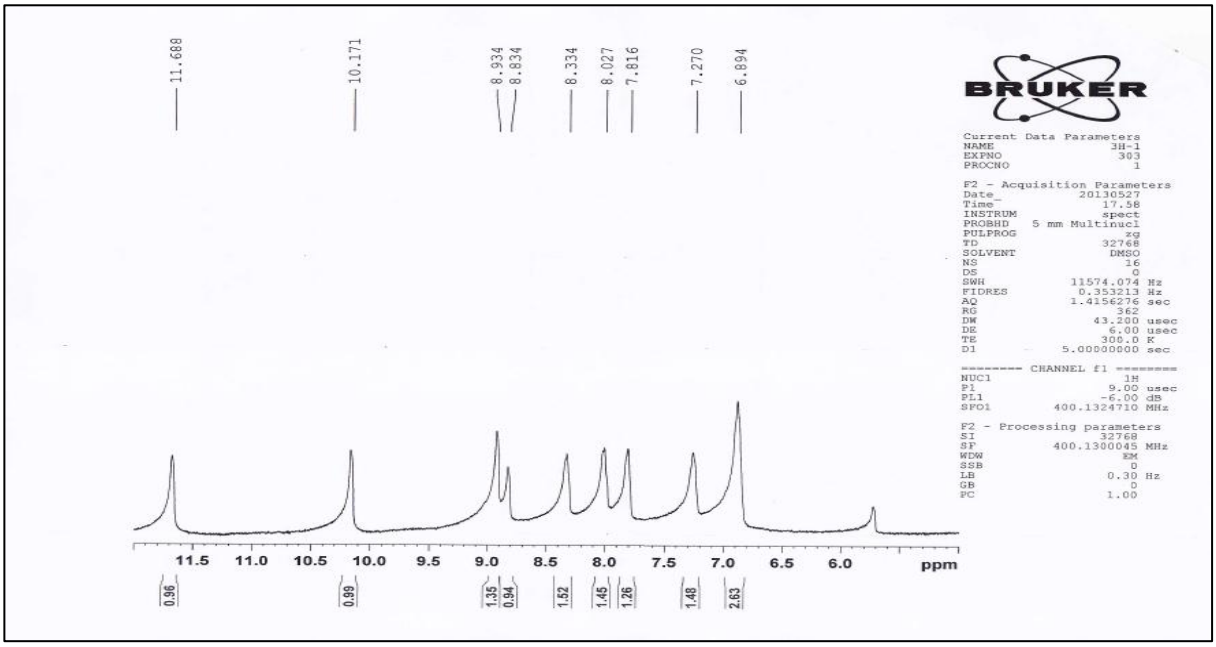

Fig. 4.3: Expansion of ^{1}HNMR spectrum of compound DNPHMP.

4.1.3 ^{13}C Nuclear magnetic resonance of DNPHMP

Fig. 4.4 shows the ^{13}CNMR spectrum for DNPHMP (dissolved in DMSO-d^6). The analysis of this spectrum shows a chemical shift at δ =117.9 ppm attributed to the C9 aromatic carbon and probably for C2 carbon atom as they have similar environment. The chemical shifts at δ =118.2, 121.09, 121.6 ppm were assigned to the aromatic carbon C12, C4, C13 respectively. The C5 and C10 aromatic carbon atoms may combines together with the same chemical shift at 124.61ppm. The signal at 128.03 ppm attributed to the C3 aromatic carbon combined with the C6 carbon atom [92]. The chemical shift at 131.29 ppm attributed to the aromatic carbon C11 which is directly bonded with the nitro group[81]. The chemical shift at 133.50 ppm attributed to the C7 carbon atom (benzylic) [94]. The chemical shift at 145.95 ppm attributed to the C8 atom which is directly bonded with hydrazone group [101]. The C1 aromatic carbon which is directly bonded with the phenolic –OH group is observed at 148.10 ppm [30]. The ^{13}CNMR spectrum of the DNPHMP is

clearly shown that the experimental result is in agreement well with suggested structure**.**

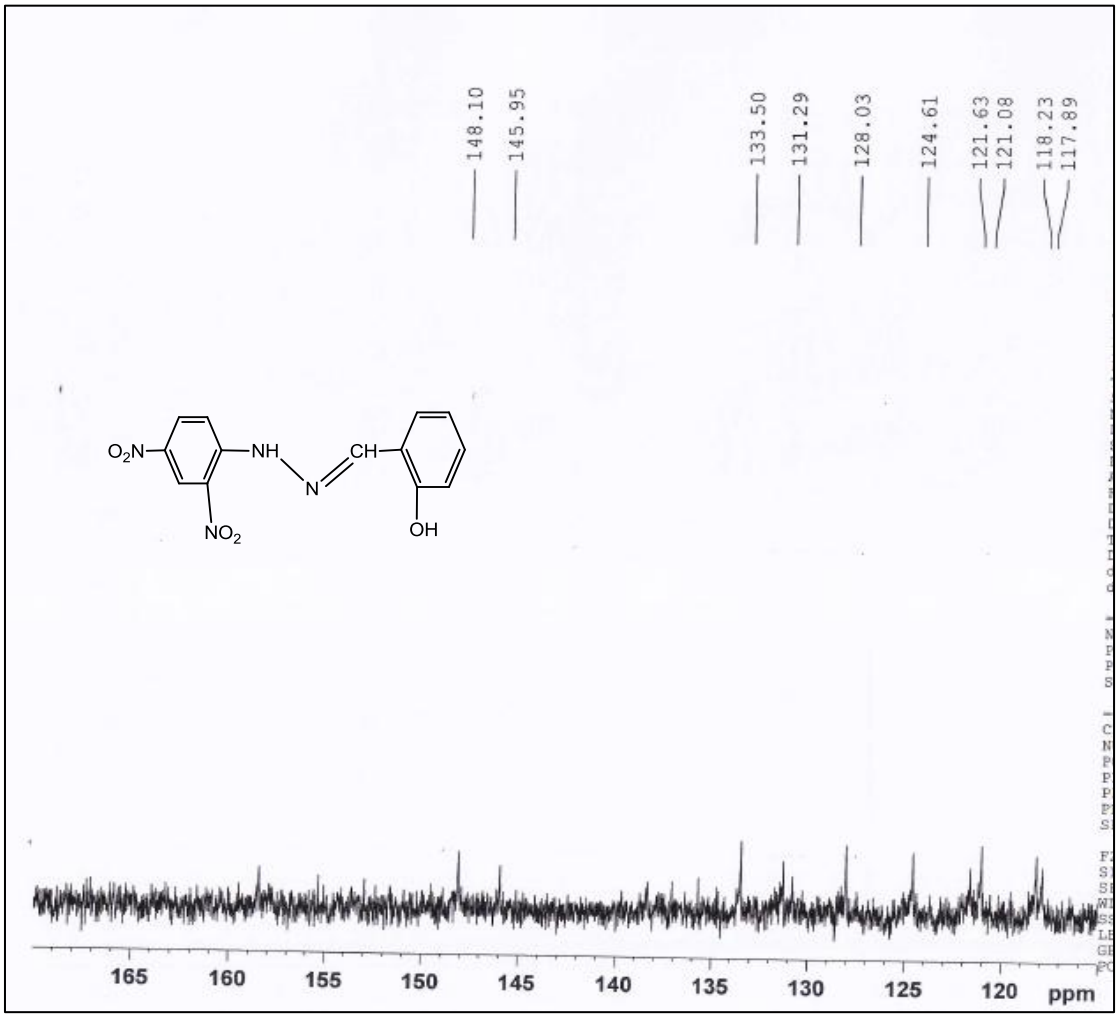

Fig 4.4: The ^{13}CNMR of DNPHMP.

4.2. The characterization of the RHDNPH

The RHDNPH catalyst was synthesis by the reaction of RHACCl with DNPHMP using toluene as a solvent under reflux condition. Scheme 4.2 shows the reaction bath for the immobilization of DNPHMP onto RHACCl. The following subtitle show the characterization which have been used to support the formation of RHDNPH.

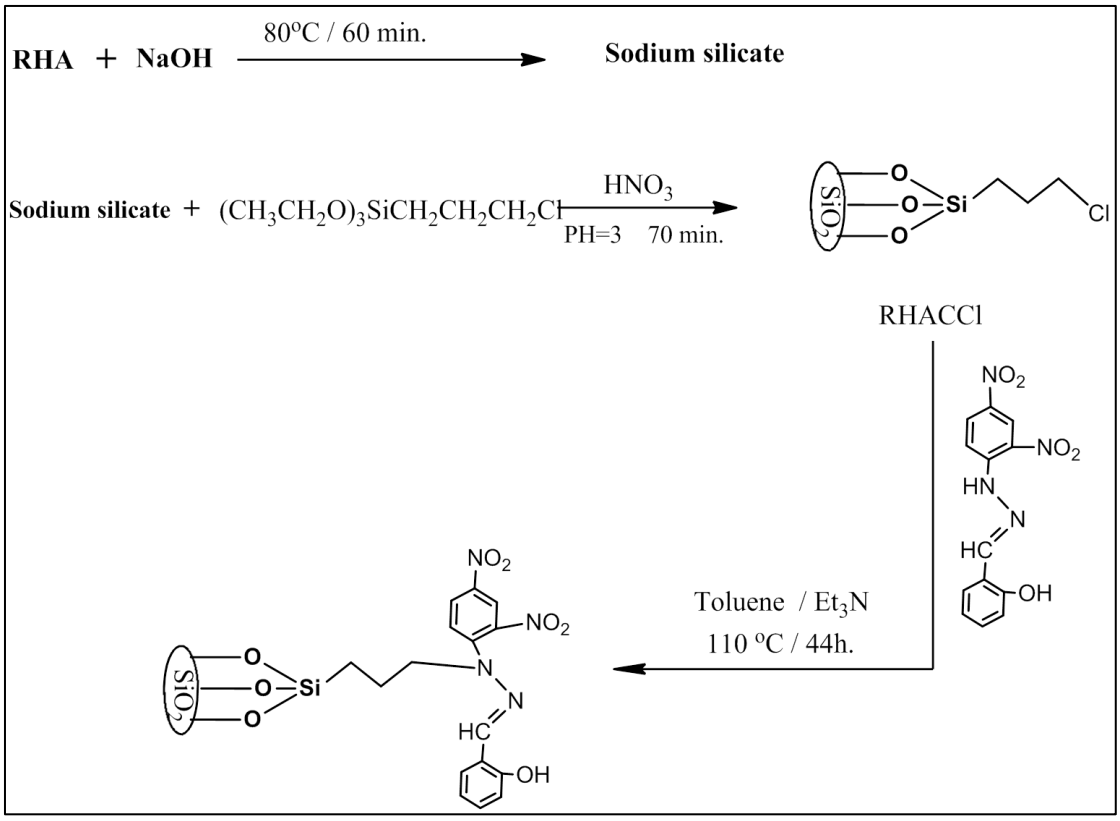

Scheme 4.2: The synthesis of RHDNPH via the immobilization of DNPHMP onto RHACCl. The possible structure of the RHDNPH was shown.

4.2.1 FT-IR analysis of RHDNPH

The FT-IR spectrum of RHDNPH is shown in Fig. 4.5. The broad band around 3425 cm^{-1} attributed to the stretching vibration of hydroxyl groups –OH in Si–O–H and free –OH phenolic group [82, 95]. The stretching vibration of C–H aromatic ring was observed at 3101cm^{-1} [85]. The stretching vibration of N-H group was not observed in the FT-IR. The stretching vibration of aliphatic C–H was observed at 2953cm^{-1} [96]. The band appear at 1649 cm^{-1} is usually assigned to the H—OH groups of absorbed water [102]. The band appear at 1620 cm^{-1} is due to stretching vibration of C=N [99]. The band of symmetrical and asymmetrical bending vibration of aliphatic CH_2 bonds is observed at 1512 cm^{-1} [27].

The band at 1332 cm^{-1} is due to stretching vibration of C-N bond [84]. The doublet and strong band at 1072 cm^{-1}, 1136 cm^{-1} attributed to Si-O-Si stretching vibration [23]. The FT-IR spectrum does not show the N-H and also show the appearance of C-H aliphatic, Si-OH, and Si-O-Si groups. These results clearly indicate that the DNPHMP was immobilized successfully onto RHACCl.

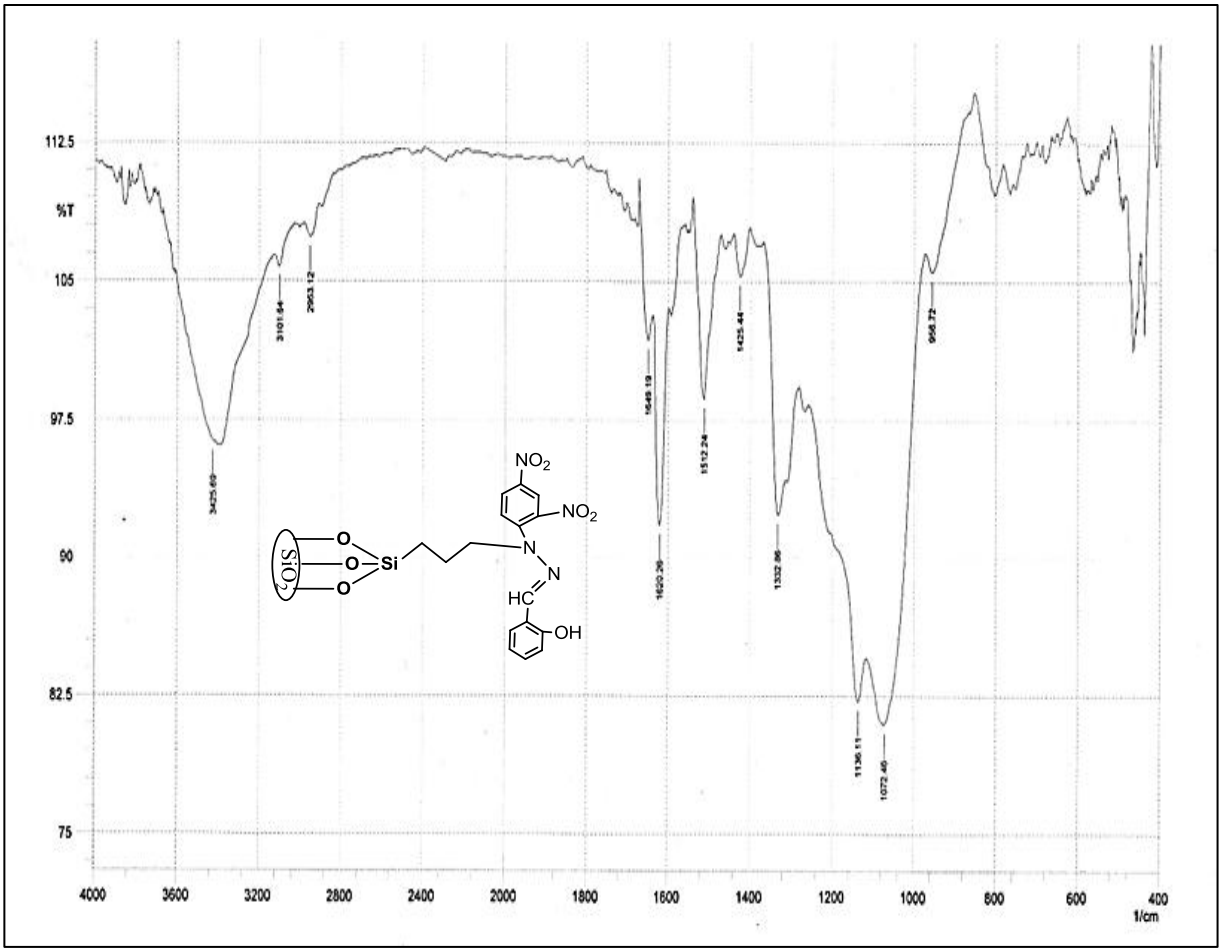

Fig 4.5 FT-IR spectrum of RHDNPH.

4.2.2 Elemental analysis

Table 4.1 shows the chemical analysis of RHDNPH. Due to the heterogeneous nature of the silica samples, these values can only be treated qualitatively. The analysis showed that carbon and nitrogen are

present in RHDNPH, while both these elements are not present in RHA as it was expected.

The elemental analysis of RHACCl showed that the percentages of C and H were 9.98 and 1.61%, respectively. RHDNPH showed a nitrogen composition of 3.14%. The C content for RHDNPH (16.49%) was slightly higher than RHACCl, which was expected. From the elemental analysis results, it can further conclude that the DNPHMP was indeed to be incorporated on the silica.

Table 4.1.Elemental analysis data of RHA, RHACCl [29] and RHDNPH.

Samples	Elemental analysis %		
	C	H	N
RHA	1.60	0.84	-
RHACCl	9.98	1.61	-
RHDNPH	16.49	2.86	3.14

4.2.3 The Nitrogen adsorption analysis

Fig. 4.6 shows the nitrogen adsorption isotherm obtained for RHDNPH. Inset is the pore size distribution graph. The hysteresis loop was observed in the range of $0.4 < P/Po < 1.0$, which is associated with capillary condensation according to the IUPAC classification. The

isotherm shown is of type IV and exhibits an H2 hysteresis loop [97]. Close observation of the program revealed that the hysteresis loop did not close but it was rather open ended. This indicates the presence of some degree of microspores retaining the nitrogen and hence failing to close the hysteresis loop. This is clearly seen in the pore size distribution curve, where the maxima in the microspore region (< 2 nm) and a major maximum at ca. 4 nm can be observed. It can therefore be concluded that RHDNPH consists of microspores with the narrow pore range of 3–4 nm.

BET analysis revealed the specific surface area of RHACCl to be 633 m^2 g^{-1} [23] . However, the specific surface area of RHDNPH was found to be 154.6 m^2 g^{-1}. Huge decrease in the surface area was observed after the modification which indicated that the DNPHMP was incorporate with the RHACCl and led to decrease in the service area. The pore size distribution showed a minor narrow pore size range below 2 nm which is in the microporous range. The average pore diameter of RHDNPH (BJH model) was obtained 1.47 nm, while for RHACCl it was reported to be 6.07 nm. It can be seen that RHDNPH had a narrower pore size compared to RHACCl. This was probably due to the presence of DNPHMP inside the silica matrix. RHDNPH showed a distinct pore size distribution between 2 and 8 nm. These fall within the mesoporous region. The results obtained by the nitrogen adsorption–desorption analysis for RHPHMP is summarized in Table 4.2.

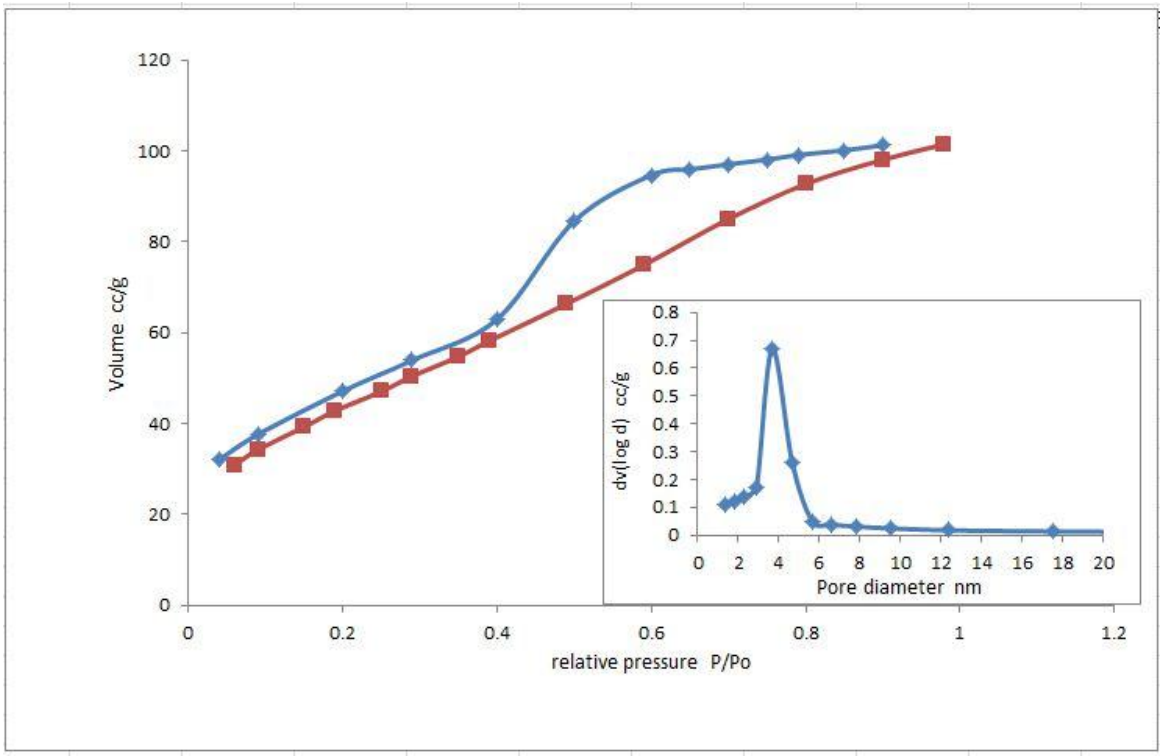

Fig 4.6: The nitrogen adsorption–desorption isotherms of RHDNPH. Inset the pore size distribution graph.

Table 4.2: The result of BET analysis for RHA [23], RHACCl and RHDNPH.

Sample	Specific surface area (m^2g^{-1})	Average pore volume (cc g^{-1})	Average pore diameter(nm)
RHA	347	0.87	10.4
RHACCl	633	0.70	6.07
RHDNPH	154.6	0.17	1.47

4.2.4 X-Ray Diffraction analyses (XRD)

The X-ray diffraction pattern of RHDNPH is shown in Fig.4.7. A band at 2θ angle of 22.5° was observed which was typical for amorphous silica. This result is similar to the X-ray of both RHA and RHACCl. This indicates that there is no change on the face after the immobilization of DNPHMP.

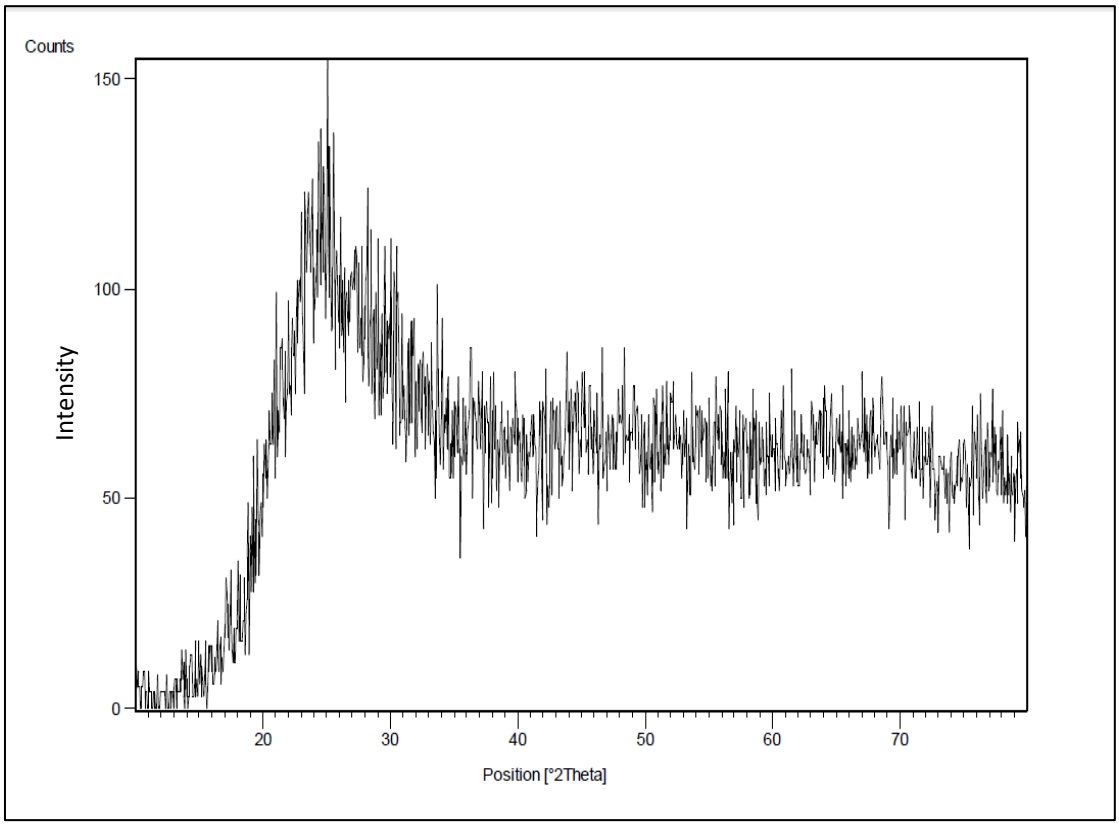

Fig. 4.7: The X-ray diffraction pattern of RHDNPH.

4.2.5 Thermogravimetric analysis (TGA)/Differential thermal analysis (DTA)

Fig. 4.8 shows the TGA/DTA of RHDNPH. The graph in Fig. 4.8 shows four characteristic decomposition stages. The first started at 40 to

185 ºC, due to the loss of adsorbed water (ca. 0.90 %), and the second mass loss (ca. 4.15 %) occurred between 185 – 273 ºC due to the decomposition of the DNPHMP and propyl groups anchored onto the silica [22]. The continuous weight loss (ca. 23.48 %) between 300 – 440 ºC was due to decomposition of the remaining organic DNPHMP and propyl anchored on the silica surface. Both those mass loss were not observed on the graph of RHA RHACCl. The forth decomposition stage between 440 – 680 ºC was due to the condensation of silanol groups at higher temperatures [103].

In the DTA curve Fig. 4.8 it was observed four exothermic transformations the first is a peak which occurs between 40 °C and 185 °C, with a maximum at 90 °C and the second occurs between 185 °C and 273 °C, with a maximum at 250 °C, while the third occurs between 300 °C and 440 °C with a maximum at 350 °C. The last exothermic transformations is occurs between 440 °C and 680 °C, with a maximum at 500 °C. The first exothermic change due to the loss of adsorbed water, while the second, third and fourth attribute to the arrangement of the structure of the polymer [98]. The TGA/DTA provided further evidence for the successful immobilization of DNPHMP onto rice husk silica.

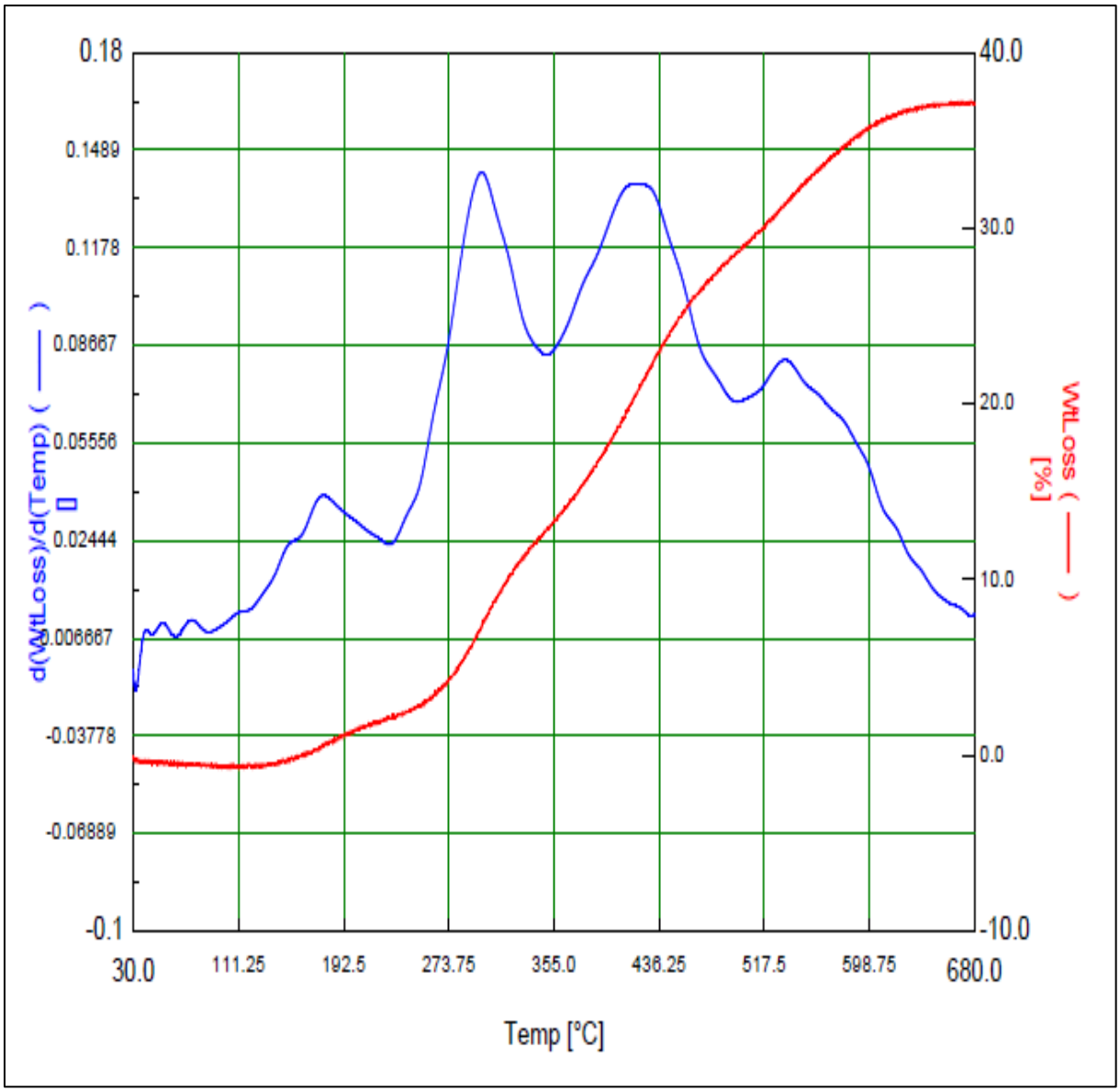

Fig. 4.8: The TGA/DTA of RHDNPH.

4.2.6 Scanning electron microscopy SEM

Fig. 4.9 shows the SEM of RHDNPH. A large particles were present onto smooth surface of silica. A randomly distribution of particles on surface were seen.

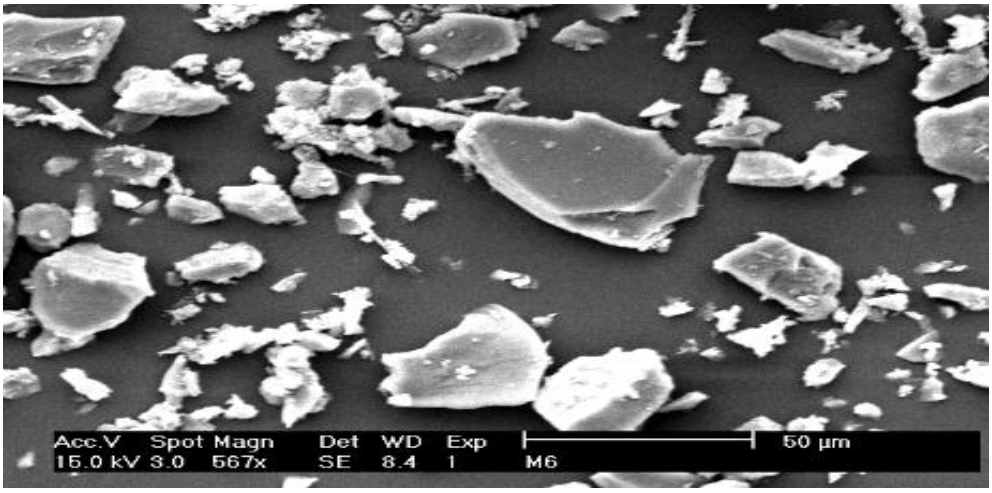

Fig. 4.9: The SEM micrograph of RHDNPH.

4.2.7 Energy dispersive X-ray analysis

Fig. 4.10 and table 4.3 show the EDX results of RHDNPH. The EDX results show the presence of C, Si, O, and N. These entire elements were found into RHACCl. The only nitrogen is not found in the formula of RHACCl. The presence of the nitrogen give very good indication for the successfully immobilization of DNPHMP onto RHACCl.

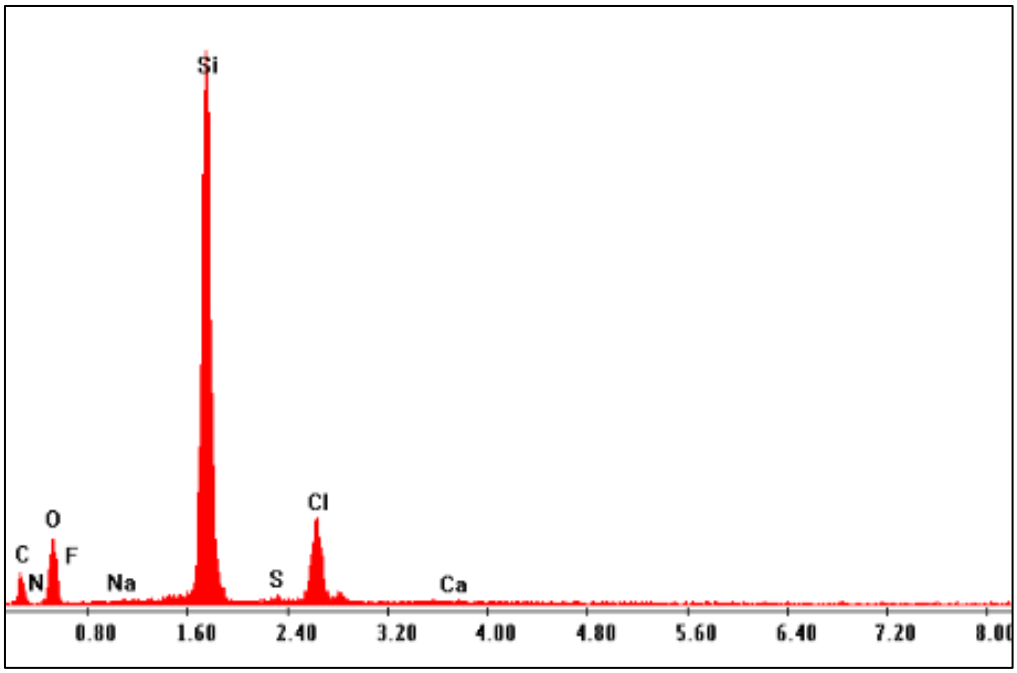

fig 4.10: The EDX result of RHDNPH.

Table 4.3: The percentage of elements obtained from EDX analysis

Elem.	%
C	11.2
N	0.9
O	34.73
Si	46.01
Cl	7.16

CHAPTER FIVE

Hydrolysis of cellulose over RHPHMP and RHDNPH

The activity of the heterogeneous catalysts RHPHMP and RHDNPH as well as homogenous PHMP and DNPHMP towards hydrolysis of cellulous to glucose were studied (Scheme 5.1).

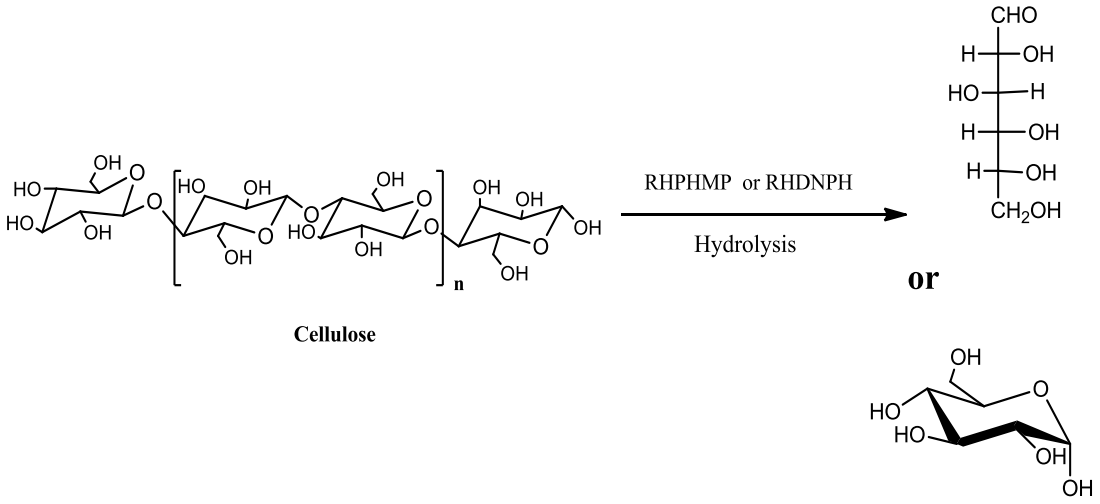

Scheme 5.1: The hydrolysis of cellulose to glucose.

The hydrolysis parameters such as hydrolysis time, catalyst mass, temperature, solvents effect and reusability of the catalysts were investigated to optimize the hydrolysis conditions. The following sections are shown the activity of the catalysts in details.

5.1 Catalytic study over RHPHMP

5.1.1 Influence of hydrolysis time

The effect of the time on the hydrolysis of cellulous over RHPHMP, RHA, and homogenous PHMP are shown in Fig. 5.1. The hydrolysis was carried out with 0.15 g of catalyst at 140 °C. The initial

hydrolysis of cellulous during the fifth hour was 10 % and it was increased to a maximum of 84.5 % in 14 h. However, it was observed that when the hydrolysis time was increased, more than 14h, there was no change on the hydrolysis of cellulose. Therefore the optimum time of the hydrolysis of cellulous over RHPHMP is 14 h. The hydrolysis of cellulose over PHMP as a homogeneous catalyst was found to be higher than 96.0 % in 14h. The activity of PHMP comparing with RHPHMP was due to the presence of hydrazon groups as homogenous active sites which may play a vital role during the hydrolysis.

The hydrolysis of cellulose over the RHA was also studied as shown in Fig. 5.1. The maximum conversion of cellulose was 20.0 % in 14 h. It is also observed that the hydrolysis of cellulose without catalyst was found to be less than 20 % in 14h.

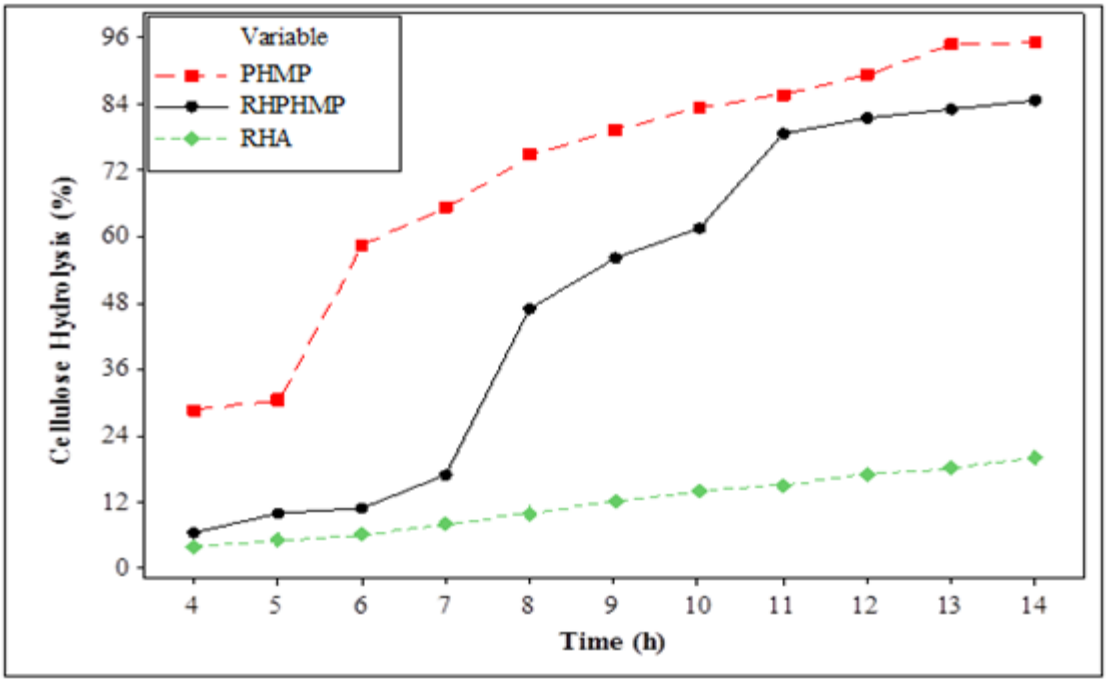

Fig 5.1: The hydrolysis of cellulose to glucose over heterogeneous RHPHMP, RHA, and homogenous RHMP as a function of the hydrolysis time.

5.1.2 Influence of catalyst's mass

The hydrolysis of cellulose was carried out by varying the amount of RHPHMP (ranged 100 and 250 mg) while keeping the other parameter fixed as 14 h hydrolysis time and temperature at 140 °C. The results are shown in Fig. 5.2.

It is clearly shown from Fig. 5.2 when the catalyst mass were increasing from 100 to 150 mg, the percentage of cellulose hydrolyzed increased too from 68 to 84 %. Further increase in the catalyst mass had no significant effect. The increased conversion with the catalyst mass could be attributed to the availability of a greater number of catalytically active sites. Therefore 150 mg was chosen as the optimum mass of the catalyst.

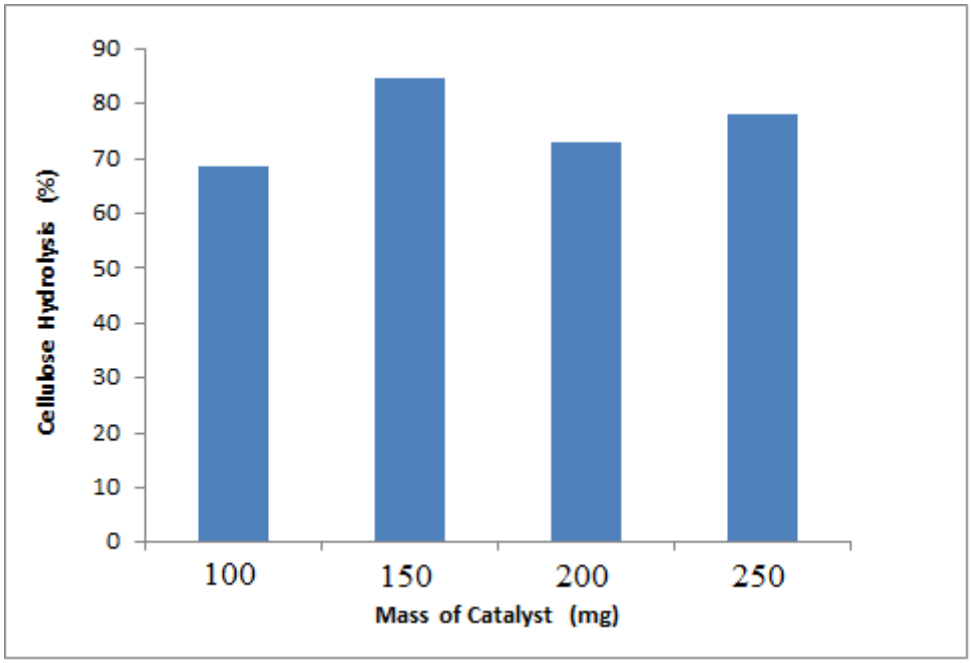

Fig 5.2: The relationship between the hydrolysis percentage of cellulose versus the used amounts of catalyst.

5.1.3 Influence of hydrolysis temperature

The effect of the temperature on the hydrolysis of cellulose over RHPHMP is shown in Fig. 5.3. The hydrolysis increased when the temperature was increased from 120 to 140 °C. The hydrolysis was ca. 84.5 % at 140 °C. There is no doubt that temperature has a great effect on the hydrolysis of cellulose. A higher hydrolysis temperature can get higher glucose yield. Taken into account the nature of the RHPHMP catalyst used (heterogeneous catalyst) in this study. This clearly indicates that the using of RHPHMP is effective to promote the hydrolysis of cellulose.

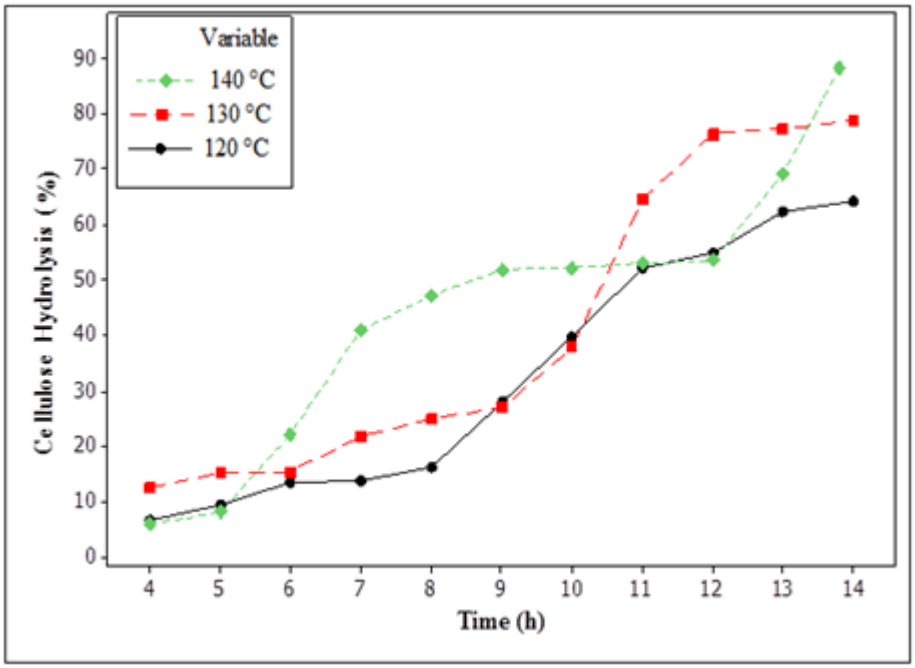

Fig. 5.3: The hydrolysis of cellulose to glucose over RHPHMP, at different temperatures.

5.1.4 Influence of solvent effect

The effect of the solvent that was used as a media on the hydrolysis of cellulose over RHPHMP is shown in Table 5.1. The hydrolysis was

studied over different solvents i. e. cyclopentanone, cyclohexanol, DMF, and butanol. It was observed that the hydrolysis of cellulose over different solvents was followed the flowing order:

DMF > cyclohexanol > 1-butanol > Cyclopentanone

The hydrolysis of cellulose was depending on the solubility of cellulose in the solvent. It was observed that the cellulose was completely soluble in the N,N-diethylacetamide containing LiCl [104] . In our study it is found that the cellulose was highly soluble in DMF and cyclohexanol containing LiCl. Most dissolution system could form a hydrogen bonding between layers of cellulose chains and the solvents. The DMF contain more than one center able to form a hydrogen bonding with the cellulose and this could lead to increasing the solubility of cellulose. This could make the hydrolysis much more easily comparing with the insoluble one.

Table 5.1: The hydrolysis of cellulose to glucose over RHPHMP, using different solvents. The hydrolysis conditions as follows: catalyst 150 mg, 140 $^{\circ}$C and 14 h reaction time.

Solvent	Cellulose hydrolysis (%)
DMF	84.54
Cyclohexanol	59.03
Butanol	57.12
Cyclopentanon	44.57

5.1.5 Catalyst's recycle experiments

The main benefit of using heterogeneous catalyst is the ability to reuse this catalyst many times. This depends on the stability of the catalyst and the activity of its active center. Since RHPHMP is a heterogeneous catalyst, so it was recycled successfully. After the first hydrolysis was run using the catalyst with the mixture, it was then washed with hot DMF (80 ^{o}C) and LiCl (this step was repeated three times) and the catalyst was heated at 110 °C for 24 h. Next, fresh cellulose and DMF with LiCl were added to the catalyst washed and a second run was conducted, as was a third, using the same procedure. As shown in Fig. 5.4 the yields in the second and third runs were very closely to that in the first run. These results indicated that catalytic performance was not lost during the course of the catalytic runs.

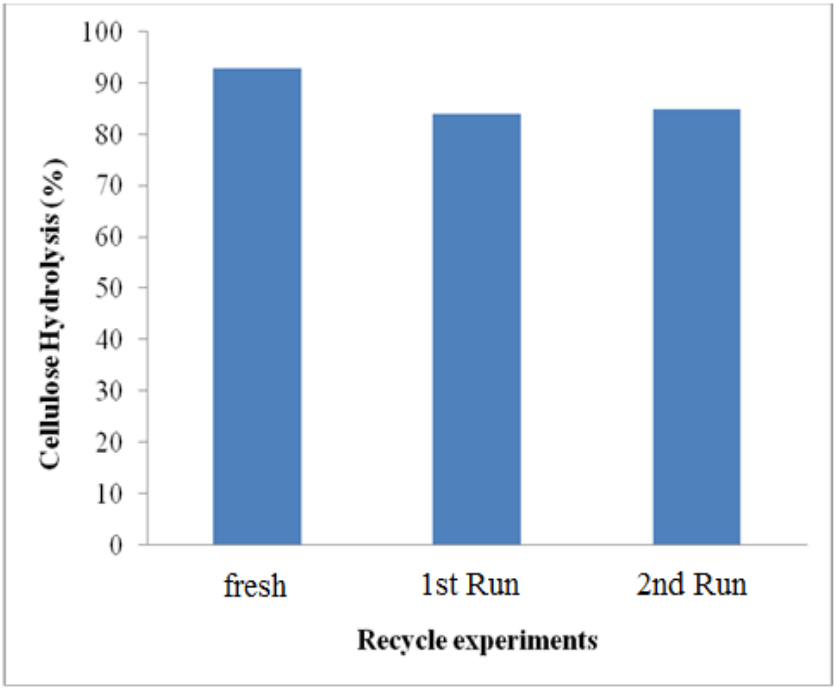

Fig. 5.4: The hydrolysis of cellulose to glucose over RHPHMP, after many times recycle.

5.2 Catalytic study over RHDNPH

5.2.1 Influence of hydrolysis time

The effect of the time on the hydrolysis of cellulous over RHDNHP, RHA, and homogenous DNHPMP are shown in Fig. 5.5. The hydrolysis was carried out with 150 mg of catalyst, at 140 °C. The initial hydrolysis of cellulous during the 5 h was 8.0 % and it was increased to a maximum of 82.5 % in 11 h. However, it was observed that when the time was increased, more than 11 h, there was no change on the hydrolysis of cellulose. Therefore the optimum time of the cellulous hydrolysis over RHDNPH is 11 h. The hydrolysis of cellulose over DNPHMP was found to be higher than 81.3 % in 11h. The activity of DNPHMP was due to the presence of amine groups as homogenous active sites which may play a vital role during the hydrolysis.

The hydrolysis of cellulose over the RHA was found 20.0 % in 14h. It is also observed that the hydrolysis without catalyst was found to be less than 20.0 % in 14 h.

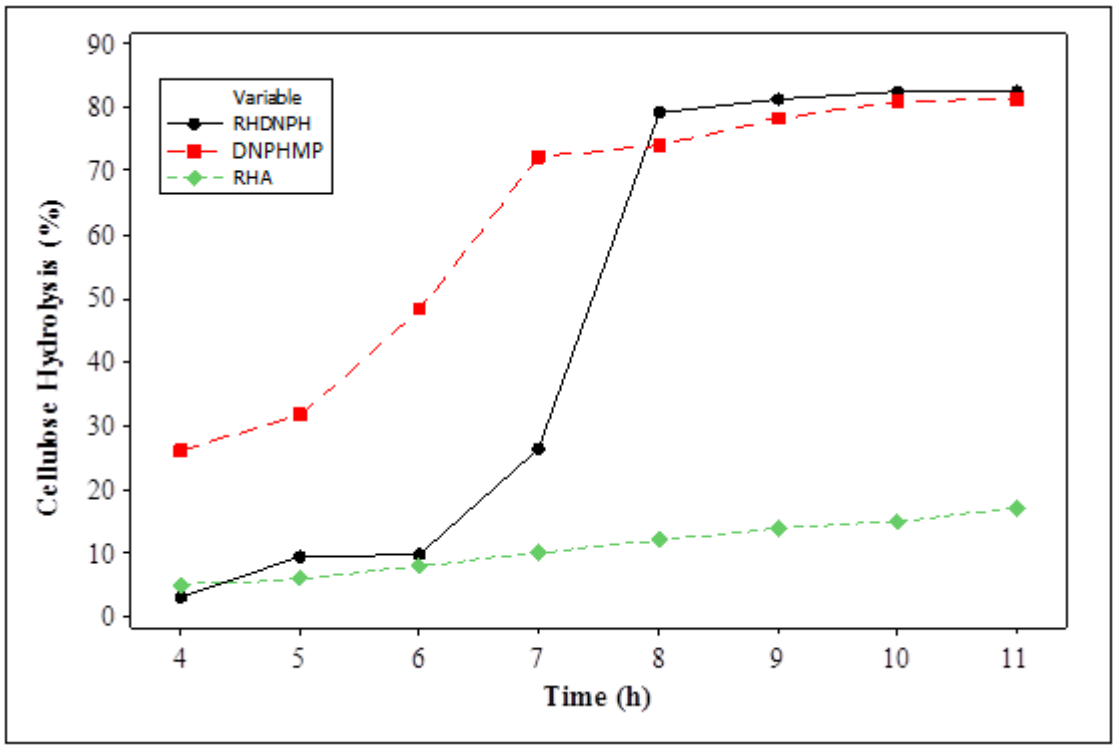

Fig 5.5: The hydrolysis of cellulose to glucose as a function of time over RHDNPH, DNPHMP, and RHA.

5.2.2 Influence of catalyst's mass

The hydrolysis of cellulose was carried out by varying the amount of RHDNPH (ranged 50 and 200 mg) while keeping the other parameter fixed as 11 h hydrolysis time at 140 °C. The results are presented in Fig. 5.6.

It is clearly shown from Fig.5.6 when the catalyst's mass were increasing from 50 to 150 mg, the percentage of cellulose hydrolyzed increased too from 49 to 82 %. Further increase in the catalyst mass had no significant effect. The increased conversion with the catalyst mass could be attributed to the availability of a greater number of catalytically active sites. Therefore 150 mg was chosen as the optimum mass of the catalyst.

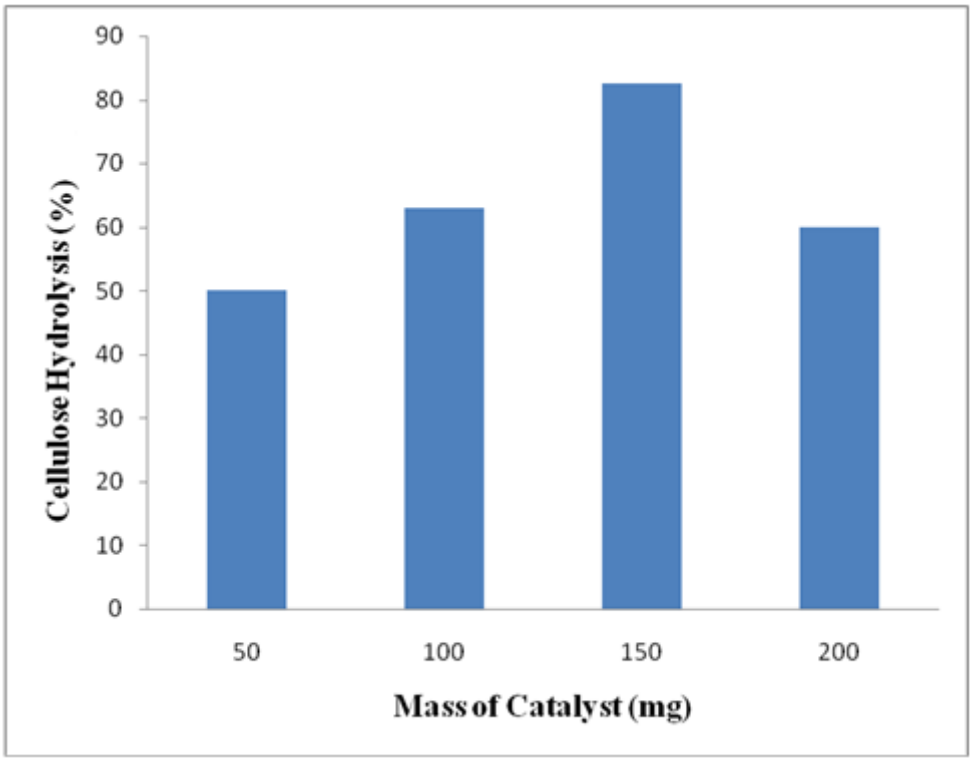

Fig 5.6: The relationship between the hydrolysis percentage of cellulose versus the used amounts of catalyst RHDNPH.

5.2.3 Influence of hydrolysis temperature

The effect of the temperature on the hydrolysis of cellulose over RHDNPH at 11 h and 150 mg of catalyst is shown in Fig. 5.7. The hydrolysis increased when the temperature was increased too from 120 to 140 °C. The conversion was ca. 82.5 % at 140 °C.

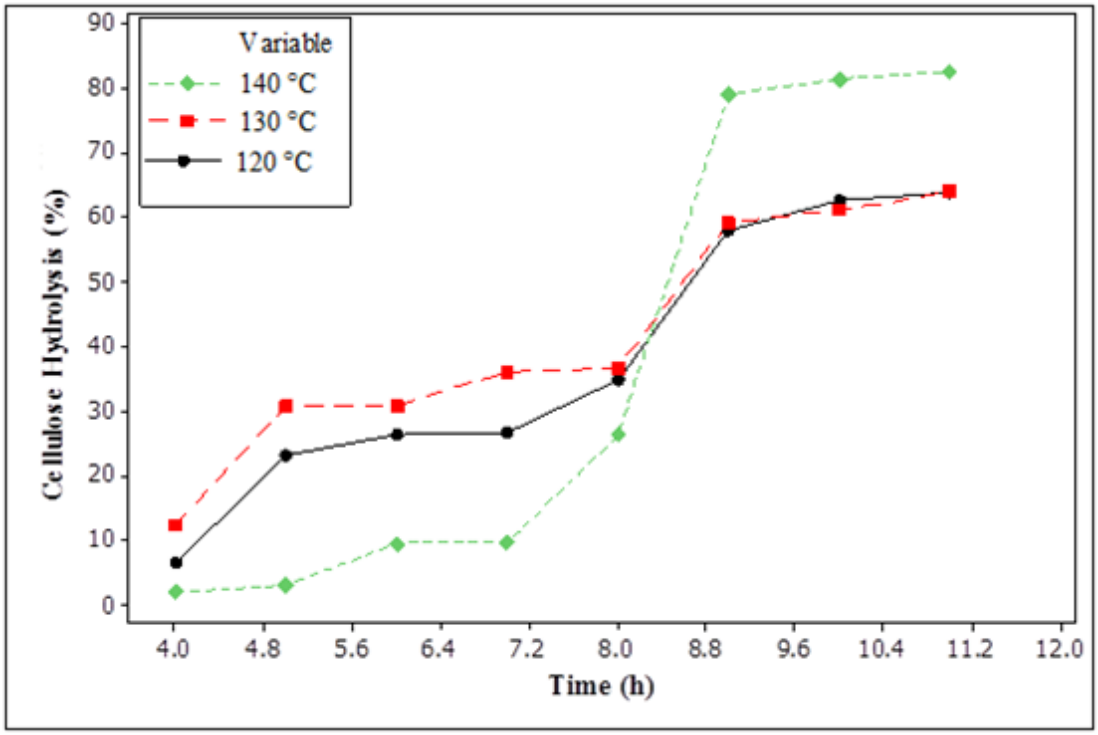

Fig. 5.7: The conversion of cellulose to glucose over RHDNPH, at different temperatures.

5.2.4 Influence of solvent effect

The effect of the solvent that was used as a media on the hydrolysis of cellulose over RHDNPH is shown in Table 5.2. The hydrolysis was studied over different solvents i. e. cyclopentanone, cyclohexanol, DMF, and butanol. It was observed that the hydrolysis of cellulose over different solvents was followed the flowing order:

DMF > Cyclohexanol > Cyclopentanone > 1-Butanol

Table 5.2: The effect of different solvents on the hydrolysis of cellulose over RHDNPH.

Solvent	Cellulose hydrolysis (%)
DMF	82.50
Cyclohexanol	61.11
Cyclopentanon	52.26
Butanol	8.56

5.2.5 Catalyst's recycle experiments

The catalytic reusability was tested after the catalyst was regenerated by washing with hot DMF (80 ^{o}C) and LiCl, and drying at 110 °C for 24 h before each reuse. Fig 5.8 shows the reusability of the RHDNPH. It was observed that there is no change on the catalytic activity after the cures of the reaction. This indicates that the catalyst was very stable during the hydrolysis running.

Fig. 5.8: The reusability of RHDNPH on the cellulose hydrolysis.

Conclusions

Phenylhydrazonomethylphenol (PHMP) was immobilized onto silica rice husk ash to form a strong catalyst denoted as RHPHMP. The BET measurements of the catalyst showed that the surface area to be 137.6 m^2 g^{-1}. The FT-IR clearly showed the presence of –NH and C=N absorption band at the expected range. The elemental and EDX analysis of RHPHMP showed the nitrogen is included into the catalyst structure. The TGA/DTA show the catalyst is stable. The RHPHMP was efficient for the hydrolysis of cellulose, with maximum glucose yields over 84 % at 140 °C in 14 h. It was found that the solubility of cellulose was very important factor to make the hydrolysis much more easily. The cellulose was hydrolyzed over RHA and the maximum hydrolysis of cellulose was 20.0 % in 14h. The low hydrolysis of cellulose over RHA comparing with high hydrolysis of cellulose over RHPHMP indicates that the activity of RHPHMP is a proportional with the active centers.

2,4-Dinitrophenylhydrazonomethylphenol (DNPHMP) was immobilized onto silica rice husk ash to form a heterogeneous catalyst denoted as RHDNPH in a good yelled. The BET measurements of the catalyst showed that the surface area to be 154.6 m2 g -1 with pore size distribution was found between 2 and 8 nm. These fall within the microporous region. The FT-IR clearly showed the presence of –NH and C=N absorption band at the expected range. The elemental and EDX analysis of RHDNPH showed the nitrogen is included into the catalyst structure. X-ray diffraction technique proved the amorphous nature of catalysts since it showed the broad band at 22.5^{o}. The RHDNPH was efficient for the hydrolysis of cellulose, with maximum glucose yields 82.5 % at 140 °C in 11 h. The catalysts were simple in its preparation, stable during the cellulose hydrolysis in addition to repeatedly without a significant loss of its catalytic activity.

Recommendations

1- Synthesis new type of catalysts by grafting of silica with different organic compounds and use it to catalyze the organic synthesis reactions especially these with slow rate.

2- Preparation a new hybrid organo-silica compounds which are suitable for industrial field.

3- Employing this catalysts to follow up the hydrolysis of cellulose by working on the produced glucose and converting it into alcohols as biofuel.

4- finding other application of extracted silica (RHA) instead of burn it as west.

References

1- Davis M. (2003). Fundamentals of chemical reaction engineering. 1st Ed. McGraw-Hill Sci./Eng./Math., pp.133.

2- Kozhevnikov, I.V., (2009). Heterogeneous acid catalysis by heteropoly acids. *J. Mol. Catal. A: Chem.*, 305, 104–111.

3- Dilip G. P. (2011). On the Role of Acidity in Amorphous Silica-Alumina Based Catalysts. PhD thesis University of Eindhoven. Nederland.

4- Avelino C., Hermenegildo G., (2008). Crossing the borders between homogeneous and heterogeneous catalysis: developing recoverable and reusable catalytic systems. *Top Catal*,. 48, 8–3.

5- Leofanti G., Tozzola G., Padovan M., Petrini G., Bordiga S., Zecchina A., (2009). Catalyst characterization: characterization techniques. *Catal. Today*., 34, 307-327.

6-Jens H., (2006). Industrial Catalysis: A Practical approach. 2nd Ed. *Wiley-Vch Verlag GmbH & Co. KGaA,Weinheim*.

7- Erica F., Dimonte R., Kaspar J., (2006). Homogeneous and heterogeneous catalysis. *Inorg. and Bio-inorg. Chem.*, 2, 1-10.

8- Farook A., Saraswathy B., Phee-Lee W., (2006). Rice husk ash silica as support material for Ruthenium based heterogeneous catalyst. *J. Phys. Chem.*, 17, 1–13.

9- [online]. [Accessed 17, October ,2013]. Available from World Wide Web. http:// www.thehindu.com/todays-paper.

10- Ajay K., Kalyani M., Devendra K., Om Parkash, (2012).Properties and industrial applications of rice husk. *Int. J. of Emerg. Tech. and Adv. Eng.*, 2, 86-91.

11- Sumrerng R., Prinya C., Rattana M., (2009). Effect of grinding on chemical and physical properties of rice husk ash. *Int. J. Miner, Metall and Mate.*, 16, 242-247.

12- Bandita D., Afzal M., (2011). Silica Sulfuric Acid: An efficient heterogeneous catalyst for the one-pot synthesis of 1,4-Dihydropyridines under mild and solvent-free conditions. *Chin. J. Catal*., 32, 1180–1184.

13- Ram P., Monika P., (2012). Rice husk ash as a renewable source for the production of value added silica gel and its application: An overview. *Bull. of Chem. React. Eng. & Catal*., 7, 1-25.

14- Sharma, N., Williams, W., Zangvil, A., (1984). Formation and structure of silicon carbide whiskers from rice hulls. *J. Am. Ceram. Soc*. 67, 715-720.

15- Kiselev A., Lygin V., (1975). Infrared spectra of surface compounds. John Wiley & Sons, New York,.

16- El-Nahhal I.M., El-Ashgar N. M., (2007). A review on polysiloxane-immobilized lig, systems: Synthesis, characterization and applications. *J. Organomet. Chem*, 692, 2861–2886.

17- Leyden D., Luttrell, G., (1975). Preconcentration of trace metals using chelating groups immobilized via silylation. *Anal. Chem*., 47, 1612-1617.

18- Hatsuo I., (1984). A review of recent progress in the studies of molecular and microstructure of coupling agents and their functions in composites, coatings and adhesive joints. *Polym. Compos*., 5, 101-123.

19- Chia-Min Y., Kuei-Jung C., (2002). Functionalization of molecularly templated mesoporous Silica. *J. Chin. Chem. Soc.*, 49, 883-893.

20- Bae, S.J., Kim, S.W., Hyeon, T., , Kim, M., (2000). New chiral heterogenous catalysts based on mesoporous silica: asymmetric diethylzinc addition to benzaldehde, *Chem. Commun*., 31–32.

21- Paul, H., Bhaduri, S., Lahiri, G.K., (2004). Platinum carbonyl derived catalysts on inorganic supports: a comparative study, J. Org. Chem., 689, 309–316.

22- Soundiressane T., Selvakumar S., Ménage S., Hamelin O., Fontecave M., Singh A.P., (2007). Ru– and Fe–based N,N′–bis(2–pyridylmethyl) –N–methyl– (1S,2S) –1,2–cyclohexanediamine complexes immobilized on mesoporous MCM– 41: Synthesis, characterization and catalytic applications, *J. Mol. Catal. A Chem.,* 270, 132–143.

23- Kasim M.H. (2010). The heterogenation of Saccharin, Melamine and their catalytic activity in esterification reaction. PhD thesis. University of Sins Malaysia, Malaysia.

24- Farook A., Kasim M.H., Hasnah O., (2010). Synthesis of Mesoporous Silica Immobilized with 3-[(Mercapto or amino)propyl]trialkoxysilane by a Simple One-pot Reaction. *China J. of Chem.*, 28, 2383-2388.

25- Farook A., Kasim M.H., Suk-Jin C., (2012). The heterogenization of l-phenylalanine–Ru(III) complex and its application as catalyst in esterification of ethyl alcohol with acetic acid. *Chem. Eng. Res. Des.*, 90, 633–642.

26- Farook A., Chew T.S., Hanushantini M., Jimmy N., Kasim M.H., (2012). Synthesis and characterization of silica–imidazole mesostructured composite from agricultural biomass. *Microporous Mesoporous Mater*., 167, 245-248.

27- Farook A, Hiba E.H., Kasim M.H., (2012). The synthesis of N-heterocyclic carbene–silica nano-particles and its catalytic activity in the cyclization of glycerol. *J. Taiwan Inst. of Chem. Eng.*, 43, 619–630.

28- Farook A., Kasim M.H., Tammar H.A., (2011). Solvent free liquid-phase alkylation of phenol over solid sulfanilic acid catalyst. *Appl. Catal., A*, 399, 42–49.

29- Hayder H. M. (2012). Synthesis and characterization of heterogeneous catalysts via silica obtained from Iraqi rice husks. PhD thesis. University of Baghdad, Iraq.

30- Gheorghe R., Mioara A., (2001). New Schiff bases from ortho-hydroxy aryl aldehydes. *Bull. of Chem. and Tech. of Macedonia*, 20, 131-136.

31- Abdul-Rauf. (2005). Synthesis and biological activities of some Schiff base compounds and their transition metal complex. PhD thesis. University of Bahauddin Zakariya, Pakistan.

32- Ahmet O., Zafer A.K., Gulhan T.Z., Gilbert R., (2010). Synthesis of some novel hydrazone derivatives and evaluation of their antituberculosis activity. *Marmara Pharm. J.*, 14, 79-83.

33- Nursabah S., Gazi I., (2005). Synthesis and complex formation of some novel vic-dioxime derivatives of hydrazones. *Turk J Chem* ,29,107 – 115.

34- Rodriguez M.C., Ferrari M.B., Bisceglie F., Pelizzi C., Pelosi G., Pinelli S., Sassi M., (2004). Synthesis, characterization and biological activity of Ni, Cu and Zn complexes of isatin hydrazones. *J.Inorganic Biochemistry*, 98, 313-314.

35- Paresh L.D., Atsushi F., (2005). Cracking of cellulose over supported metal catalysts. *Catalysis Research Center, Hokkaido University*, Sapporo 001-0021, Japan.

36- Moumita S., Hong G., Jeremy C.S., (2010). Catalytic mechanism of cellulose degradation by a cellobiohydrolase CelS. *Plosone*, 5, 1-10.

37- Jagrati P., Tiwari C.K., Akhilesh A., Verma R.K., (2012). Bio degradation of cellulose by wood decaying fungi. *J. of Appl. Sci. in Environ. Sanitation*, 7, 209-214.

38- Perez J., Munoz-Dorado J., Rubia T., Martinez J., (2002). Biodegradation , biological treatments of cellulose, hemicellulose , lignin: an overview. *Int. Microbiol J*.,5, 53–63.

39- Halliwell G., (1965). Catalytic decomposition of cellulose under biological conditions. *Biochem. J*., 95, 35-36.

40- Rosa M.M., (2005). Brief on biomass and cellulosic ethanol, *California Research Bureau, California State Library*. [Online]. [Accessed 20 August 2013]. Available from World Wide Web: http:// (www.library.ca.gov)

41- Pengfei Y., Hirokazu K., Atsushi F., (2011). Recent developments in the catalytic conversion of cellulose into valuable chemicals. *Chin. J. Catal*., 32, 716–722.

42- Haibo X., Zongbao K.Z., (2011). Selective breakdown of (Ligno)cellulose in Ionic Liquids. From ebook Ionic Liquids applications, perspectives. (Ed.)Prof. Alexander Kokorin. [online]. [Accessed 15, September, 2013]. Available from World Wide Web. www.intechopen.com.

43- Joung W.H., Hyunjoo L., (2012). Direct conversion of cellulose into sorbitol using dual-functionalized catalysts in neutral aqueous solution. *Catal. Commun.*, 19, 115–118.

44- Franz M.H. (2011). The cellulose gap (the future of cellulose fibers). *Lenzinger Berichte*, 89, 12-21.

45- John R.R., (2010). Cellulosic biofuels got gasoline. [online]. [Accessed 12, August,2013]. Available from World Wide Web. http://genomicsgtl.energy.gov/biofuels/b2bworkshop.shtml.

46- Tomas M., Josef P., Petra O., Igor B., (2010). The using of enzymes for degradation of cellulose substrate for the production of biogas. *37th International Conference of Slovak Society of Chemical Engineering.*

47- Camacho F., Gonzalez P., Jurado E., Robles A., (1996). Microcrystalline-cellulose hydrolysis with concentrated sulphuric acid. *J. Chem. Tech. Biotechnol.*,67, 350-356.

48- Sean J., Alexis T., (2011). A Study of the acid-catalyzed hydrolysis of cellulose dissolved in ionic liquids and the factors influencing the dehydration of glucose and the formation of humins. *ChemSusChem*., 4, 1166 – 1173.

49- Mohit S.M., Chandrashekhar B., Tanushree C., Kanwal S., (2011). Production of bio-ethanol from jatropha oilseed cakes via dilute acid hydrolysis and fermentation by Saccharomyces cerevisiae. *Int. J. of Biotech. Appl.*, 3, 41-47.

50- Changzhi L., Zongbao K., (2007). Efficient Acid-Catalyzed Hydrolysis of Cellulose in Ionic Liquid. *Adv. Synth. Catal.*, 349, 1847 – 1850.

51- Dongli A., Aihua Y., Weiping D., Qinghong Z., Ye W., (2012). Selective conversion of cellobiose and cellulose into gluconic acid in water in the presence of Oxygen and catalyzed by polyoxometalate-supported Gold nanoparticles. *Chem. Eur. J.*, 18, 2938 – 2947.

52- Flora C., Franck R., Catherine P., Amandine C., Emmanuelle G., Nadine E., (2011). Cellulose hydrothermal conversion promoted by heterogeneous Bronsted and Lewis acids: Remarkable efficiency of solid Lewis acids to produce lactic acid. *Appl. Catal. B: Environ.*, 105, 171–181.

53- Mingxing C., Tian S., Hongyu G., Shengtian W., Xiaohong W., Zijiang J., (2011). Clean production of glucose from polysaccharides using a micellar heteropolyacid as a heterogeneous catalyst. *Appl. Catal. B: Environ.*, 107, 104– 109.

54- Mingxing C., Tian S., Hongyu G., Shengtian W., Xiaohong W., (2011). Fabrication of micellar heteropolyacid catalysts for clean

production of monosaccharides from polysaccharides. *Catal. Commun.*, 12, 1483–1487.

55- Guozhi F., Chongjing L., Tao F., Min W., Guangsen S., (2013). Hydrolysis of cellulose catalyzed by sulfonated poly (styrene-co-divinylbenzene) in the ionic liquid 1-n-butyl-3-methylimidazolium bromide. *Fuel Process. Technol.*, 116, 142–148.

56- Jinxu X., Yu Z., Qineng X., Xiaohui L., Jiawen R., Guanzhong L., Yanqin W., (2013). Direct conversion of cellulose into sorbitol with high yield by a novel mesoporous Niobium phosphate supported Ruthenium bifunctional catalyst. *Appl. Catal. A*, 459, 52– 58.

57- Lanzafame P., Temi D.M., Perathoner S., Spadaro A.N., Centi G., (2012). Direct conversion of cellulose to glucose and valuable intermediates in mild reaction conditions over solid acid catalysts. *Catal. Today*, 179, 178– 184.

58- Rick O., James R. K , Joby M., (2012). Hemicellulose hydrolysis using solid acid catalysts generated from biochar. *Catal. Today*, 190, 89– 97.

59- Dong S., Xi X., Xi P., Lin M., Chun X., Wei H.Y., Chun H., Zhe K., (2013). Catalytic hydrolysis of cellulose to reducing sugar over acid-activated montmorillonite catalysts. *Appl. Clay Sci.*, 74, 147–153.

60- Shuguang S., Chunyan W., Bei C., Huanmei L., Yong H., Tao W., Haifeng Q., (2013). Heterogeneous hydrolysis of cellulose into glucose over phenolic residue-derived solid acid. *Fuel*, 113, 644–649.

61- Christos D.T., Vasilis N.B., (2004). Pore-Structure Analysis by Using Nitrogen Sorption and Mercury Intrusion Data. *AIChE J.*, 50, 489-511.

62- Derivation of the BET and Langmuir Isotherms. "[online]. [Accessed 20 March 2013]. Available from World Wide Web http://chem.colorado.edu/chem.

63- Sari W., (2000). Use mercury porosimetry and Nitrogen adsorption in characterization of the pore structure of mannitol and microcrystalline

cellulose powders, granules and tablet, PhD thesis. University of Helsinki, Finland.

64- Frangoise R., lean R., Hennet S., (1999). Adsorption by powders , porous solids principles, methodology and applications 1st Ed., Academic press.

65- Chunrong Z., Weikun W., Zhongbao Y., Hao Z., Anbang W., Yusheng Y., (2009). Nano-$CaCO_3$ as template for preparation of disordered large mesoporous carbon with hierarchical porosities. *R. Soc. of Chem*., 20, 976-980.

66- Basics of X-ray Diffraction. "[online]. [Accessed 15 March 2013]. Available from World Wide Web www.scintag.com.

67- Maslen E.N, Fox A., Okeefe M.A., (2004). X-ray Scattering. (Ed), International Tables for Crystallography, Vol. C (Kluwer Academic, Dordrecht, pp 554.

68- Scott A.S., (2000). Basics of X-Ray Powder Diffraction. [Online]. [Accessed 10 March 2013]. Available from World Wide Web: http://www.prism.mit.edu.

69- Hatakeyama T., Quinn F.X., (1999). Thermal Analysis: Fundamentals and Applications to Polymer Science. 2nd Ed. *John Wiley & Sons*

70- Grega K., Jozef M. , Primož M., (2010).Differential thermal analysis (DTA) and differential scanning calorimetry (DSC) as a method of material investigation. *RMZ – Mater.* and *Geoenviron.*, 57, 127–142.

71- P. Gabbott (2008). Principles and Applications of Thermal Analysis. *Blackwell Pub.*

72- Geoffrey E.L., (1987). Atomic number and crystallographic contrast images with the SEM: a review of backscattered electron techniques. *Mineral. Mag.*, 51, 3-19.

73- Russell P., Batchelor D., Thornton J,. SEM , AFM: Complementary techniques for high resolution surface investigations. [Online].

[Accessed 10 October 2013]. Available from World Wide Web http://www.microscopy-analysis.com

74- Goldstein, J. I., Newbury, D.E., Echlin, P., Joy, D.C., Fiori, C, Lifshin, E., (1981). Scanning electron microscopy and X-ray Microanalysis. 1st Ed. John Wiley & Sons. pp.60

75- Neves B., Salmon M., Russell P., Troughton, E., (1999). Comparitive study of field emission-scanning electron microscopy and atomic force microscopy to access self- assembled monolayer coverage on any type of substrate. *Microscopy and Microanalysis*, 5, 413-420.

76-Michael D., Adaskaveg J.E, (1997). Introduction to the scanning electron microscope theory, practice and procedures. facility for advanced instrumentation. [Online]. [Accessed 17 October 2013]. Available from World Wide Web https://imf.ucmerced.edu/downloads/semmanual.pdf

77- Farook A., Radhika T., (2010). Oxidation of benzene over bimetallic Cu–Ce incorporated rice husk silica catalysts. *Chem. Eng. J.*, 160, 249–258.

78- Adil E.A., Farook A., (2007). Indium incorporated silica from rice husk and its catalytic activity. *Microporous and Mesoporous Mater.*, 103, 284–295.

79- Farook A., Hasnah O., Kasim M.H., (2009). The immobilization of 3-(chloropropyl)triethoxysilane onto silica by a simple one-pot synthesis. *J. of Coll. and Interface Sci.*, 331, 143–147.

80- Diganta K. D., Priyanka G., Smita S., (2013). Salicylaldehyde phenylhydrazone: A new highly selective fluorescent lead (II) probe. *J Fluoresc*. DOI 10.1007/s10895-013-1167-0.

81- Hassan H.M., Omid P., Christoph J., (2007). Synthesis and spectral characterization of hydrazone Schiff bases derived from 2,4-

dinitrophenylhydrazine. crystal structure of salicylaldehyde-2,4-dinitrophenylhydrazone. *Z. Naturforsch*., 62, 717 – 720.

82- Barbra S., (2004). Infrared Spectroscopy: Fundamentals and Applications. *John Wiley & Sons, Ltd* pp.67.

83- Tagreed N. O., (2007). Synthesis of Schiff bases of benzaldehyde , salicylaldehyde as anti-inflammatory agents. *Iraqi J.Pharm.Sci*.,16 (2),5-11.

84- Gary D.W., (2003). Analytical chemistry, 6th Ed. *John Wiley & Sons, Ltd*, pp 80.

85- Mohammed Q.M., (2011). Synthesis and characterization of new Schiff bases and evaluation as Corrosion inhibitors. *J. of Basrah Res. Sci.*, 37, 116-130.

86- Skoog D.A, Donald M.W., James F.H., Stanley R.C., (2004). Fundamentals of analytical chemistry.8th Ed., pp 817.

87- Hugo E. G., Vadim K., Abraham N., (1997). NMR chemical shifts of common laboratory solvents as trace impurities. *J. Org. Chem.*, 62, 7512-7515.

88- Ioannis P. G., Anastassios T., Vassiliki E., Klimentini B., (2002). Nuclear magnetic resonance (NMR) spectroscopy basic principles, phenomena and their applications to chemistry, biology and medicine. *Gerothanassis trogains, exarchou, & barbarossou*, 3, 229-252.

89- Roger S.M., (1988). NMR spectroscopy, basic principles and applications. 1st Ed., *Harcourt College Pub*.

90- Muhammad A.A., Mahmood K., Abdul Wajid, (2011). Synthesis, characterization and biological activity of Schiff bases. *International Conference on Chemistry and Chemical Process*, 10, Singapore.

91- Hegazy W. H., Gaafar A., (2012). Synthesis, characterization and antibacterial activities of new Pd(II) and Pt(IV) complexes of some unsymmetrical tetradentate Schiff bases. *Am. Chem. Sci. J.,* 2, 86-99.

92- Brian E.L., Edward G.J., (1999). The use of salicylaldehyde phenylhydrazone as an indicator for the titration of organometallic reagents. *J. Org. Chem.*, 64, 3755-3756.

93- Michael G.B., Brian V., Gerald R., (1982). Phenylhydrazone derivatives of dimedone : Hydrogen bonding, spectral (^{I3}C , H nuclear magnetic resonance) and conformational considerations. crystal and molecular structures of 5,5-Dimethylcyclohexane- 1,2,3-trione 2-(4-Methylphenylhydrazone) and 5,5-Dimethylcyclohexane- I ,2,3-trione 2-(4-Nitrophenylhydrazone). *J. Chem. Soc. Perkin Trans.*, 2, 1297-1303.

94- Jugal K.P., Raghubir S., Varinder K.C., Raj P.S., (2009). Novel hexacoordinate organosilicon(IV) complexes of diethylenetriamine Schiff base with SiO_2N_3 skeleton. *Arkivoc*., 11, 247-256.

95- Farook A., Adil E.A., Sia L.M., (2008). Silver modified porous silica from rice husk and its catalytic potential. *J Porous Mater*.,15,433–444.

96- Farook A., Kasim M.H., Hasnah O., (2010). The heterogenation of melamine and its catalytic activity. *Appl. Catal., A,* 382, 115-121.

97- Thommes M., (2010). Physical adsorption characterization of nanoporous materials, *Chem. Ing. Tech*.,82,1059–1073.

98- Nassar, E.J., Neri, C.R., Calefi, P.S., Serra O.A, (1999). Functionalized silica synthesized by sol-gel process. *J. Non-Cryst. Solids*, 247, 124-128.

99- Ndahi N.P., Nasiru Y.P., (2012). Complex of Cobalt(II), Nickel(II) and Zinc(II) with Schiff bases derived from 4- Anisaldehyde. *Int. J. of Pharm. Sci. , Res*., 3, 5116-5120.

100- John C.E., (1990). Principles of NMR. *J. Phys. Chem.*, 94, 553.

101- Antonin L., Josef J., (1995). ^{1}H, ^{13}C , ^{15}N NMR spectra of some anthracenedione phenylhydrazones. *Dyes and Pigments*, 28, 207-216.

102- Farook A., Kasim M.H., Maysun R., (2011). The synthesis of heterogeneous7-amino-1-naphthalenesulfonicacid immobilized silica nanoparticles and its catalytic activity. *J. of the Taiwan Inst. of Chem. Eng*., 42, 843-851.

103- Díaz, I., Mohino, F., Pérez–Pariente, J., Sastre, E. (2001). Synthesis, characterization and catalytic activity of MCM–41–type mesoporous silicas functionalized with sulfonic acid, *Appl. Catal., A.*,205,19–30.

104- Charles L.M., Peter A.C., and Brewer H.J. (1985). Cellulose in Lithium Chloride and N,N-Dimethylacetamide. *Macromolecules*, 18, 2394-2402.